Copyright Warning & Restrictions

The copyright law of the United States (Title 17, United States Code) governs the making of photocopies or other reproductions of copyrighted material.

Under certain conditions specified in the law, libraries and archives are authorized to furnish a photocopy or other reproduction. One of these specified conditions is that the photocopy or reproduction is not to be "used for any purpose other than private study, scholarship, or research." If a, user makes a request for, or later uses, a photocopy or reproduction for purposes in excess of "fair use" that user may be liable for copyright infringement,

This institution reserves the right to refuse to accept a copying order if, in its judgment, fulfillment of the order would involve violation of copyright law.

Please Note: The author retains the copyright while the New Jersey Institute of Technology reserves the right to distribute this thesis or dissertation

Printing note: If you do not wish to print this page, then select "Pages from: first page # to: last page #" on the print dialog screen

ABSTRACT

ALCOHOL AS A CATALYST FOR HIV-ASSOCIATED NEUROINFLAMMATION AND TBI-INDUCED IRON TOXICITY

by
Agnieszka Agas

Alcohol has long been considered an exacerbator of diseases, disorders, and injuries as well as many of the accompanying symptoms. As an alternative approach, this dissertation explores alcohol as a catalyst for two different human disease conditions, human immunodeficiency virus (HIV)-associated neuroinflammation and traumatic brain injury (TBI)-induced iron toxicity. In HIV-1 infection, this dissertation presents a novel anti-viral drug, called Drug-S, for a possible inhibition and treatment of HIV-1 disease progression.

The ***first aim*** explores the influence of alcohol with HIV-associated neuroinflammation on macrophage migration across an *in vitro* model of the blood brain barrier. There is a gap in knowledge on the effects of low dose alcohol under HIV-associated injury in people living with HIV-1 who have achieved viral suppression. The model, consisting of a quad-cultivation of neuroimmune cells including endothelial, astrocyte, macrophage, and neuron cells, is challenged with low dose (10 mM) alcohol and the viral protein trans-activator of transcription (TAT). It was then observed for changes to barrier integrity and neuronal injury upon macrophage migration. Results show that combined alcohol and viral injuries significantly increases migration even under the clinically lowest concentrations of alcohol. The cause of enhanced macrophage migration and related neurotoxicity is implicated to alcohol-induced nitric oxide production by endothelial cells and TAT's chemoattractant properties.

The ***second aim*** analyzes a compound called Drug-S as a possible therapeutic for inhibiting HIV-1 replication and HIV-1 disease progression. Although the combination of highly active antiretroviral therapy can remarkably control HIV-1, it is not a cure. Current therapy is unable to eliminate persistent HIV-1 contained in latent reservoirs in the central nervous system and to prevent rebound viral replication and resurgence when treatment is withdrawn. Treating HIV-1 infected macrophage with Drug-S shows inhibition of infection and persistence at a low concentration without causing any toxicity to neuroimmune cells. Results suggest that Drug-S may have a direct effect on viral structure, prevent rebounding of HIV-1 infection, and arrest progression into acquired immunodeficiency syndrome.

The ***third aim*** explores the role of low level of alcohol use in TBI-induced hemolytic iron management. As hemorrhage is a major component of TBI, the accumulated red blood cells in the tissue layers undergo hemolysis and release free iron into the central nervous system. As a secondary stressor, prior alcohol consumption can increase iron aggregation and alter its management. The effects of alcohol on TBI- induced iron toxicity is explored in an *in vivo* model of chronic alcohol exposure subjected to fluid percussion injury. Results show that alcohol increases the iron overload and alters iron management following injury by changing the expression profile of the iron regulatory proteins lipocalin 2, heme oxygenase 1, ferritin light chain, and hemosiderin. Accompanying these results, it was also found that microglia can similarly play a significant role in iron management by phagocytosing red blood cells and retaining iron.

Overall, the results of this dissertation demonstrate the pervasive impact of alcohol use in neuropathophysiology arising from HIV protein TAT toxicity or TBI-induced iron

toxicity. In addition, the newly discovered DrugS can be an effective antiviral drug for a possible HIV/AIDS disease prevention and progression.

ALCOHOL AS A CATALYST FOR HIV-ASSOCIATED NEUROINFLAMMATION AND TBI-INDUCED IRON TOXICITY

by
Agnieszka Agas

A Dissertation
Submitted to the Faculty of
New Jersey Institute of Technology
and Rutgers University Biomedical and Health Sciences – Newark
in Partial Fulfillment of the Requirements for the Degree of
Doctor of Philosophy in Biomedical Engineering

Department of Biomedical Engineering

August 2021

APPROVAL PAGE

ALCOHOL AS A CATALYST FOR HIV-ASSOCIATE NEURINFLAMMATION AND TBI-INUCED IRON TOXICITY

Agnieszka Agas

Dr. James Haorah, Dissertation Advisor — Date
Associate Professor of Biomedical Engineering, NJIT

Dr. Kevin D. Belfield, Committee Member — Date
Professor of Chemistry and Environmental Science, NJIT

Dr. Pranela Rameshwar, Committee Member — Date
Professor of Medicine-Hematology/Oncology,
Rutgers University New Jersey Medical School, Newark, NJ

Dr. Jiang-Hong Ye, Committee Member — Date
Professor of Anesthesiology,
Rutgers University New Jersey Medical School, Newark, NJ

Dr. Vivek Kumar, Committee Member — Date
Assistant Professor of Biomedical Engineering, NJIT

BIOGRAPHICAL SKETCH

Author: Agnieszka Agas

Degree: Doctor of Philosophy

Date: August 2021

Undergraduate and Graduate Education:

- Doctor of Philosophy in Biomedical Engineering,
  New Jersey Institute of Technology, Newark, NJ, 2021
  Rutgers University Biomedical and Health Sciences, Newark, NJ, 2021

- Master of Science in Biomedical Engineering,
  New Jersey Institute of Technology, Newark, NJ, 2017

- Bachelor of Science in Biomedical Engineering,
  New Jersey Institute of Technology, Newark, NJ, 2015

Major: Biomedical Engineering

Publications:

Agas, A., A. Ravula, X. Ma, Y. Cheng, K. Belfield, J. Haorah (2021). "Hemolytic iron regulation in traumatic brain injury and alcohol use." Under review in TBD.

Agas, A., R. Garcia, J. Kalluru, B. Leiser, and J Haorah (2021). "Synergistic effects of alcohol and HIV TAT protein on macrophage migration and neurotoxicity." Under review in the Journal of Neuroimmunology.

Agas, A., J. Kalluru, B. Leiser, R. Garcia, H. Kataru, and J. Haorah (2021). "Possible mechanisms of HIV neuro-infection in alcohol abuse: interplay of oxidative stress, inflammation, and interruption of energy metabolism." Alcohol Apr 14:S0741-8329(21)00049-5.

Mishra, V.*, **A. Agas***, H. Schuetz, J. Kalluru and J. Haorah (2020). "Alcohol induces programmed death receptor-1 and programmed death-ligand-1 differentially in neuroimmune cells." Alcohol 86: 65-74. (*co-lead author).

Agas, A., H. Schuetz, V. Mishra, A. M. Szlachetka and J. Haorah (2019). "Antiretroviral drug-S for a possible HIV elimination." International Journal of Physiology, Pathophysiology, and Pharmacology 11(4): 149-162.

Presentations:

Agas, A., R. Garcia, J. Kalluru, and J. Haorah. "Profiling the effects of HIV protein TAT in an interactive neuroimmune cell culture." 2019 Biomedical Engineering Society Annual Meeting, October 17th, 2019, Philadelphia, PA.

Agas, A. and J. Haorah. "Profiling the effects of TAT on the blood-brain barrier during active HIV-1 infection." New Jersey Institute of Technology-Institute for Brain and Neuroscience Research Graduate Student/Post-Doctoral Research Showcase, April 29th, 2019, Newark, NJ.

Agas, A. and J. Haorah. "Profiling the effects of TAT on neurotoxicity during active HIV-1 infection." New Jersey Institute of Technology-Institute for Brain and Neuroscience Research Graduate Student/Post-Doctoral Research Showcase, March 29th, 2018, Newark, NJ.

Agas, A., R. Garcia, and J. Haorah. "Profiling the neurovascular cell interactions in alcohol exposure and HIV-1 Infection." Rutgers 10th Annual Pioneers in Endocrinology Workshop, October 11th, 2017, Piscataway, NJ.

To my dad, in loving memory.
Dla kochanego zmarłego taty.

ACKNOWLEDGMENT

Firstly, I would like to thank my supervisor, James Haorah, for his incredible mentorship and guidance through each stage of the process.

I would also like to thank my committee members, Vivek Kumar, Jiang Ye, Pranela Rameshwar, and Kevin Belfield for their valuable suggestions.

I thank the Department of Biomedical Engineering for the financial support as well as acknowledge Esther Hom, Selenny Fabre, Monuel Aulov, and Fatima Ejallali for their technical support.

I would like to thank my lab-mates and colleagues, Xiaotang Ma, Yiming Cheng, Arun Reddy Ravula, Tulika Das, Ricardo Garcia, Jagathi Kalluru, and Brooke Leiser for providing a wonderful research environment full of support and stimulating conversation.

I would like to acknowledge my co-authors, Harisritha Kataru, Heather Schuetz, Vikas Mishra, Adam M Szlachetka, as well as those already mentioned above for their contributions.

Finally, I would like to thank my mom, Danuta Agas, and brother, Michael Agas, for their sympathetic ear and never-ending love and encouragement. Mamo i Michał, dziękuję wam za ciągłą miłość i wsparcie.

TABLE OF CONTENTS

TABLE OF CONTENTS
(Continued)

TABLE OF CONTENTS
(Continued)

TABLE OF CONTENTS
(Continued)

LIST OF TABLES

LIST OF FIGURES

LIST OF FIGURES
(Continued)

CHAPTER 1

INTRODUCTION

1.1 A Note on the Text

All the work presented in my dissertation has already been published or is under review for publication. Each chapter (except for Chapter 5) is a direct derivative of 1 article and, therefore, a self-contained study. For this reason, each chapter will have its own Introduction, Methods and Materials, Results, Discussion, and Conclusion sections wherever applicable. Prior to the start of each chapter will be an acknowledgment of the co-authors that have helped me complete the work described. It is with their help that I was able to accomplish such a large and varied body of work and I look for every opportunity to thank them. Also, I note the journal, year, and volume number in which the work was published or is under review for publication.

Here in Chapter 1, I introduce the idea that alcohol can be perceived as a catalyst for diseases, injuries, or disorders by researching and analyzing current studies describing its effects on HIV infection in the brain. I take an alternative approach at understanding the exacerbating effects of alcohol use by focusing on the energy metabolism. This work was published as a review article entitled *Possible Mechanisms of HIV Neuro-Infection in Alcohol Use: Interplay of Oxidative Stress, Inflammation, and Energy Interruption* and it was published in volume 94 of *Alcohol* on August 2021. My co-authors, Jagathi Kalluru, Brooke Leiser, Ricardo Garcia, Harisritha Kataru, and James Haorah, helped me with the literature research.

1.2 Literature Survey

1.2.1 Introduction

Human immunodeficiency virus type-1 (HIV-1) continues to be one of the leading causes of death worldwide with new infections reaching millions each year, totaling 75.7 million people infected so far [1]. Of the 38 million people currently living with HIV-1, less than 67% receive treatment with 1 in 7 people being unaware of infection [1, 2]. In the United States, 1.2 million people are currently living with HIV-1 with over 100 new diagnoses every day [3]. The most affected populations are men who have sex with men, African American/black people, and young people ages 13-29 [4]. Despite almost 90% of the United States population being able to access treatment, only 76% initiates treatment, 58% retains care and 65% achieves viral suppression [5]. In the HIV-1 treatment cascade, viral suppression is an ultimate objective, although not a cure, it signifies that replication of the virus has been reduced to a point where viral load is at an undetectable level [6]. Therefore, someone with viral suppression is less likely to transmit the virus to their sexual partners and their treatment regimen is considered very successful [7]. The continual persistence of HIV-1 and difficulty in reaching viral suppression in this era of highly active antiretroviral therapy (HAART) treatment may then be due to other circumstances [8]. Many people infected with HIV-1 also abuse substances such as alcohol, as a result, alcohol may have some interplay on progression into acquired immunodeficiency syndrome (AIDS) [9, 10]. Much research has been focused on the exacerbating effects of alcohol use and HIV-1 infection, supporting the idea that infection renders the body more conducive to alcohol-induced metabolic changes and vice versa [11]. The purpose of this introduction is to contextualize these exacerbating effects as an interplay of oxidative stress, inflammation,

and an interruption of the energy metabolism, and, in so doing, generate a hypothesis for the accelerated progression of HIV neuro-infection seen with alcohol abuse.

1.2.2 Risk factors of alcohol on HIV/AIDS transmission

The frequency of alcohol abuse and likelihood of developing HIV-1 are mutually affected by several factors. Epidemiological studies have found that the probability of abusing alcohol in a lifetime has been shown to increase with educational inequality as incongruous levels of education can cause discrepancies in external stressors such as communication, financial status, and societal perception, and lead to both social and economic marginalization [12, 13]. Poorer education has been shown to limit access to knowledge of preventive care measures and contribute to the increasing population size affected by HIV-1 infection [14]. Racial and homophobic stigma can generate additional discrimination against alcohol abusers and people living with HIV-1 and discourage them from seeking appropriate medical care [15, 16]. A significant link between alcohol abuse and HIV-1 infection is poverty due to income inequality [15]. Impoverished communities are inclined towards increased alcohol intake and decreased condom use, both as methods of stress-relief, prompting alcohol abuse and a higher transmission of HIV-1 [17-19].

Alcohol use has been attributed with feelings of depression and anxiety, reducing inhibitions to provoke risky sexual behavior (such as engaging in prostitution or unprotected sex), among drug users, needle sharing, and, in those already infected, decreased adherence to HAART, all of which can support opportune HIV-1 transfection and increase susceptibility for HIV/AIDS transmission [20-25]. By interrupting regular functions involved with intelligence and rational thinking, chronic alcohol use may pervert

the user towards harmful behaviors, especially in regard to impulsive decision-making, taking on the form of a positive valence system whereby reward (euphoria) is chosen to outweigh risk (infection) no matter the severity of that risk (lifelong infection) [26, 27]. However, alcohol dependency and addiction are developed as a result of the negative valence system with constant intoxication being a relief from negative emotional states [28]. Recently, low to moderate alcohol drinking has been associated with improved cognitive function following evidence that information processing shows acute tolerance to alcohol [29, 30]. Conversely, the stigma of being HIV-positive can provoke unhealthy alcohol use and trigger a self-perpetuating, vicious cycle towards HIV-1 progression [31]. In obstructing mental health, alcohol instigates harmful behavior and increases risk for HIV/AIDS contraction and transmission.

Alcohol use also has implications beyond its behavioral associations. Physiologically, the effects of alcohol on immune defenses can further encourage HIV-1 acquisition [32]. The link between alcohol consumption and risk of infection is the immune response. There have been no direct associations found between alcohol use and viral load in people receiving HAART even with hazardous alcohol consumption except reduced adherence [23, 33, 34]. An enhanced immune response can improve host defenses while a substandard response can weaken defenses and increase vulnerability to infection. For the innate immune response, moderate prenatal alcohol exposure following liposaccharide administration has been shown to downregulate the MyD88-independent pathway of the tool-like receptor 4 (TLR4) response [35]. For the adaptive immune response, low to moderate doses of alcohol have been shown to increase differentiation of T-regulatory cells (Tregs) which work to suppress other cells of the immune system. These doses have also

been shown to increased differentiation of T helper 17 (Th17) cells, a subset of pro-inflammatory T helper cells that release IL-17 to recruit neutrophils [36]. This response creates a link between innate and adaptive immunity. Conversely, chronic heavy drinking has been shown to increase peripheral coagulation and inflammation following liposaccharide stimulation in a dose-dependent manner [37]. Therefore, low to moderate, inebriating doses have an immunomodulatory effect that can affect immune response time and produce a diffuse suppressed immune reaction to increase risk of infection and replication of virus, while heavy, chronic doses activate the immune system through inflammation and oxidative injury to damage the vasculature and promote HIV-1 infected cell entry into the brain. However, factors such as drinking pattern, beverage type, and gender can also influence alcohol consumption and the immune system [38]. Alcohol and HIV-induced chronic immune activation have also been shown to create an anergic effect on immune cells to increase surreptitious viral entry into the brain and viral persistence in the central nervous system (CNS) [39, 40]. These ability changes are caused by alcohol-triggered interferences in B-cell and T-cell tasks, including suppression of antiviral factors and decreases in some antigen presenting functions making cells more susceptible to viral infection [41-44]. Therefore, alcohol-impaired immune defenses combined with HIV-1's ability to evade immune attack through quick antigenic variation make cells very susceptible to infection [45]. In effect, alcohol use augments and accelerates HIV-1 transmission. Alcohol's additive effects for furthering risk of infection and transmission have been very well studied [46].

1.2.3 Influences of alcohol on HIV/AIDS entry and persistence in the brain

People living with HIV-1 (PLWHA) have reported faster alcohol-associated behavioral effects (such as feeling tipsy) with fewer drinks than people not infected with HIV-1 [47]. Therefore, HIV-1 may play a role in delaying metabolism of alcohol by the liver resulting in its sustained circulation in the blood [48]. Persistent presence of alcohol in the bloodstream allows vascular cells to admit and metabolize increasingly more alcohol, a result which can be especially problematic for the integrity of the blood-brain barrier (BBB) [49]. The liver metabolizes alcohol into acetaldehyde by alcohol dehydrogenase (ADH) from the cytosol (main pathway), cytochrome P4502E1 (CYP2E1) from microsomes, and catalase from peroxisomes as well as into H_2O_2 also by CYP2E1 [50]. Since the brain does not contain alcohol dehydrogenase, it uses the enzymes CYP2E1 and catalase to metabolize alcohol [51, 52]. Interestingly, class III ADH activity was found in brain endothelial cells, neurons, and astrocytes of various brain regions as well as Purkinje cells of the cerebellum, however this class of ADH in the CNS is not involved in ethanol metabolism. ADH III is more likely used to reduce surplus acetaldehyde in brain cells possessing low acetaldehyde dehydrogenase (ALDH) activity. CYP2E1 activity is induced after alcohol administration and is the form of CYP450 that actively oxidizes ethanol. CYP2E1 presence has been shown in all types of glial cells, neurons, and brain microvascular endothelial cells. Although distributed heterogeneously among all the brain regions, CYP2E1 was distinctly found in the frontal cortex, hippocampus, striatum, substantia nigra, and neuropils of various regions of the brainstem such as the pons, superior olivary complex, and trigeminal nerve nuclei. Catalase is located in microperoxisomes and only found in the perikaryons of aminergic neurons and in glial

cells. Maximum catalase activity has been shown in the ependymocytes of the third ventricle and in the solitary nucleus of the brainstem [53].

Since the CYP450 pathway metabolizes multiple drugs and regulates their bioavailability, HAART treatment may be altered with alcohol use through reductions in concentrations of antiretroviral drugs [54]. Interestingly, since HAARTs are designed for CD4-dependent infection, they are less effective on CD4-independent infection such as in hepatocytes making the liver a possible silent reservoir of HIV-1 infection [55]. In vitro studies have shown that hepatocyte cell lines may permit low levels of HIV-1 infection through CD4-independent entry mechanisms, but these levels can be significantly potentiated by secondary stressors such as alcohol [56, 57]. The increases in HIV-1 replication observed in monocyte-derived macrophages exposed to chronic levels of alcohol have been attributed, in part, to CYP2E1-mediated oxidative stress [58]. Acetaldehyde is very reactive and can form adducts with various brain signaling chemicals such as neurotransmitters, only when it is metabolized by ALDH into acetate does alcohol become least active [59]. Similar to CYP2E1, ALDH activity is broadly dispersed in the brain structure although less so in aminergic neurons. This presents an idea of localized accumulations of acetaldehyde in certain brain regions [53]. In the pancreas, the less common nonoxidative pathway of alcohol metabolism produces fatty acid ethyl esters (FAEE) that can also cause tissue injury, specifically mitochondrial dysfunction [60]. The brain has also been shown to participate in this pathway, regulating FAEEs production with three synthases, two being glutathione S-transferases. Activity of these synthases is predominant in gray matter, the regions containing neuronal cells [61, 62]. In neurons, the acetaldehyde produced activates NADPH/xanthine oxidase (NOX/XOX) and inducible

nitric oxide synthase (iNOS) to generate reactive oxygen species (ROS) and nitric oxide (NO) while H_2O_2 reacts with copper/iron to produce additional ROS [63, 64]. This activated iNOS and NADPH oxidase can further produce reactive nitrogen species (RNS) from NO and superoxide (O2-) [65].

Accumulation of RNS/ROS can unbalance redox to increase oxidative stress and cause vascular injury [66]. Specifically, excess oxidative stress can stimulate the inositol 1,4,5-triphosphate receptor and release of Ca^{2+} leading to activation of myosin light chain kinase (MLCK) and subsequent phosphorylation of the myosin light chain (MLC) and tight junction (TJ) proteins (occludin, claudin-5, and zonula occludens) of the endothelial cells that constitute the BBB [67, 68]. Degree of permeability across the BBB depends on the integrity of TJ proteins, therefore, decreases in TJ proteins injures the microvasculature permitting influx of otherwise restricted substances such as HIV-1 virions [69, 70]. The BBB appears most vulnerable to oxidative stress because prenatal exposure to alcohol has not been shown to disrupt the BBB [71]. Presence of alcohol alone or HIV-1 regulatory proteins such as the trans-activator of transcription (Tat) and the envelope glycoprotein gp120 is enough to destabilize BBB integrity because they induce formation of stress fibers and ROS that can redistribute tight junction proteins [72, 73]. Furthermore, decreases in occludin have also been shown to increase HIV-1 transcription and promote infection [74]. TJ proteins are the gatekeepers of the BBB, their injury emphatically compromises the permeability of the BBB. Ethanol metabolites such as acetaldehyde and FAEE can also directly affect the BBB. Acetaldehyde can traverse the BBB only when concentrations saturate the ALDH of the brain microvasculature [75]. Alone, acetaldehyde does not damage the BBB, however the addition of another stressor, such as malnutrition, may be

sufficient in reducing barrier function [76, 77]. The effects of FAEEs on BBB integrity have been largely unexplored, however free FAEEs are themselves bioactive and can be potentially toxic to the BBB.

However, HIV-1 virus does not need to rely on a damaged BBB to enter the CNS, it can bypass the barrier with the Trojan horse mechanism [78]. HIV-1 can infect monocytes/macrophage (as well as T-lymphocytes and dendritic cells) and use them as a veil of resident protein to enter the CNS in a Trojan horse manner. Inflammation of the BBB by oxidative stress can further entry by causing an immune response and more of these infected monocytes/macrophages to gather at the BBB [79-81]. Then, especially in alcohol users, vascular oxidative injury can promote HIV-infected cell entry into the brain [82]. Upon entering the CNS, HIV-1 begins infecting microglia via CD4 receptor binding and astrocytes via cell-to-cell contact, along with establishing latent reservoirs [83-85]. Infection is currently treated with HAART however, the unique anatomy of the brain makes treatment a constant challenge and viral persistence a certainty [86, 87]. The geometry of the brain, including the folds and convoluted surface created by gyri and sulci, distinct shapes of the lobes and hemispheres divided by fissures, and many important enclosed, internal structures, makes drug penetration and distribution difficult [88]. Transporters at the BBB such as P-glycoprotein (P-gp), the multidrug resistance associated protein (MRP1), and the breast cancer resistance protein (BCRP) prevent HAART drugs from entering the CNS or work as active efflux pumps to throw them back into circulating blood [89]. A disrupted BBB can facilitate penetration of HAART drugs [90, 91]. Even though HAARTs are effective, studies have shown BBB impairment persists because HARRT drugs carry their own risks of toxicity and tolerability [92, 93]. They have been

shown to cause mitochondrial toxicity and changes to neurotransmitter levels as well as impairment of the electron transport chain and glucose metabolism [94]. Oxidative stress, induced by alcohol or HARRT drugs themselves, can exacerbate their toxicity.

Even if they are able to circumvent all these obstacles, HAARTs cannot eradicate viral DNA compartmentalized in latent reservoirs, hideouts containing non-replicating, dormant forms of the virus, inside the CNS [95]. Therefore, any interruption or withdrawal of HAART regimens can cause a rebound effect in which the dormant virus is activated to re-start replication and, being that the BBB is a bi-directional barrier, re-infect the body [96, 97]. Alcohol use exacerbates these consequences by diminishing HAART adherence wherein the person forgets to take the drug or is afraid of taking the drug while using alcohol [98, 99]. Alcohol can also interrupt treatment by attenuating the effects of these drugs [100]. Overlapping pathways in HAART and alcohol metabolism may explain these limiting and/or disrupted effects of HAART and even aggravation of HIV-associated neurological disorders (HAND) [101].

HAART metabolism is largely governed by CYP450, also the chief pathway for alcohol metabolism in the brain. Certain HAART drugs, such as the protease inhibitor nelfinavir, form active metabolites that can also exert an antiviral effect [102]. PLWHA experience drug interaction due to the use of multiple drugs in their HAART treatment as well as other substances such as alcohol. Many of these drugs also inhibit CYP enzymes to facilitate sustained exposure of HAARTs and, when used together, alcohol in the body and the brain. This increased exposure of HAART drugs and alcohol has the potential for creating toxicity [103]. In addition, HAART drugs induce mitochondrial toxicity much earlier in the liver than the brain, therefore liver damage may prevent proper elimination

of these drugs and cause their bioaccumulation [104]. Furthermore, some treatment regimens require drug boosting which can increase toxicity and aggravate side effects. Alcohol consumption has not been shown to affect the pharmacokinetics of HAART drugs [105]. However, pharmacological interventions for alcohol use disorder (AUD) have reduced alcohol use to improve viral suppression without changes to HAART adherence which implies there may be some interaction between alcohol and HAART drugs that moderates treatment [106]. There has been some suggestion that an interaction between immune cells and astrocytes through the CYP pathway can lead to an increase in oxidative stress and subsequent deceased response to HAART [107]. Another suggestion is that alcohol decreases the activity of membrane-associated drug transporters of testicular cells by altering properties of the lipid bilayer thereby diminishing uptake of HAART drugs [108]. Studies involving alcohol-drug-protein interactions are needed to understand the affect alcohol has on HAART efficacy.

1.2.4 Effects of HIV-1 infection and alcohol use on the neuroenergetic balance

1.2.4.1 Impeded glucose uptake. As the most energy demanding organ of the body, the brain requires a significant supply of glucose, especially when active [109]. Proopiomelanocortin and agouti-related peptide neurons sense glucose and regulate its supply to the brain [110]. Unfortunately, both alcohol and HIV-1 have been shown to alter uptake of glucose into the brain [111]. Studies measuring glucose analog ^{18}F2-fluoro-2-deoxy-D-glucose (^{18}F-FDG) uptake and regional cerebral blood flow using imaging techniques have found overall reduced uptake in symptomatic HIV-1 participants [112, 113]. However, results of asymptomatic HIV-1 participants (those receiving HAART)

were varied and brain regions showing this deficient uptake changed depending on participant demographics and presence of comorbid conditions. Some of these first studies, done throughout the 1990s, found increased uptake in the basal ganglia and thalamus [114]. However, these early studies were done on participants not receiving treatment who had already progressed to AIDS, therefore this increased uptake of glucose by the brain may occur in the late stages of HIV-1 disease when the virus is most virulent and neurodegeneration is most severe.

Most early studies on alcohol have documented decreased uptake of glucose by the brain [115]. In fact, in a previous study done on human neurons and astrocytes our lab has shown that ethanol downregulates uptake of D-(2-3H)-glucose by reducing expression of uniporter glucose transporter proteins (GLUTs), GLUT1 in astrocytes, oligodendrocytes, endothelial cells (of the BBB), and microglia, and GLUT3 in neurons [116]. In disturbing the activity of acetylglucosamine, ethanol prevents glycosylation of these GLUTs thereby impairing their function and impeding transport of glucose in the brain. However, several recent studies have shown increased glucose and lactate levels in the CNS [117]. These studies were performed on C57BL/6J mice exposed to chronic intermittent ethanol concentrations with glucose and lactate levels measured in the CNS and not individual cell populations. This indicates that alcohol, through impairing the uptake of glucose by astrocytes and neurons, is likely disrupting the utilization of glucose by these cells and causing metabolic dysfunction in the CNS. In a study exploring the effects of oxygen and glucose deprivation conditions on brain cells, exposure caused neurons to rapidly release the tissue-type plasminogen activator to induce adenosine monophosphate-activated protein kinase activation in astrocytes and endothelial cells and recruitment of GLUT1 to

their membranes [118]. Subsequent increase of glucose uptake was followed by astrocyte-neuron lactate shuttling (ANLS) as a means of promoting neuronal survival [119].

1.2.4.2 Use of imaging techniques for glucose metabolism. Many of these studies adopted imaging techniques for diagnostic and treatment discovery purposes. One study found that, in the early stages of HIV-1 disease, there is no real evidence of structural changes, based on magnetic resonance imaging (MRI), but rather some metabolic differences, based on positron emission tomography (PET) scans [120]. However, these differences did not appear indicative of disease onset. Subsequent studies began using imaging techniques, such as ^{18}F-FDG coupled with PET-computed tomography (PET/CT) or MRI scanning to assess glucose metabolism in the body. Since many of these studies were not followed-up with specific experiments determining the activity of reactions involved with glucose breakdown, metabolism is impossible to confirm. As such, it would be more appropriate to assert that these techniques only measured glucose uptake. The overall caveat of these techniques is that they fail to explain the fate of glucose once it is taken up. Metabolism activity cannot be directly observed because current imagining technologies do not have the spatiotemporal resolution to measure this fast-acting process [121]. Furthermore, results may be misconstrued if abnormal uptake of glucose is due to secondary HIV-related pathologies such as inflammation or neuronal damage [122, 123]. ^{18}F-FDG-type imaging requires knowledge of individual patients' conditions, viremia, and treatment history for proper interpretation and more convincing results [112, 124]. Although certain HIV-related cerebral pathologies such as primary central nervous system lymphoma can be differentiated from infection with this technique [125]. Alternatively,

increases in brain glucose metabolism have been shown to be visible if HAART becomes interrupted [126].

Another method used to study neurometabolic states under HIV-1 disease is the use of magnetic resonance spectroscopic (MRS) imaging to study distributions and concentrations of metabolites such as N-acetylaspartate (NAA), choline (Cho), creatine (Cr), glutamate (Glu), and myo-inositol (MI). In studies involving HIV-1 infection and chronic alcohol consumption, concentrations of phosphodiester (PDE) and phosphocreatine (PCr) have also been examined [127]. The ratios of these metabolites are correlated to viral load and cerebral spinal fluid (CSF) biomarkers and then extrapolated to draw conclusions about monocyte activation and chemotaxis, inflammation, gliosis, neuronal dysfunction, and regional metabolic changes [128-131]. This generalization is a non sequitur because metabolite ratios can vary depending on the type of disease, its severity, and the afflicted brain region. Correlation cannot imply causation without additional confirmation. An immunoPET study may help resolve this controversy however labeled antibodies cannot cross the BBB. More experimental evidence is needed to support the imaging results on glucose metabolism.

1.2.4.3 Alternative energy sources. Other ethanol-induced secondary effects can also lead to deficiencies in glucose uptake. Ethanol consumption mimics the inhibitory neurotransmitter γ-aminobutyric acid (GABA), ergo the sedative effects of alcohol, and GABA metabolism has been shown to trigger insulin secretion [132, 133]. Ethanol-damaged insulin signaling increases insulin levels to produce a hypoglycemic effect [134]. Increased levels of alternative energy sources in the bloodstream has also been linked to

decreased glucose utilization [135]. Glucose cannot be replaced as the main supplier of energy, but other sources can be used to supplement it. Alternative sources include ketone bodies during periods of low caloric energy intake, glycogen, locally stored in astrocytes, during strenuous exercise, and acetate during periods of heavy alcohol consumption [136-140]. Fatty acids are not a viable source of energy for the brain because they are bound to albumin and therefore cannot pass through the BBB [141]. Under HIV-1 infection, glutamine-glutamate has also been used as energy by infected macrophage [142]. Glutamate can be converted to α-ketoglutarate (α-KG), a tricarboxylic acid (TCA) cycle component, by glutamate dehydrogenase or the alanine or aspartate transaminases and be used in adenosine 5'-triphosphate (ATP) production or be further converted to citrate by isocitrate dehydrogenase to synthesize other intermediates [143]. However, during periods of increased brain activity and neuronal firing, lactate has been considered the preferred energy substrate [144]. The purpose of these supplementary energy sources is to conserve glucose during alcohol consumption and HIV-1 infection when glucose uptake is impeded, and overall glucose levels are low. In another way, this shift to metabolic substrates is an adaptive response to mitigate the glucose deficiency following alcohol abuse and HIV-1 infection. However, increased presence of other metabolites has been shown to promote HAND [145]. Increased levels of acetate and citrate have been linked to worsened cognitive status in HIV+ patients [146].

Lactate is often the end-product of glycolysis in astrocytes, getting shuttled through both monocarboxylate transporters (MCT) and MCT-independent lactate transporters and conduits [147]. 1H MRS of NOD/scid-IL-2Rgcnull mice transplanted with human CD34+ hematopoietic stem cells have shown a notably large increase in lactate levels at the

cerebral cortex after HIV-1 infection [148]. In addition, a decrease in glucose levels in the brain, especially the hypothalamus, by alcohol can cause increased AMP activated protein kinase (AMPK) activity and may even indirectly inhibit oxidative phosphorylation (OXPHOS) [149]. Muraleedharan, et., al. has shown that AMPK is required for astrocytic glycolysis as well as increased lactate production and shuttling as a source of energy. AMPK-null astrocytes were deficient in glycolysis and reduced production of lactate and other energy metabolites. Reduction in citrate presents the possibility that pyruvate-derived acetyl CoA and the TCA cycle may also be decreased. AMPK activity preserves astrocytic GLUT1 by phosphorylating and destabilizing thioredoxin-interacting protein (TXNIP) to enable lactate production. Finally, AMPK-null neurons co-cultured with wild type astrocytes prevented neuronal death, providing further evidence for the ANLS hypothesis in energy management and distribution [119]. Ethanol reduces AMPK activity in the liver and the brain while increasing acetyl-CoA carboxylase activity and malonyl CoA content, both enzymes important in fatty acid synthesis [150]. However, ethanol does not decrease total AMPK levels, rather AMPK activity is impeded through reductions of its phosphorylation [151].

1.2.4.4 Increased lactate shuttling. Within the CNS, glucose uptake among brain cells is disproportionate [152]. While astrocytes are located closest to the source of available glucose, the bloodstream, neurons have limited access. Astrocytic expansions and end-feet are in contact with vascular capillaries to the extent that microvessels are entirely covered in these perivascular astroglial sheaths [153]. This requires neurons to receive deliverable energy in an indirect manner. Astrocytes' position next to blood vessels allows them to

traffic energy substrates to areas demanding energy. For these reasons, neurons (and even oligodendrocytes) favor lactate as an energy source during homeostasis [154]. Neurons, expressing their own glucose transporter protein, can process glucose glycolytically but do so under conditions involving extremely high energy demand, preferentially, this glucose is used to produce reducing agents (electron sources) including nicotinamide adenine dinucleotide (NADH) and nicotinamide adenine dinucleotide phosphate (NADPH) through the pentose phosphate pathway or biosynthetic precursors for other compounds, since the restrictive BBB requires they be synthesized from glucose within the brain [155]. In addition, ions such as sodium, potassium, and calcium do not require much energy for signaling purposes because they move according to concentration gradients however recharging these gradients is a significant energy consuming process for the brain.

Interestingly, in intestinal cells, moderate alcohol use has been shown to alter the sodium gradient and diminish affinity of the co-transporter for glucose [156]. This has been supported with studies that show astrocytes as the predominate consumers of glucose during synaptic activity [152]. It is also well documented that during brain excitation, the glycolysis of glucose-to-lactate rate temporarily exceeds that of OXPHOS because there is an upregulation of glucose activity compared to oxygen consumption [157, 158]. The ANLS model describes that astrocytes respond to the release of synaptic signaling by increasing utilization of glucose and triggering glycolytic production and release of lactate into the extracellular space to be absorbed by surrounding neurons for oxidation [159, 160]. However, since its formulation, this hypothesis has been fraught with controversy. Lack of experimental evidence as well as issues with the metabolic requirements for significant lactate shuttling creates doubt about the energetic contributions of ANLS [161, 162]. The

decreased energy supply in the CNS caused by HIV-1 infection and alcohol abuse may strengthen the case for ANLS as the central energy source, glucose, becomes diminished. Fresh evidence from new and sophisticated technologies, techniques, and experimental models are necessary to circumstantiate this model. Recently, Barros et al. have expanded on this concept by proposing that under increased neuronal activity, astrocytes, through a compounded outcome of the Warburg and Crabtree effects, take up aerobic glycolysis [163]. During aerobic glycolysis, lactate is produced regardless of the sufficient levels of oxygen, conversely, during anaerobic glycolysis, lactate is mass produced under hypoxia conditions. ANLS has also been referred to as the Reverse Warburg effect because astrocyte glycolysis metabolically supports adjacent neurons [164]. The lack of a rate-limiting demand for energy in brain activities permits for the rapid and tuned synthesis of ATP done by aerobic glycolysis. Hexokinase, which phosphorylates glucose to glucose-6-phosphate, has a very low half-saturation constant and can perform this conversion at its highest speeds. In addition, hexokinase IV, an isoform of hexokinase in the brain, is not inhibited by glucose-6-phosphate to prevent more uptake of glucose by cells [121].

Although less energetically favorable, aerobic glycolysis produces more lactate and, in reducing the need for OXPHOS and the electron transport chain, conserves oxygen for neuronal oxidative metabolism. In this respect, ANLS does not reflect an inefficient production of energy but the organizing of astrocytes for neuronal energy assembly. However, the question remains, how do astrocytes overcome the Pasteur effect? With the abundance of oxygen present in the CNS, astrocytes should favor OXPHOS as it produces more ATP. An idea is that astrocytes tradeoff their energy for the common good of the biomass (or the brain). This idea has not yet been studied but presents a possible

multifaceted view of neuroenergetics. Controversially, another idea of metabolic coupling is that neurons shuttle lactate to astrocytes instead, to release accumulating lactate from the brain. In the neuron-astrocyte lactate shuttle (NALS) model, glucose travels through endothelial cells and between astrocyte endfeet gaps to be taken up by neurons which release accumulating lactate to be absorbed by astrocytes, dispersed to astrocyte endfeet, and released to the surrounding vasculature or lymphatic drainage systems [165]. Transport of glucose to more distant neurons is also facilitated by astrocyte endfeet. NALS explains that GLUT3, the glucose transporter for neurons, has a much higher transport rate than GLUT1, the glucose transporter for astrocytes, while astrocytes have a higher capacity for lactate uptake [121]. Lactate is not considered a source of energy in this model, instead its accumulation is thought to cause cerebral lactic acidosis which can be mitigated by NALS. However, this model does not explain why glycolysis exceeds the OXPHOS metabolism of glucose. This controversy surrounding lactate is due to limited studies on the cause of lactate production in vivo and its viability as a suitable energy substrate. More studies with direct experimental proof are needed for a comprehensive understanding of lactate metabolism in the brain.

A recent study of the effects of alcohol on glucose and lactate homeostasis has shown that alcohol causes the brain to adopt more of the astrocyte-neuron lactate transfer as a source of energy. Chronic intermittent ethanol increases CNS concentrations of glucose and lactate, as well as augments the expression of the membrane protein, MCT, a carrier for lactate, pyruvate, and ketone bodies [117]. However, the increased glucose and lactate concentrations have not been linked to the increased MCT expression. A previous study of astrocyte metabolism exposed to acute levels of ethanol used MRS to show

decreased fluxes of pyruvate dehydrogenase and pyruvate carboxylase reactions alongside an increased flux of glycolysis and an increased ratio between lactate formation and glucose consumption [166]. Infection has been shown to further increase the rate of glycolysis both directly, by increasing the activity of enzymes involved in glycolytic pathways, and indirectly through viral proteins [167]. HIV-1 proteins such as the envelope gp120, Tat, and viral protein R (Vpr) increase energetic demands by stimulating synaptic excitation [168, 169]. This combination of increased glucose consumption, lactate production and dispersal, and glycolysis metabolism in astrocytes is a reaction to the stress induced by alcohol exposure and HIV-1 infection. This response may be an evolution on the survival mechanism, enabling the brain to react to neurotoxins created by these stressors to preserve neurons. Alternatively, Mason et al. have proposed that, during infection, astrocytes shuttle more lactate to activated microglia rather than neurons [170]. The argument for astrocyte-microglia lactate shuttling (AMLS) is that it is to the advantage of the CNS for microglia to perform immune responses. By targeting, engulfing, and clearing away pathogens, microglia destroy harmful substances to protect neurons and the CNS. A study of the effects of tuberculous meningitis on lactate levels found elevated host lactate acid as a response to infection [171]. Furthermore, this lactate appeared to be used as an energy substrate by microglia, preferentially over glucose, with neuroprotective outcomes. To date, AMLS has only been studied in the context of tuberculous but these results merit studies in other infectious diseases such as HIV-1.

In any respect, the twofold increase in glycolysis rate caused by alcohol and HIV-1 infection may go beyond the usual fluctuations readily maintained by cellular maintenance mechanisms. The consequence to an inability to accommodate increased

glycolysis may be the development of an abnormal redox state. A change in the generation of NAD+/NADH and NADP+/NADPH, normally maintained by the malate-aspartate shuttle (MAS) for the TCA cycle and lactate dehydrogenase when an overactive glycolytic flux overwhelms MAS, may affect their concentrations as well as levels of ROS and lead to allostatic overload. In neurons, this overextension of maintenance mechanisms might cause an inverse Warburg effect whereby overworked ROS maintenance mechanisms break down ROS homeostasis and cause persistent, irreversible metabolic impairment [164]. This damage could cause cortical spreading depolarizations to neighboring neurons and lead to diffuse injury and massive neuronal loss [172]. This type of damage is typical of HIV-1 infection and exacerbated with alcohol use, it can lead to associated neurodegeneration and neurocognitive disorders.

1.2.4.5 Exaggerated microglia activity. Another effect of cortical spreading depolarization is the stimulation of glial cell proliferation and activity [173, 174]. Like microgliosis, this can be instigated with injury caused by alcohol use and HIV-1 infection [175, 176]. Microglia's roles in the immune system are to scavenge for debris and pathogens, and phagocytose them in an effort to repair tissue, promote neuronal survival, and maintain homeostasis. Neurons damaged by insults, such as Tat, release more of the chemoattractant fractalkine (CX3CL1) in order to stimulate their uptake and removal [177]. However, in a study done on primary rat microglial cells and BV2 cells exposed to HIV-1 Tat, increased microglial activation was attributed to disruption of the CX3CL1/CX3CR1 axis, an immune cell migration controller, and subsequent decreased response of microglia to cells presenting CX3CL1 [178]. Ethanol has been shown to

downregulate expression of CX3CL1 and also altered the CX3CL1/CX3CR1 axis [179]. By suppressing their scavenging functions, microglia are prevented from expending their energy and remain highly active, that is, their energy is thought to be 'held back'. Importantly, CX3CL1/CX3CR1 control extends to rescuing neurons by attenuating the production and release of cytokines from microglia as well as modulating phagocytic activity [180]. The microglia-neuron interaction is complex, and the fate of a damaged neuron to be either protected or destroyed does not depend on CX3CL1/CX3CR1 signaling alone but is contingent on the presence or absence of co-stimulatory signals. Disruptions in the CX3CL1/CX3CR1 pathway are being studied as a mechanism for neurodegeneration.

This microglia-neuron communication is also involved with inducing HIV-1 expression in latently infected microglia containing dormant forms of the virus. Damaged neurons, specifically GABAergic cortical and dopaminergic neurons, as well as substantial neurodegeneration have been shown to stimulate HIV-1 virus from latency by disrupting the cross-talk between healthy neurons and infected microglia restraining HIV-1 expression [181]. For this purpose, HIV-1 has evolved mechanisms to extend the lifespan of infected microglia [182]. Since the byproducts of alcohol consumption and HIV-1 infection can damage neurons, both alcohol and HIV-1 can be involved with viral rebound. Astrocytes also serve as latent reservoirs, however, viral replication in astrocytes is triggered by inhibiting host restriction factors [183].

For macrophage/microglial cell respiration, the presence of HIV-1 infection and alcohol use has been shown to affect the TCA cycle with no detectable changes in glycolysis [142]. HIV-1 infection silences mitochondrial metabolism and, consequently,

disrupts the tricarboxylic acid cycle to reduce ATP production. To compensate, infected microglia/macrophage consume glutamine/glutamate as an alternative major source of energy [184]. A result of this utilization is the elevated expression of glutaminase 1 (GLS1), the amidase that generates glutamate from glutamine. Ectopic expression of GLS1 then induces microglial activation and pro-inflammatory exosome release by regulating glutaminolysis activity and its downstream production of α-KG [185, 186]. In a study examining the role of HIV-1 Vpr in energy metabolism, Datta et al. found an increase in glucose uptake and accumulation of α-KG and glutamine in the extracellular environment of Vpr expressing macrophage, but pools of glutamate and several TCA intermediates, such as glucose-6-phosphate, fructose-6-phosphate, citrate, malate, α-KG, and glutamine, exhibited a decreased trend [187]. Datta, et al. suggests that an increase in TCA cycle activity can be the cause for these observed reductions in TCA metabolite pools. Therefore, HIV-1 infection causes an increased production of energy due to greater energetic demand. However, the reason of this additional energy has not been abundantly studied. Infected cells may be utilizing this energy to further infection, working at a cross-purpose in the interest of the virus, disregarding clear disadvantages to the immune system. In contrast, this energy may be simply accumulated and wasted in order to decrease total energy supply and instigate the demise of non-infecting cells. More research should be directed at the energy requirement and utilization of HIV-1 infected cells.

The primary pathway through which alcohol induces microglia activity appeared to be via the stimulation of a TLR4 response and subsequent signaling cascades that change microglia from a ramified to an ameboid form. This type of activation can also stimulate endocytic and phagocytic activity [188, 189]. Alcohol mimics actions of endogenous TLR4

ligands to activate TLR4 signaling. For example, activation of NLRP3-inflammasome in glial cells, a protein that triggers an immune response, was shown to be mediated by ethanol-induced TLR4 signaling [190]. Robust viral replication without immune activation has not been shown to cause development of AIDS [191]. Conversely, virologic suppression with chronic immune activation has shown progression of HIV-1 disease severity [192]. As an immunomodulator, alcohol can modify the activity of an immune response. People who have achieved viral suppression on HAART but drank heavily have shown increased immune activation [193]. Immune activation can be a powerful indicator of clinical outcome.

1.2.4.6 Disrupted neuronal mitophagy. The impacts of alcohol and HIV-1 infection on neuronal cells concern the stability of their mitochondria. In vivo studies have not substantiated support for neuronal infection by HIV-1 because neurons lack the CD4 receptor necessary for targeting intended cells. Instead, viral proteins such as gp120, Tat, and Vpr, secreted during active infection, can produce neurotoxic effects. These viral proteins have been shown to directly interact with the neuron to disrupt and injure synaptodendritic function as well as mediate signal transduction cascades to cause mitochondrial dysfunction and neuronal cell death [194]. Presynaptic terminals, one side of the synaptodendritic compartment, hold abundant amounts of mitochondria, therefore, loss of synaptodendritic function may also be reflective of mitochondrial dysfunction. Studies on primary rat cortical neurons have shown that by increasing oxidative stress, ATP levels, and mitochondrial membrane potential, Tat induces mitochondrial hyperpolarization [195]. Similar studies done of gp120 have shown reduced mitochondrial

respiratory capacity by observing decreased oxygen consumption rate, maximal and spare respiratory capacity, and mitochondrial distribution and movement as well as increased abnormal mitochondrial fusion/fission [142, 196]. Consequently, HIV-1 secreted proteins exhaust mitochondrial bioactivity as well as increase the level of stimulus required to initiate further activity. Interestingly, HARRT has also been shown to deplete mitochondrial respiratory capacity by reducing interterminal ATP levels as a means to decrease production and generation of the byproduct ROS [197]. Stimulation by viral proteins at presynaptic terminals can increase energetic demands, however defective mitochondria cannot produce enough energy. The unused fuel molecules and oxygen can then build up in the mitochondria and cause additional damage.

Under homeostasis conditions, mitochondria damage checkpoints respond to oxidative stress to repair damage or trigger mitophagy in order to restore function and protect the cell [198]. Mitophagy is a form of macroautophagy that reverses mitochondrial dysfunction by clearing away damaged mitochondria before the cell can activate apoptosis. Even though dysfunctional mitochondria initiate mitophagy, alcohol has been shown to prevent its completion. In a study of SIV (simian immunodeficiency virus) -infected macaques administered chronic binge doses of alcohol, muscle samples showed upregulated expression of mitophagy-related genes in SIV infection alone but downregulation of these genes and increased expression of pro-apoptotic genes when alcohol was introduced [199]. Mitophagy is disrupted when the defective mitochondria are prevented from being trafficked to lysosomes for degradation. In neurons, the combination of HIV-1 infection and alcohol use may cause mitochondrial dysfunction and activate mitophagy pathways that eventually get interrupted, then superseded by apoptosis. This

forcing towards apoptosis may either be due to bolstering of activators to rate-limiting enzymes in the apoptosis pathways, inhibition of enzymes in the mitophagy pathways, or both. So far, studies have shown that the root cause may be cell stress from generated ROS and/or defective antioxidant mechanisms [200]. More mechanistic studies involving the competition between mitophagy and apoptosis pathways are necessary. There may be a tug-of-war-like contest between these competing pathways.

1.2.4.7 Decreased food consumption. While there are many studies on HIV-associated wasting, research into the misuse of energy by HIV infected or uninfected cells in the CNS remains scarce. The invasion and multiplication of virus increases daily energy expenditure, therefore someone with HIV/AIDS disease requires more food to compensate for this upregulated metabolic rate [201]. Despite this, HIV-1 infection tends to reduce appetite and, in so doing, slowly deteriorates the nutritional status that, over time, can develop into malnutrition [202]. Even though HAART therapies have been shown to increase appetite, wasting may not be due to decreased energy intake alone. HIV-1 has also been shown to cause malabsorption by reducing intestinal villi numbers as well as increasing susceptibility for contracting gut infections [203]. Ineffective utilization and metabolism of food by the body can perpetuate a negative energy balance and lead to malnutrition. At the same time, malnourishment can compromise the immune system and, with HIV-1, increase immunosuppression and severity of infection [204]. Importantly, body weight depends more so on the composition of the diet, as evident by the varying degrees of malnutrition among HIV/AIDS patients. Alcohol use has been shown to exacerbate wasting [205]. Prolonged consumption of alcohol has been associated with poor

appetite, malnutrition, and vitamin deficiencies (thiamine deficiency can cause Wernicke-Korsakoff syndrome) [206]. Therefore, both late-stage alcoholism and HIV/AIDS become wasting diseases as patients experience skeletal muscle atrophy [207]. Energy misuse may be the perpetrator of this eventual wasting.

1.2.5 HIV-1 infection and alcohol use on oxidative damage, inflammation, and neurodegeneration

HIV-1 does not cause disease through a direct infection of neurons, instead it is predominantly infected resident microglia and perivascular macrophage as well as released HIV-1 proteins that promotes neuroinflammation and neurotoxicity [208, 209]. In this way, the amount of viral burden in the CNS correlates with disease severity and generation of neurotoxins. Alternatively, alcohol can act directly on neurons and alter neurotransmitter systems to cause damage and disease [210, 211]. Therefore, the most studied facets of alcohol consumption and HIV-1 infection have concerned their detrimental effects to brain function and, when co-occurring, the exacerbation of these effects. Oxidative damage, inflammation, and neurodegeneration are interdependent insults to the CNS and, for this reason, the regulation of one can impact the strength of another to either aggravate or alleviate injuries. For example, a study using HIV-1 transgenic rats found neurodegeneration, from activation of apoptosis-inducing pathways and events, following upregulation of nitroxidative stress and elevated inflammation [212]. Different studies have also speculated the reverse, that HIV-1-induced neurodegeneration can produce inflammation through the activation of microglia cells, although direct data to this effect has been scarce [213]. To support this, HIV-1 viral proteins have been shown to induce neurotoxicity alone, independent of an inflammatory response and without affecting viral

replication [214, 215]. This three-way interaction explains the exacerbating effects of HIV-1 infection under alcohol use as a three-way causal relationship between oxidative damage, inflammation, and neurodegeneration. However, oxidative damage and inflammation can still act independently, and each can induce neurodegeneration alone. In a cohort study of HIV-infected patients oxidative stress was a predictor of all-cause mortality regardless of subclinical inflammation [216]. However, with alcohol use, oxidative stress, inflammation, and neurodegeneration are all concomitantly present, and can cooperatively interact to promote HIV-1 infection and disease. Specifically, alcohol use and HIV-1 infection generate oxidative stress, which then impedes proper regulation of the inflammatory response and leads to neurodegeneration.

Glial cells, excessively activated from both infection and unhealthy alcohol use, ROS/RNS, proinflammatory factors, and other potential cytotoxic molecules to induce oxidative stress [217]. HIV-1 protein Tat has been shown to stimulate calcium release from inositol 1,4, 5-trisphosphate sensitive intracellular stores and activate protein kinase C isoforms to produce the cytopathic cytokine tumor necrosis factor alpha while gp120 can enhance microglia outward K(+) current to cause secretion of more neurotoxins [218-220]. Potassium fluctuations have been shown to affect mitochondrial membrane potentials that can affect neuronal death downstream [221]. Inhibition of microglial/macrophage activity abrogated neurodegeneration caused by activation of their chemokine receptors; however this did not prevent stromal cell-derived factor 1-induced neurotoxicity since this chemokine may be acting directly on neuron and astrocyte cells [222]. Alcohol-induced oxidative stress is associated with overproduction of ROS/RNS and impairment of antioxidant mechanisms during ethanol metabolism [223]. Persistent accumulation of this

ROS/RNS can contribute to immune dysfunction by affecting lipid raft mechanisms and antigen presentation, diminished proteasome activity and immunoproteasome contents by disrupting the prooxidant/antioxidant balance, as well as cellular protein inactivation and oxidative DNA damage that can lead to mutations and interruptions in functions such as glycolysis and OXPHOS [224, 225]. It is the presence of an unpaired electron that causes ROS/RNS to be highly reactive to all molecules inadvertently damaging them. In their role, alcohol and HIV-1 infection act as stress factors to increase ROS/RNS production. Microglia respond to this stress by adopting a pro-inflammatory, M1, phenotype to elicit a neuroinflammatory response. Once inflammation subsides, microglia shift to an anti-inflammatory, M2, phenotype to stop immune activation and promote recovery [226]. The persistent stress induced by HIV-1 infection and alcohol use may prevent inflammation from decreasing and inhibit M1 microglia from polarizing to M2 microglia, or this stress may lead M2 microglia to revert to the M1 phenotype. However, microglia have been shown to still scavenge during inflammation, done largely by M2b and M2c microglia [227]. It is not known whether this phagocytosis is activated because of an intrinsic defect or as a pathological response. More research is required on the effects of HIV-1 infection and alcohol use on microglia polarization.

The primary mechanism for protecting the CNS from alcohol use and HIV-1 infection mediated insults is the neuroinflammatory response. The combination of these injuries creates enough trauma to result in an uncontrolled, maladaptive neuroinflammatory response that can damage the CNS. Alcohol induces neuroinflammation by activating TLR4 signaling in glial cells and initiating mitogen-activated protein kinase (MAPK) induction of the nuclear factor κB (NF-κB), a key

regulator of inflammation [228]. Concomitant HIV-1 infection also leads to NF-κB mediated neuroinflammation but as a result of the phosphorylation of cytosolic phospholipase A2 (cPLA2) [229, 230]. Alcohol can also enhance the neuroinflammation present under HIV-1 infection by augmenting glial activation and increasing oxidative stress while reducing elimination of infected cells [231]. Inflammatory reactions can further release toxins to feed-forward the neuroinflammatory response and exacerbate it. The consequences of a chronic neuroinflammatory response are an excess production of ROS/RNS, proinflammatory cytokines/chemokines, and other inflammatory intermediaries that can cause neuronal damage [232]. Co-occurring alcohol and HIV-1 infection may disturb or impair resolution of this neuroinflammatory response and create a state of persistent neuroinflammation that can lead to inflammation-associated pathologies and neurodegeneration. For these reasons, reducing neuroinflammation is the target of most therapeutic approaches aimed at ameliorating neurological disorders including HAND [145]. In addition, there is a metabolic cost to neuroinflammation that can unbalance the amount of available energy. Chronic neuroinflammation may reduce the energy pool and cause cells to shift towards processes that require less energetic investment such as aerobic glycolysis in replacement for the less energy efficient oxidation phosphorylation. Inflammation is a response that is consistently present in both alcohol use and HIV-1 infection and, as such, many be involved in sustaining their detrimental effects.

The short-run effects of oxidative stress and inflammation can lead to neurodegeneration that can cause long-term neurological complications and loss of brain function [233]. Multispectral imaging microscopy of humanized NOD/scid-IL-2Rγcnull mice transplanted with human CD34-positive hematopoietic stem cells showed loss of the

microtubule-associated protein 2, synaptophysin, and neurofilaments after HIV-1 infection [234]. As survival continues to improve, occupancy of the virus in the CNS increases and, accordingly, so do the amounts of released neurotoxic metabolites. However, suppressed viral levels have not been shown to arrest active HIV-related injury, therefore other neurochemical irregularities may be involved in continued neurodegeneration [235]. Neuronal progenitor cells are especially susceptible to ethanol-induced damage. Prenatal exposure to ethanol has been shown to reduce hippocampal somatostatin and brain-derived neurotrophic factor (BDNF) levels, two important supporters of neuronal survival and synaptic growth [236]. Adolescent drinking has led to long-term decreases in pro-BDNF, a precursor to BDNF [237]. Deficits in neurotrophin signaling have been associated with early alcohol exposure-derived effects on cognition [238]. BDNF has been shown to reduce the degeneration of neuronal synapses caused by HIV-1 TAT and gp120. BDNF protects synapses by enhancing mitochondrial health and preventing their alteration by these viral proteins [239]. Presence of both alcohol and HIV-1 infection exacerbates neurodegeneration by decreasing vital levels of BDNF.

The combination of drugs used to treat HIV-1 infection, HAART, have also been associated with several risks. Lifelong treatment with HAART can dispose a person to opportunistic infections as well as cardiovascular diseases, kidney diseases, and decreases in bone mineral density [240]. Other studies have also reported drug-related neurotoxicity associated with HAART. By only suppressing viral load and not fully eliminating the virus, HAARTs only improve quality of life. However, even with successful HAART, HIV-associated neurological disorders persist, especially neuropsychological deficits [241]. This can be seen clinically by the manifesting neurocognitive disorders and impairments,

brain size and volume deficits, and progression of the infection into AIDS. What with impeding energy uptake and shifting energy trafficking, HIV-1 may be upsetting neuronal energy balance and, in so doing, causing further neurodegeneration. In a study of elite controllers, loss of spontaneous virologic control was attributed to increased aerobic glycolytic metabolism, oxidative stress, immune activation, and dysregulation of mitochondria function, all of which are involved in maintaining homeostatic energy balance [242]. Alcohol can exacerbate neurodegeneration by further coercing these processes.

1.2.6 Possible mechanism(s) for accelerated HIV neuro-infection progression in alcohol use

Previous research has established that alcohol aggravates HIV-1 progression, however this does not explain the accelerated progression of HIV neuro-infection. The exacerbating effects of alcohol on HIV-1 infection as well as the role both play at unbalancing metabolic energy suggests alcohol may have a more severe impact on disease progression [111]. That is, alcohol is not just a co-factor in progression, but an active participant. Alcohol-mediated deprivation of glucose to the brain parenchyma reduces energy for cells [116]. Additional total energy reductions are caused by disruption to nutrient metabolic pathways [202]. Depletion of glucose by alcohol and energy wasting by HIV-1 infection can interrupt the energy supply to a point where demand exceeds supply and leads to a state of malnutrition in the CNS environment. I propose this resulting state of malnutrition as a mechanism for accelerated HIV-1 progression.

Competition for energy between cells becomes complex as supply decreases. It is to the advantage of microglia to receive the most energy in an effort to fulfill their

protective function, with HIV-1 infection, energetic demand is intensified to sustain infection [171]. Alcohol further promotes demand by acting as a stimulant to increase cellular metabolism [243]. Highly energy demanding cells like neurons, further stimulated by oxidative stress produced by alcohol and neurotoxins released by HIV-1 infection and antiviral treatment, undergo neurodegeneration [244]. Alternatively, infected microglia may resort to scavenging for energy and, in this way, infected microglia hijack the energy utilization during interruption of energy supply. I postulate that when metabolic reprogramming of infected microglia renders them reactive and subsequently deficient in biosynthetic precursors, in this now nutrient deprived environment these infected microglia resort to an ingestion of any available energy [245].

1.2.7 Conclusion

This chapter presented current knowledge of HIV-1 infection and alcohol use on the energetic interplay in the CNS. A hallmark of HIV-1 infection in the CNS is the sustained activation of immune cells with subsequent high metabolic energy utilization by infected neuroimmune cells in the brain, with at-risk alcohol use, where the exacerbated brain environment demands an increased supply of energy needed to maintain homeostasis. Unfortunately, both alcohol use and HIV-1 infection deter the uptake of glucose into the CNS and cause a significant depletion of this CNS energy source. Thus, metabolic shifts are expected following HIV-1 infection in alcohol use as indicated by neuropathological evidence. I postulated that the comorbidity of HIV-1 infection and alcohol consumption might likely cause a redistribution of energy metabolism. Specifically, when there is shortage of nutrients supply during HIV-1 infection and alcohol use, the paradigm shift of

energy wasting in infected cells and malnutrition in non-infected cells is likely to accelerate HIV neuro-infection progression in alcohol abuse (**Figure 1.1**). Treatment strategies must consider alleviating this energy imbalance in order to help impede progression of HIV-1 disease and alcohol associated neurological disorders.

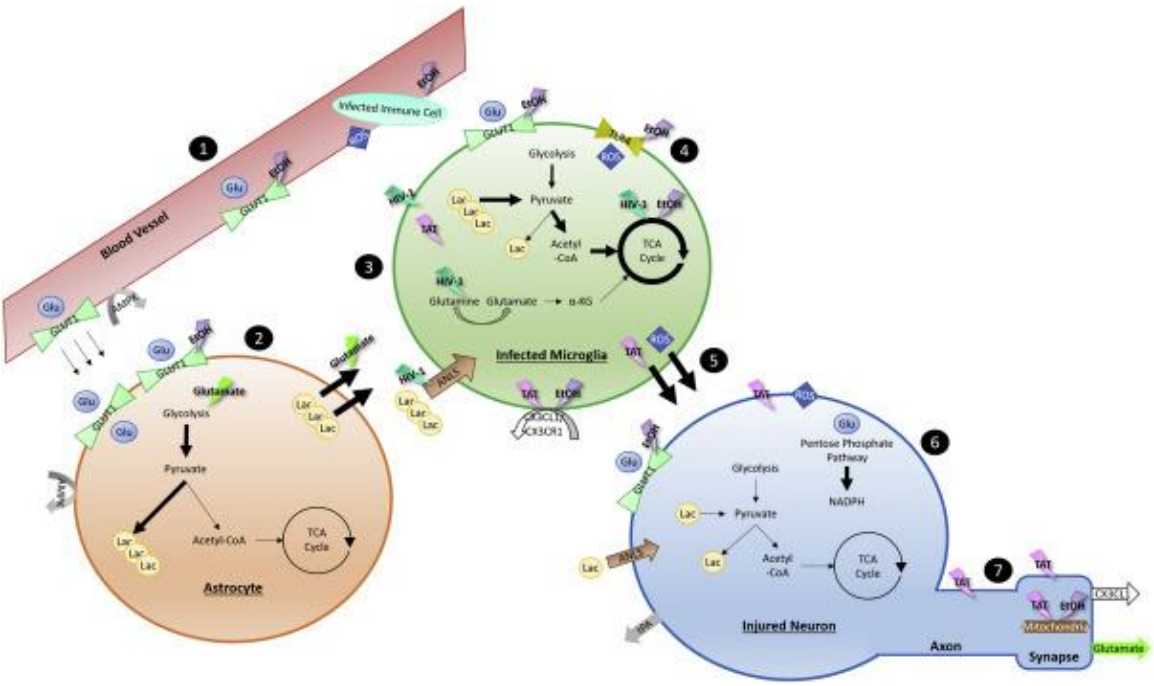

Figure 1.1 Schematic of disrupted neuroenergetics. Alcohol use reduces total available energy while infection renders microglia highly active. It is to the advantage of the CNS to concentrate its energy supply to microglia, consequently, deprived of energy, neurons deteriorate. (1) Alcohol and HIV-generated RNS/ROS disrupt the BBB and GLUT1, this permits entry of infected cells into the CNS but impedes glucose uptake [66, 116]. (2) AMPK, glutamate, and neuronal activity increases astrocytic glycolysis and lactate production [118, 159, 163]. (3) HIV-1 infected microglia require more shuttling of lactate for energy and the use of alternative energy sources [83, 116, 142]. (4) Alcohol triggers TLR4 signaling for further microglial activation and ROS/RNS production [228]. (5) ROS/RNS and TAT accumulation released from infected microglia cause neuronal damage [194, 246]. (6) Any glucose absorbed by neurons is used to produce biosynthetic precursors while lactate shuttled from astrocytes is used for energy [155, 159]. (7) ROS/RNS and TAT disrupt mitochondrial stability and synaptodendritic functions of neurons as well as the removal of these damaged neurons. Signaling to neighboring neurons may spread injury and lead to massive neurodegeneration [172, 178, 194].

CHAPTER 2

SYNERGISTIC EFFECTS OF ALCOHOL AND HIV TAT PROTEIN ON MACROPHAGE MIGRATION AND NEUROTOXICITY

This chapter represents my first aim where I looked at the effects of alcohol and HIV-associated injury on neuroinflammation by way of macrophage migration across an in vitro model of the blood-brain barrier. This work is under review in the *Journal of Neuroimmunology* as of July 2021. My co-authors, Ricardo Garcia, Jagathi Kalluru, Brooke Leiser, James Haorah, assisted me with the experiments and data acquisition.

2.1 Introduction

The trans-activator of transcription (TAT) is a regulatory protein found in HIV-1 that greatly enhances viral transcription. After serving its purpose, TAT is actively sloughed by infected cells as a byproduct of the infection. In the presence of ethanol, TAT-induced toxicity has been shown to potentiate. In a study of calcium responses in cultured neurons, short exposure to 50 mM ethanol increased the fast-onset, short-lasting calcium overload elicited by 10 mM TAT and the slow-onset, sustained calcium overload elicited by 500 mM TAT [247]. A study involving treatment of neuronal cells with combined 100 ng/mL TAT or 100 ng/mL gp120, another toxic viral protein, and 16.7, 50, or 83 mM EtOH found increased expression of death receptor and N-methyl-D-aspartate (NMDA) receptor-related programmed cell death pathways [248]. In vivo studies with intracerebral injection of 25 μg/μL TAT and intraperitoneal injections of 3 g/kg ethanol confirmed these results [249]. Even after its withdrawal, EtOH still caused marked potentiation of TAT concentrations as low as 0.1 nM [250]. Up to now, studies of TAT and ethanol exposure

involved moderate to high doses of alcohol usually found in binge drinking or alcoholism. Although many people living with HIV-1 (PLWH) abuse substances such as alcohol, others may be classified as casual drinkers who consume 1-3 drinks at a given time and have blood alcohol concentration (BAC) below the legal drinking limit. Therefore, there is a gap in knowledge on the effects of low dose alcohol under HIV-associated injury.

Central nervous system (CNS) inflammation is a common feature of HIV-1 infection even in the absence of detectable viral loads [208]. Alcohol consumption does not appear to affect viral load even for viral suppression [251]. Neuroinflammation under alcohol use has been shown to involve infiltration of peripheral macrophage [252]. As key egression cells of the body, macrophage may be migrating the blood brain barrier (BBB) under HIV-associated injury and, with low dose alcohol, this migration may be potentiated. This study used an in vitro blood brain barrier model to examine the role of ethanol and TAT injuries, along with the combination, on macrophage infiltration. Specifically, I resolved to observe migratory effects under low doses of ethanol with TAT concentrations found in PLWH who have achieved viral suppression as well as those on antiretroviral drugs who have been unsuccessful at suppressing detectable viral loads and replication. In so doing, I study the effects of casual drinking on PLWH under the currently best possible clinical outcome.

2.2 Methods and Materials

2.2.1 Reagents

Rat brain microvascular endothelial cells (#R1000) and rat astrocyte cells (#R1800) along with rat endothelial cell medium (#1021), bovine plasma fibronectin (#8248) and astrocyte

medium (#1831) were purchased from ScienCell. Rat macrophage colony stimulating factor (#300-523P) was purchased from Gemini. Poly-D-lysine hydrobromide (#P7280), lipopolysaccharides from Escherichia coli O127:B8 (#L4516), Evans Blue dye (#E2129), and absolute ethanol were purchased Sigma. B-27 Supplement (50X), serum free (#17504044), neurobasal medium (#21103049), CellTracker red CMTPX dye (#C34552), and MTT (3-(4,5-dimethylthiazol-2-yl)-2,5-diphenyltetrazolium bromide) (#M6494) as well as Alexa Fluor secondary antibodies were purchased from Thermo Fisher. S-nitroso-N-acetyl-D,L-penicillamine (SNAP) (#82250) was purchased from the Cayman Chemical Company. Anti-neurofilament antibody (#ab24574) and anti-caspase-3 antibody (ab32351) were purchased from Abcam. The 6.5 mm transwell with 3.0 μm pore polycarbonate membrane inserts (#3415) were purchased from Corning. The HIV-TAT protein was generously donated by Professor Eliseo Eugenin.

2.2.2 Cell culture

2.2.2.1 Astrocyte and endothelial cells. Astrocyte and rat brain microvascular endothelial cells (RBMEC) were cultured according to manufacturer's recommendations. Briefly, cryopreserved astrocytes were seeded on a 2 μg/cm2 poly-D-lysine-coated flask to initiate the culture. Confluent cultures were further expanded for 3 population doublings. Finally, astrocytes were harvested for transwell culture. Cryopreserved RBMECs were seeded on a 2 $\mu g/cm^2$ fibronectin-coated flask to initiate the culture. Similarly, confluent cultures were further expanded for 3 population doublings. Finally, RBMECs were harvested for transwell culture.

2.2.2.2 Neurons. Primary neuronal cells were obtained by neuronal isolation as we have previously described [253, 254]. Briefly, cortices were removed from the embryos of a Sprague Dawley timed pregnant rat (Charles River) 16 days post gestation. Cortices were washed with sterile PBS, mechanically agitated with a pipette, and strained through a 40 μm pore filter to extract neurons. Neurons were seeded in 20 μg/mL poly-D-lysine (PDL) coated wells at a density of 50,000 cells/cm^2 and cultured in complete neurobasal medium containing neurobasal media, 2% B-27 antioxidant supplement, 1% penicillin-streptomycin, and 0.2% L-glutamine for 7 days.

2.2.2.3 Macrophage. Primary macrophage cells were derived from bone marrow and differentiated in vitro in the presence of macrophage colony-stimulating factor (M-CSF) [255]. Briefly, the femurs and tibia of euthanized rats were removed intact, cleaned of excess muscle, and washed with 75% ethanol. Inside a cell culture hood, bones were severed proximal to each joint and the shafts were flushed with PBS. Cells were centrifuged to remove PBS and resuspended in macrophage differentiating medium containing DMEM, 0.2% gentamicin, 1% L-glutamine, 10% fetal bovine serum, 10 μg/mL ciprofloxacin, and 20 ng/mL M-CSF. Cells were seed at a density of 10,000 cells/cm^2 and cultured for 7 days. On day 7 macrophage became fully differentiated and macrophage differentiating medium was replaced with medium not containing M-CSF. Macrophage were stimulated to an M1 or pro-inflammatory phenotype with lipopolysaccharide (LPS)-activation [256]. Only pro-inflammatory macrophage have been shown to cross the BBB. Briefly, a suspension of 100,000 macrophage cells were incubated with a 1:500 dilution of 0.1 mg/mL LPS for 4 hrs. After LPS stimulation, macrophage undergo a morphological

change and begin releasing macrophage-derived cytokines into the medium. Prior to adding them to the transwell, stimulated macrophage cells were labeled with CellTracker Red CMTPX fluorescent dye. Briefly, medium was removed and replaced with medium containing 1 μM CellTracker dye. Cells were incubated for 45 mins. under growth conditions after which time medium was removed.

2.2.2.4 BBB models. An interactive coculture model of the BBB involved quad-cultivation of primary RBMECs, astrocytes, neurons, and macrophage cells on a transwell system. The culture of RBMECs/astrocytes on the transwell insert was performed similar to previously described endothelial/astrocyte coculture models [257-259]. First, 3.0 μm pore inserts were filled with 2 μg/cm^2 fibronectin and suspended in a well containing 2 μg/cm^2 poly-D-lysine overnight after which time these solutions were removed. This ensures that the surface of the transwell is coated in fibronectin while the underside is coated with poly-D-lysine. Next, the insert was inverted, and astrocyte cells were seeded at a density of 5,000 cells/cm^2 onto this underside of the transwell insert. Astrocytes were cultured in this manner with medium supplemented every 15 mins. to ensure attachment. After 2 hrs., the insert was inverted back and suspended in a well filled with astrocyte medium. Next RBMECs were seeded at a density of 10,000 cells/cm^2 onto the surface of the transwell insert already holding astrocyte cells. Endothelial cell medium was added to the transwell insert while astrocyte medium remained in the well. This RBMEC/astrocyte transwell was cultured for 7 days. After 7 days, this RBMEC/astrocyte transwell was suspended over a culture of primary neuronal cells that have also been in culture for 7 days. Finally, the RBMEC medium in the insert was removed and replaced with fluorescently

labeled, stimulated macrophage cells suspended in medium free of phenol red. The medium in the well was also replaced with phenol red free medium. This coculture model was then immediately used for experiments.

The effects of ethanol and TAT injuries on macrophage migration was observed by modification of this base interactive BBB model. 0, 10, 20, or 50 mM ethanol was added to the apical (RBMEC) side of the insert for an EtOH-BBB model and examination of ethanol injury in the vasculature. Heat-inactivated, 5 ng/mL, 25 ng/mL, or 50 ng/mL TAT was added to the basolateral (neuron) side of the insert for a TAT-BBB model and examination of HIV-associated injury in the CNS. Simultaneous addition of 10 mM ethanol to the apical and 5 ng/mL or 25 ng/mL TAT to the basolateral sides of the insert was used for an EtOH-TAT-BBB model and examination of combined ethanol and HIV-associated injuries.

2.2.3 Evans blue extravasation

2% (w/v) Evans blue dye was prepared in phenol red-free medium [260]. This solution was added to the apical side of the transwell BBB model with or deficient of a cell coculture as well as injury by treatment with apical 50 mM ethanol for 24 hrs. 20 μL of medium from the basolateral side was collected a read on a plate reader at 620 nm excitation/680 nm emission. Percentage of Evans Blue permeation was calculated by a standard curve assay of Evans Blue dye.

2.2.4 Nitric oxide measurement

Cells cultured in the wells of a 24-well plate were treated with 0, 10, 20, or 50 mM ethanol and examined for NO production. NO was measured in real time with a World Precision Instruments Free Radical Analyzer TBR4100/1025. First, the ISO-NOP NO probe was polarized in a solution of copper chloride for 12 hrs. or until the current reached a steady baseline value. Next a calibration curve was created by decomposition of SNAP because SNAP corresponds to equivalent NO concentration. Briefly, increasing concentrations of SNAP were sequentially injected into the copper chloride solution and signal output (pA) was plotted against SNAP concentration (nM) to construct the curve. Measurement of NO release by cells was performed by inserting the NO probe directly into the culture for several minutes or until the response reached a plateau. Finally, this redox current was converted to NO concentration using the calibration curve.

2.2.5 Cell viability assay

The viability of neuronal cells exposed to HIV-TAT protein concentrations and RBMECs exposed to ethanol doses was determined with an MTT assay. Actively respirating cells convert MTT dye to purple formazan. Cells were cultured in the wells of a 96 well plate under appropriate growth conditions. The medium from each well was aspirated and replaced with medium containing 5 mg/mL MTT solution. Plates were incubated for 4 hrs. at 37^{o}C after which time the solution was removed and replace with dimethyl sulfoxide (DMSO). Plates were left to stand for 15 mins. at room temperature before reading by a plate reader at 570 nm. Percentage of viable cells was calculated by a standard curve assay.

2.2.6 Immunofluorescence and imaging

Primary neuronal cells were cultured on coverslips pre-coated with poly-D-lysine solution. Following 7 days in culture, neurons were exposed to TAT with or without presence of ethanol for 24 hrs, after which time cells were stained for expression of neurofilament and caspase-3 protein. Prior to staining, phase contrast images of these cells were captured with a Leica DMi1 inverted microscope. Briefly, cells were fixed onto the coverslips with 4% paraformaldehyde and permeabilized with 0.4% Triton X-100. Nonspecific antigen binding was blocked with incubation with 5% bovine serum albumin at room temperature for 1 hr. in the presence of 0.4% Triton X-100. Cells were incubated with mouse anti-neurofilament (1:200 dilution) and rabbit anti-caspase-3 (1:250 dilution) at 4^{o}C overnight. After washing with PBS, cells were incubated with goat anti-mouse IgG Alexa Fluor 594 (1:400 dilution) and goat anti-rabbit IgG Alexa Fluor 488 (1:400 dilution) at room temperature for 1 hr. Finally, coverslips were mounted onto glass slides with mounting medium containing DAPI. Fluorescent images were acquired with an Olympus IX81 inverted epifluorescence microscope.

2.2.7 Statistical analysis

Results were analyzed using two-way mixed-design analysis of variance (ANOVA), with a within-subjects factor of time (6 levels) and a between-subjects factor of EtOH or TAT concentration (3-4 levels). This allowed testing for a significant effect of individual groups as well as any possible interactions. Next, one-way ANOVA was performed to determine whether there were any statistically significant differences between the times as well as EtOH or TAT concentrations. Statistically significant results indicated that not all the

means in the group were equal and, thus, were further analyzed with post hoc Tukey's Honest Significance tests for multiple comparisons of pairs. In both the bar and line graphs, data are presented as mean ± standard error from the mean (SEM). The threshold for statistical significance was $p \leq 0.05$ (* $p \leq 0.05$, ** $p \leq 0.01$ and *** $p \leq 0.001$). Statistical analysis was performed using the Rcmdr package of R software [261].

2.3 Results

2.3.1 An interactive in vitro model of the blood-brain barrier

To examine the effects of ethanol and TAT exposure on macrophage infiltration in vitro I developed an interactive coculture model of the BBB. For the diffusion barrier portion of the model, I used a modified version of previously described endothelial/astrocyte coculture models [96]. These models utilize a transwell system to create a chemokine concentration gradient and simulate a chemotactic environment. Primary astrocyte cells were seeded (5,000 cells/cm^2) on the underside of a 3 μm pore 24-well plate transwell insert coated in poly-D-lysine. Next, primary brain microvascular endothelial cells were seeded (10,000 cells/cm^2) on the opposite, upper side of the same insert coated in bovine plasma fibronectin. This transwell coculture was then immersed in a well containing culture medium and grown to confluency. I developed this model further by suspending the transwell coculture over primary neurons (50,000 cells/cm^2) cultured for 7 days in the wells of a 24-well plate coated in poly-D-lysine (**Figure 2.1.B**). Then I added 40,000 fluorescently labeled, M1 polarized macrophage to the apical side of the transwell insert (**Figure 2.1.A**).

Evans blue dye extravasation was performed to determine the integrity of this in vitro model because Evans blue cannot normally pass through the BBB. Penetration to the basolateral side of the insert was examined with and without the inclusion of a cells. Model efficacy was tested by injuring cells to a degree that would allow for increased Evans blue penetration. Injury was induced by treating the endothelial cells (apical side) with 50 mM ethanol for 24 hrs. Protein expressions of tight junction proteins claudin-5, occludin, and ZO-1 have been shown to be markedly decreased after 24 hrs. treatment with 50 mM ethanol while cell viability remains unchanged. An analysis of variance on percentage of Evans blue penetration revealed significant variation among conditions ($p<0.001$). A post hoc Tukey's Honest Significance test showed that a coculture of cells significantly decreases Evans blue movement ($p<0.001$) even when the model is injured ($p<0.001$). However, the injury itself did not cause a significant increase in penetration ($p=0.003$) (**Figure 2.1.C**). Therefore, this model provides an appropriate response and an in vitro representation of the BBB.

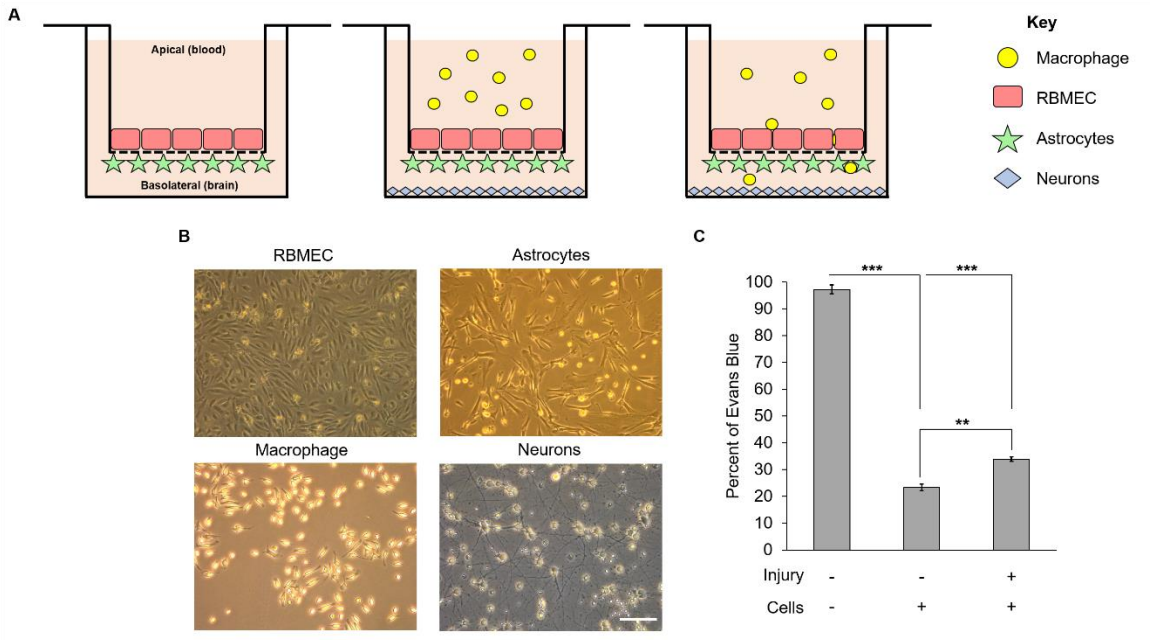

Figure 2.1 In vitro model of the BBB. A) Cartoon depicts coculture of macrophage, RBMECs, astrocytes, and neuron cells. Left image: RBMECs were seeded on the surface of a 3 μm pore transwell insert while astrocytes were seeded underneath. Middle image: This transwell coculture was suspended over neurons in a 24-well plate. Finally, fluorescently labeled stimulated macrophage in suspension were added to the apical side of the insert. Right image: The model was challenged with ethanol concentrations on the apical side, TAT concentrations on the basolateral side, or both. Migration of macrophage was then observed. B) Images of the different cell types used in the model. White bar represents 100 μm. C) Percentage of Evans Blue dye able to reach the basolateral side of the insert. Penetration was examined with and without the inclusion of a cell coculture as well as injury by treatment with 50 mM ethanol for 24 hrs. Results are presented as mean values (±SEM, N = 3 individual transwell models). Significant difference is indicated by ** $p \leq 0.01$ and *** $p \leq 0.001$.

2.3.2 Ethanol and TAT increase macrophage migration in a time dependent manner

Ethanol injury was performed on the apical side of the transwell BBB model to replicate alcohol circulation in the vasculature. The RBMECs were treated with either PBS (vehicle), 10 mM, or 20 mM ethanol. In the neurobiology, ≤ 10 mM ethanol represents low doses or concentrations below the legal driving limit (< 0.08% BAC or < 17.5 mM) while ≥ 20 mM represents moderate doses or concentrations above the legal driving limit (> 0.08% BAC or > 17.5 mM) [262]. TAT injury was performed on the basolateral side to

replicate sloughing of TAT protein by infected microglial cells into the CNS. The neurons were treated with either heat-inactivated, 5 ng/mL, or 25 ng/mL TAT concentrations. In the CSF of PLWH, TAT concentrations of 200 pg/mL to 6.5 ng/mL are found in those virally suppressed on antiretroviral therapy while concentrations ranging from 10-1000 nM (≈16 ng/mL to 1.6 μg/mL) are found in those with detectable levels of the virus regardless of therapy adherence [263, 264]. Therefore, 5 ng/mL was chosen to represent a suppressed status and 25 ng/mL was chosen to represent a non-suppressed status.

Macrophage migration was observed at 0, 2, 4, 8, 24, and 48 hrs. post-treatment by a fluorescent plate reader. Prior to reading, the suspension of fluorescently labeled macrophage on the apical side of the insert was gently removed and replaced with PBS. The detector of the reader was located below the plate to allow for bottom-up read measurements and simultaneous detection of macrophage at the bottom of the well, in suspension on the basolateral side of the insert, and actively traversing the barrier. Number of macrophage cells was calculated by a standard curve assay of fluorescently labeled macrophage. To confirm migration, images of infiltrated macrophage at 48 hrs. were also captured with a fluorescent microscope.

A two-way mixed design analysis of variance showed a significant effect of time ($p<0.001$) and dose ($p<0.001$) but no time-dose interaction ($p=0.519$) on macrophage migration in the EtOH-BBB model. EtOH significantly affected migration of macrophage at 24 hrs. ($p=0.042$) and 48 hrs. ($p=0.014$). A post hoc Tukey's Honest Significance test showed significant migration to 10 mM EtOH treatment at 48 hrs. ($p=0.027$) and to 20 mM EtOH treatment at 24 ($p=0.044$) and 48 hrs. (0.018) (**Figure 2.2.A**). These results reveal

that EtOH injury induces macrophage migration at late timepoints. There was no significant difference in migration between 10 mM and 20 mM EtOH treatment.

Similarly, a two-way mixed design analysis of variance showed a significant effect of time ($p<0.001$) and concentration ($p<0.001$) but no time-concentration interaction ($p=0.988$) on macrophage migration in the TAT-BBB model. TAT significantly affected migration of macrophage at 0 hrs. ($p<0.001$), 2 hrs. ($p=0.014$), 4 hrs. ($p=0.003$), 8 hrs. ($p=0.022$), 24 hrs. ($p=0.022$), and 48 hrs. ($p=0.013$). A post hoc Tukey's Honest Significance test showed significant migration to 5 ng/mL TAT treatment at 0 ($p<0.001$), 2 ($p<0.05$), and 4 hrs. ($p<0.01$) and to 25 ng/mL TAT treatment at 0 ($p<0.001$), 2 ($p<0.05$), 4 ($p<0.01$), 8 ($p<0.05$), 24 ($p<0.05$), and 48 hrs. ($p<0.05$) (**Figure 2.2.B**). These results reveal that TAT injury induces macrophage migration at early timepoints. There was no significant difference in migration between 5 ng/mL and 25 ng/mL TAT treatment. Time significantly affected migration of stimulated macrophage regardless of treatment condition for both the EtOH-BBB and TAT-BBB models (**Figure 2.3**). A post hoc Tukey's Honest Significance test observed no significance of time up to 4 hrs. This suggests that time is a greater determinant of migration performance than either ethanol dose or TAT concentration.

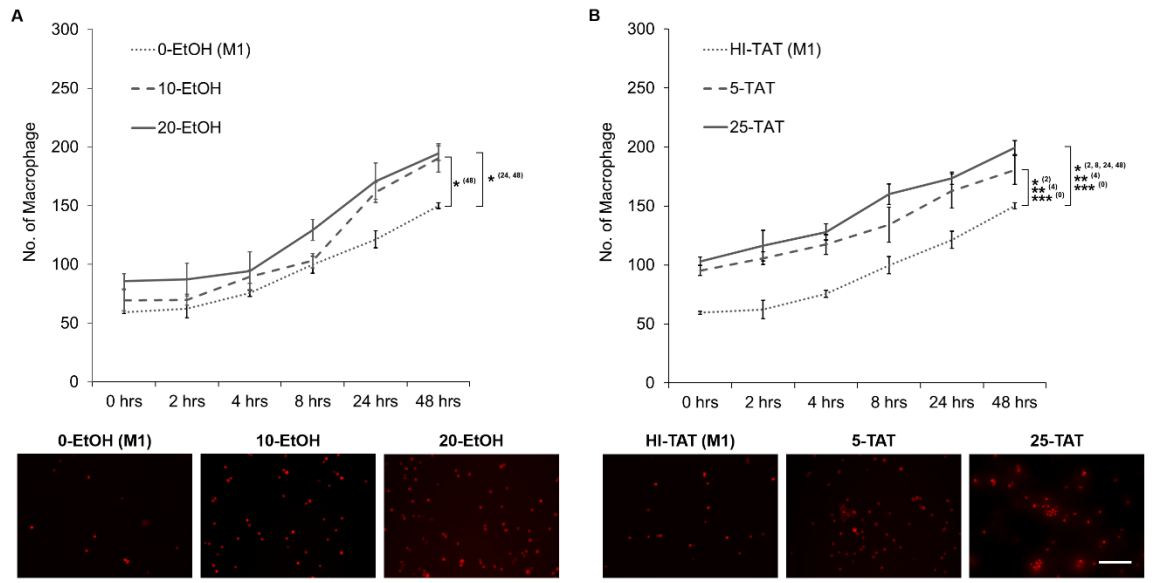

Figure 2.2 Macrophage migration after treatment with ethanol or TAT concentrations alone. A) Only the apical side of the model was treated with 0, 10, or 20 mM ethanol. B) Only the basolateral side of the model was treated with heat-inactivated, 5 ng/mL, or 25 ng/mL TAT. A and B) Macrophage migration was observed at 0, 2, 4, 8, 24, and 48 hrs by a fluorescent plate reader. Bottom panels are representative images of infiltrated macrophage at 48 hrs. White bar represents 100 μm. Results are presented as mean values (±SEM, N = 3 individual transwell models). Brackets designate treatment groups being compared. Superscript describes timepoint compared. Significant difference is indicated by $* p \leq 0.05$, $** p \leq 0.01$ and $*** p \leq 0.001$.

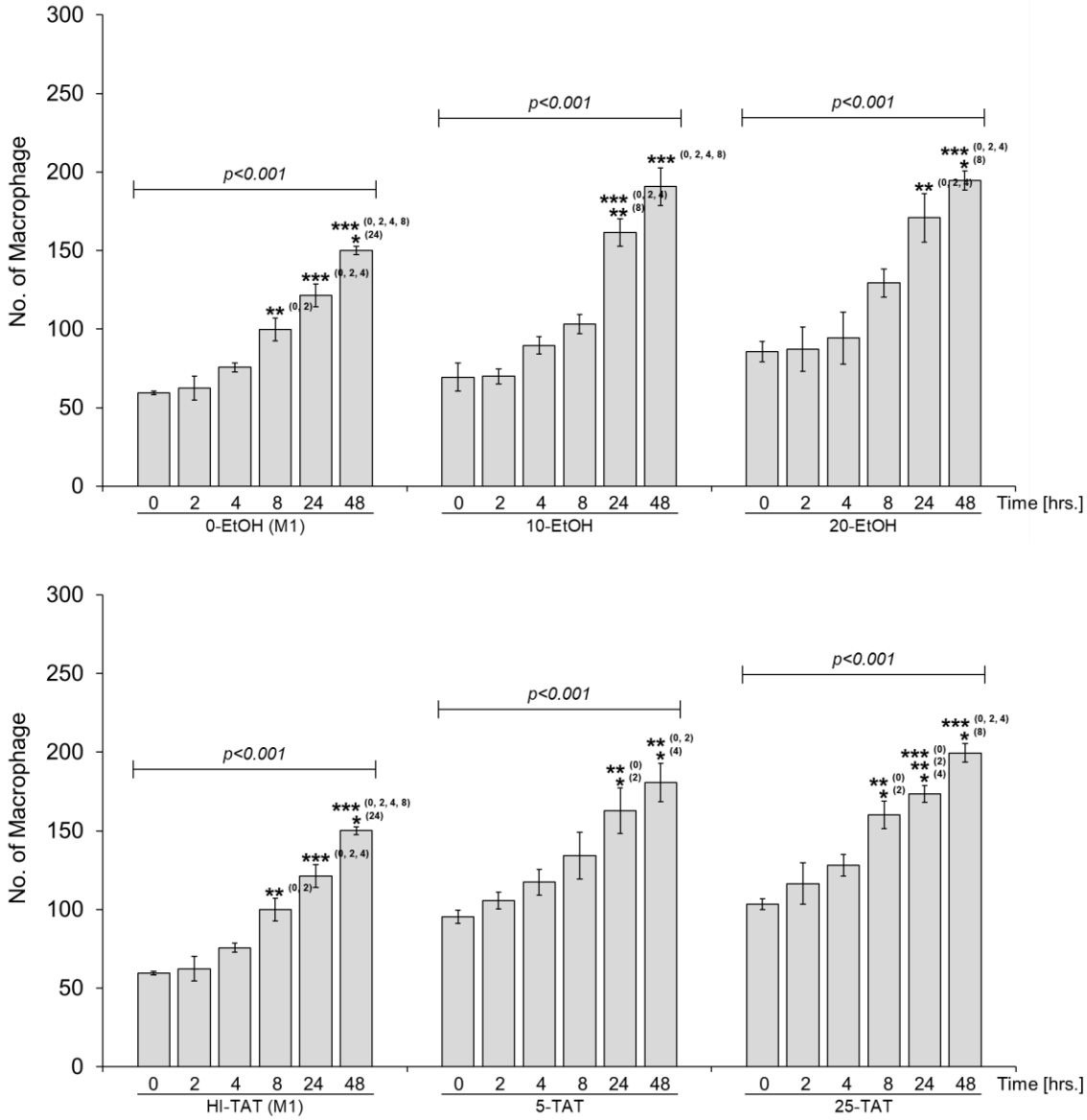

Figure 2.3 Effect of time on macrophage migration. Graphs plot number of infiltrating macrophage cells for each timepoint of a treatment condition. Graphs compliment those found in **Figure 2.2**. Results are presented as mean values (±SEM, N = 3 individual transwell models). Superscript describes timepoint compared. Significant difference is indicated by $* p \leq 0.05$, $** p \leq 0.01$ and $*** p \leq 0.001$

2.3.3 Combined presence of low dose ethanol and TAT increases migration across all timepoints

Co-presence of ethanol and TAT injuries was explored to observe the combined effect on macrophage migration. 10 mM dose was chosen for ethanol injury while 5 ng/mL or 25

ng/mL concentration was chosen for TAT injury. This combination investigates macrophage infiltration in PLWH with and without viral suppression who occasionally drink alcohol. The 10 mM ethanol was introduced to the apical side while a TAT concentration was added to the basolateral side of the insert. Stimulated macrophage cells were placed on the apical side and migration was observed at 0, 2, 4, 8, 24, and 48 hrs. A two-way mixed design analysis of variance showed a significant effect of time ($p<0.001$) and treatment ($p<0.001$) as well as a time-treatment interaction ($p=0.025$) on macrophage migration in this EtOH+TAT-BBB model. EtOH+TAT significantly affected migration of macrophage at 0 hrs. ($p=0.011$), 2 hrs. ($p<0.001$), 4 hrs. ($p<0.001$), 8 hrs. ($p=0.001$), 24 hrs. ($p<0.001$), and 48 hrs. ($p<0.001$). A post hoc Tukey's Honest Significance test showed significant migration to ethanol with 5 ng/mL TAT treatment at 0 ($p<0.05$), 2 ($p<0.01$), 4 ($p<0.01$), 8 ($p<0.01$), 24 ($p<0.01$), and 48 hrs. ($p<0.001$) and to ethanol with 25 ng/mL TAT treatment at 0 ($p<0.05$), 2 ($p<0.01$), 4 ($p<0.001$), 8 ($p<0.01$), 24 ($p<0.001$), and 48 hrs. ($p<0.001$). Significant migration was also shown in ethanol with 5 ng/mL TAT treatment compared to ethanol with heat-inactivated TAT at 2 ($p<0.05$), 4 ($p<0.05$), 8 ($p<0.01$), and 48 hrs. ($p<0.01$) as well as in ethanol with 25 ng/mL TAT treatment compared to ethanol with heat-inactivated TAT at 2 ($p<0.01$), 4 ($p<0.01$), 8 ($p<0.01$), 24 ($p<0.05$), and 48 hrs. ($p<0.001$) (**Figure 2.4.A**). Therefore, the combination of ethanol and TAT injuries causes significant macrophage migration for all timepoints. There was no significant difference in migration between ethanol with 5 ng/mL and ethanol with 25 ng/mL TAT treatment. As with the EtOH-BBB and TAT-BBB models, time significantly affected migration of stimulated macrophage regardless of treatment condition for the EtOH+TAT-BBB model (**Figure 2.5**).

The dichotomy in significant migration between EtOH and TAT injuries was explored by challenging the BBB model with severe concentrations of ethanol or TAT. The model was treated with 50 mM EtOH on the apical side, 50 ng/mL TAT on the basolateral side, or no treatment on either side of the insert. Migration of stimulated, M1 polarized macrophage was observed at 0, 2, 4, 8, 24, and 48 hrs. post-treatment. A two-way mixed design analysis of variance showed a significant effect of time ($p<0.001$) and treatment ($p<0.001$) as well as a time-treatment interaction ($p<0.001$) on macrophage migration. Treatment significantly affected migration of macrophage at 0 hrs. ($p=0.005$), 2 hrs. ($p=0.009$), 4 hrs. ($p=0.005$), 8 hrs. ($p=0.006$), 24 hrs. ($p=0.004$), and 48 hrs. ($p<0.001$). A post hoc Tukey's Honest Significance test showed significant migration to 50 mM EtOH at 2 ($p<0.05$), 4 ($p<0.05$), 8 ($p<0.01$), 24 ($p<0.01$), and 48 hrs. ($p<0.001$) and to 50 ng/mL TAT at 0 ($p<0.01$), 2 ($p<0.01$), 4 ($p<0.01$), 8 ($p<0.05$), 24 ($p<0.05$), and 48 hrs. ($p<0.001$) (**Fig. 2.4.B**). These results reveal that TAT injury triggers migration first, but after 6 hrs. post-treatment ethanol injury progresses and causes greater migration. The significant migration observed at all timepoints under co-presence of ethanol and TAT may be the combination of an initial TAT effect followed by subsequent ethanol injury. There was no significant difference in migration between 50 mM EtOH and 50 ng/mL TAT treatments. Similar to the EtOH-BBB, TAT-BBB, and EtOH+TAT-BBB model results, time significantly affected migration of stimulated macrophage regardless of treatment condition (**Figure 2.6**).

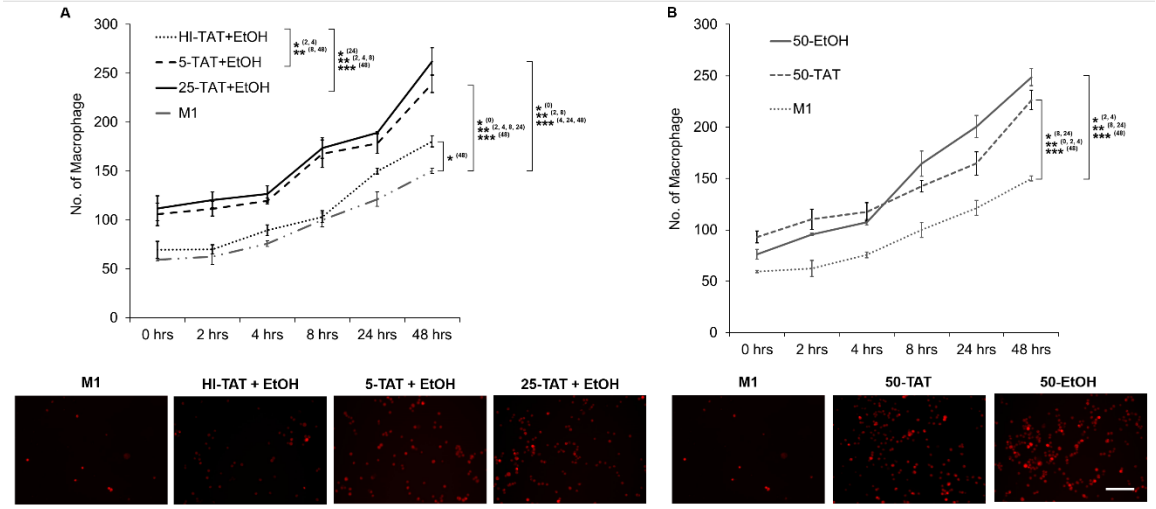

Figure 2.4 A) Macrophage migration following combined treatment 10 mM ethanol with 5 ng/mL or 25 ng/mL TAT. The apical side of the model was treated with 10 mM ethanol and the basolateral side was treated with 5 ng/mL or 25 ng/mL TAT. B) Results of migration to severe ethanol or TAT injuries. The model was treated with apical 50 mM ethanol, basolateral 50 ng/mL TAT, or no treatment, stimulated macrophage only (M1). A and B) Macrophage migration was observed at 0, 2, 4, 8, 24, and 48 hrs by a fluorescent plate reader. Bottom panels are representative images of infiltrated macrophage at 48 hrs. White bar represents 100 μm. Results are presented as mean values (±SEM, N = 3 individual transwell models). Brackets designate treatment groups being compared. Superscript describes timepoint compared. Significant difference is indicated by $* p \leq 0.05$, $** p \leq 0.01$ and $*** p \leq 0.001$.

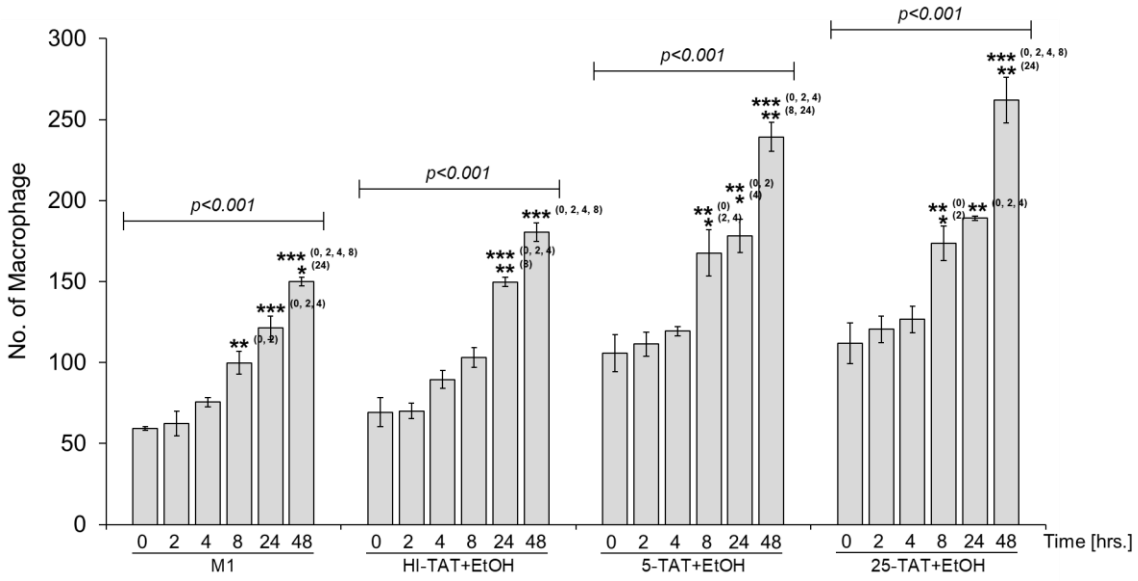

Figure 2.5 Effect of time on macrophage migration. Graph plots number of infiltrating macrophage cells for each timepoint of a treatment condition. Graph compliments **Figure 2.4.A**. Results are presented as mean values (±SEM, N = 3 individual transwell models). Superscript describes timepoint compared. Significant difference is indicated by $* \; p \leq 0.05$, $** \; p \leq 0.01$ and $*** \; p \leq 0.001$.

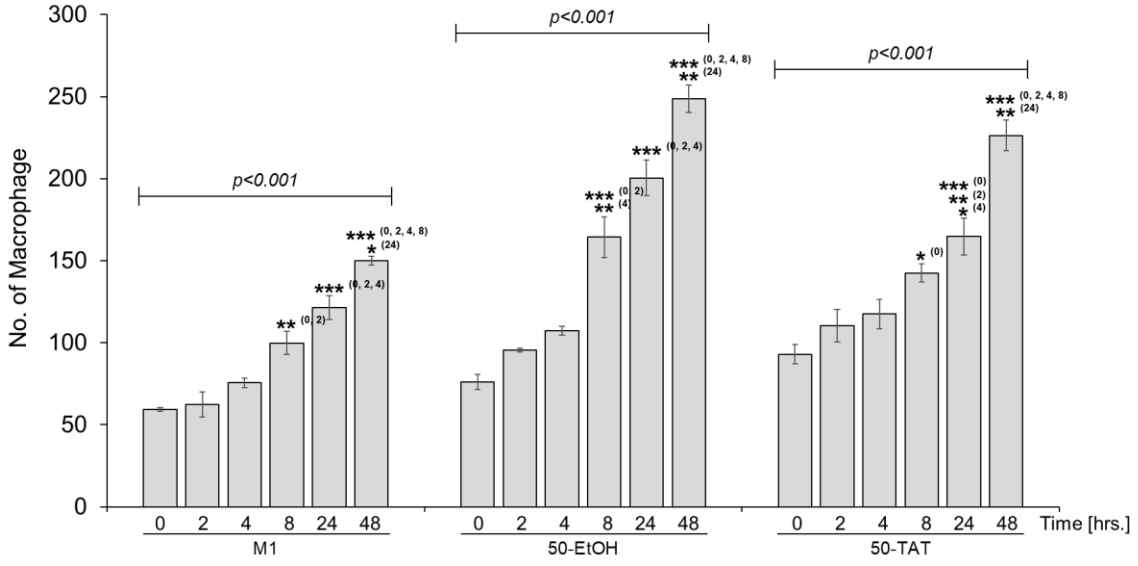

Figure 2.6 Effect of time on macrophage migration. Graph plots number of infiltrating macrophage cells for each timepoint of a treatment condition. Graph compliments **Figure 2.4.B**. Results are presented as mean values (±SEM, N = 3 individual transwell models). Superscript describes timepoint compared. Significant difference is indicated by $* \; p \leq 0.05$, $** \; p \leq 0.01$ and $*** \; p \leq 0.001$.

Results of the EtOH-BBB, TAT-BBB, and EtOH+TAT-BBB models were compared to review and evaluate which treatment produces greatest macrophage migration. A comparison between treatment with 10 mM EtOH, 5 ng/mL TAT, 10 mM ethanol with 5 ng/mL TAT, and no treatment examines PLWH with viral suppression who are causal alcohol drinkers. An analysis of variance showed a significant effect of treatment at 0 hrs. ($p=0.008$), 2 hrs. ($p=0.001$), 4 hrs. ($p<0.001$), 8 hrs. ($p=0.009$), 24 hrs. ($p=0.018$), and 48 hrs. ($p<0.001$). Combined ethanol with 5 ng/mL TAT treatment caused the greatest number of macrophage migration at every timepoint while 10 mM ethanol treatment only instigated significant migration at 48 hrs. and 5 ng/mL TAT treatment only instigated significant migration at 0, 2, and 4 hrs. A post hoc Tukey's Honest Significance test also showed significant migration in 5 ng/mL TAT compared to 10 mM ethanol at 2 ($p<0.05$) and 4 hrs. ($p<0.05$), ethanol with 5 ng/mL TAT compared to 10 mM ethanol at 2 ($p<0.01$), 4 ($p<0.05$), 8 ($p<0.05$), and 48 hrs. ($p<0.05$), and ethanol with 5 ng/mL TAT compared to 5 ng/mL TAT at 48 hrs. ($p<0.05$) (**Figure 2.7.A**). A comparison between treatment with 10 mM EtOH, 25 ng/mL TAT, 10 mM ethanol with 25 ng/mL TAT, and no treatment examines PLWH without viral suppression who are causal alcohol drinkers. An analysis of variance showed a significant effect of treatment at 0 hrs. ($p=0.004$), 2 hrs. ($p=0.003$), 4 hrs. ($p<0.001$), 8 hrs. ($p<0.001$), 24 hrs. ($p<0.001$), and 48 hrs. ($p<0.001$). Ethanol with 25 ng/mL TAT treatment caused the greatest number of macrophage migration at every timepoint while 10 mM ethanol treatment only instigated significant migration at 48 hrs. 25 ng/mL TAT treatment also produced significant migration at all timepoints, however ethanol with 25 ng/mL TAT caused greater migration numbers. A post hoc Tukey's Honest Significance test also showed significant migration in 25 ng/mL TAT compared to 10 mM

ethanol at 2 ($p<0.05$), 4 ($p<0.05$), 8 ($p<0.01$), and 24 hrs. ($p<0.01$), ethanol with 25 ng/mL TAT compared to 10 mM ethanol at 0 ($p<0.05$), 2 ($p<0.05$), 4 ($p<0.05$), 8 ($p<0.01$), 24 ($p<0.001$), and 48 hrs. ($p<0.01$), and ethanol with 25 ng/mL TAT compared to 25 ng/mL TAT at 24 ($p<0.05$) and 48 hrs. ($p<0.01$) (**Figure 2.7.B**).

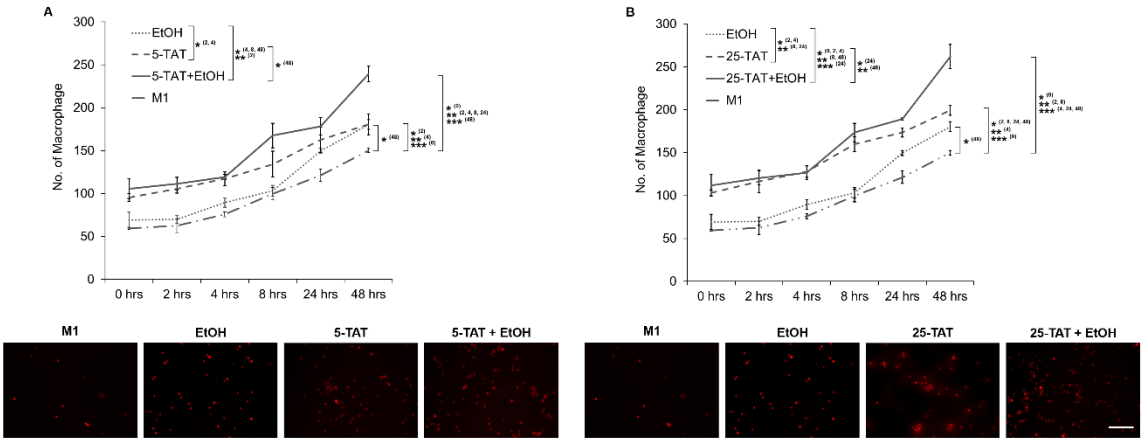

Figure 2.7 Assessment of migration between 10 mM ethanol, TAT concentrations, and treatment with both. A) Comparing to 5 ng/mL TAT, a concentration found in PLWH under viral suppression. B) Comparing to 25 ng/mL TAT, a concentration found in PLWH with a detectable viral load. A and B) Results from **Figures 2.2 and 2.4** were plotted on one graph for comparison. Bottom panels are representative images of infiltrated macrophage at 48 hrs. White bar represents 100 μm. Results are presented as mean values (±SEM, N = 3 individual transwell models). Brackets designate treatment groups being compared. Superscript describes timepoint compared. Significant difference is indicated by $* \ p \leq 0.05$, $** \ p \leq 0.01$ and $*** \ p \leq 0.001$.

2.3.4 NO production by endothelial cells may explain the dichotomy in migration pattern

Nitric oxide (NO) has been shown to modulate the expression of monocyte chemoattractant protein 1 (MCP-1/CCL2) in cultured endothelial cells [265]. MCP-1 is a key regulator of monocyte/macrophage migration and infiltration [266]. Increases to NO production above basal levels can downregulate endothelial MCP-1 secretion. NO production by RBMECs was measured in real-time with a free radical analyzer after cells were treated with 0, 10,

20, and 50 mM ethanol for 24 hrs. (**Figure 2.8.A**). These ethanol concentrations did not significantly affect cell viability (**Figure 2.9.B**). An analysis of variance on NO released by RBMECs revealed significant variation among ethanol doses ($p<0.001$). A post hoc Tukey's Honest Significance test showed that 10 mM ethanol significantly increased NO release ($p<0.01$) while 20 mM and 50 mM ethanol decreased NO release (both $p<0.001$) (**Figure 2.8.B**). Therefore, NO production in RBMECs was significantly increased with 10 mM ethanol but inhibited with 20 mM and 50 mM ethanol after 24 hrs. treatment.

NO production by neuronal cells was also measured in real-time with a free radical analyzer after cells were treated with 0, 10, 20, and 50 mM ethanol for 24 hrs. (**Figure 2.8.C**). Acute ethanol treatment has been shown to decrease NO synthesis by cortical neuron cells [267]. The lipophilic properties of ethanol allow for it to easily cross the BBB. Therefore, treatment with ethanol on the apical side may result in some transfer of ethanol to the basolateral side of the insert. An analysis of variance on NO released by neurons revealed significant variation among ethanol doses ($p<0.001$). A post hoc Tukey's Honest Significance test showed that 10, 20, and 50 mM ethanol significantly decreased NO release ($p<0.01$, $p<0.001$, $p<0.001$), in addition, 20 and 50 mM ethanol caused even greater decrease of NO release than 10 mM (both $p<0.001$) (**Figure 2.8.D**). Therefore, NO production in neurons was significantly decreased with all ethanol treatments.

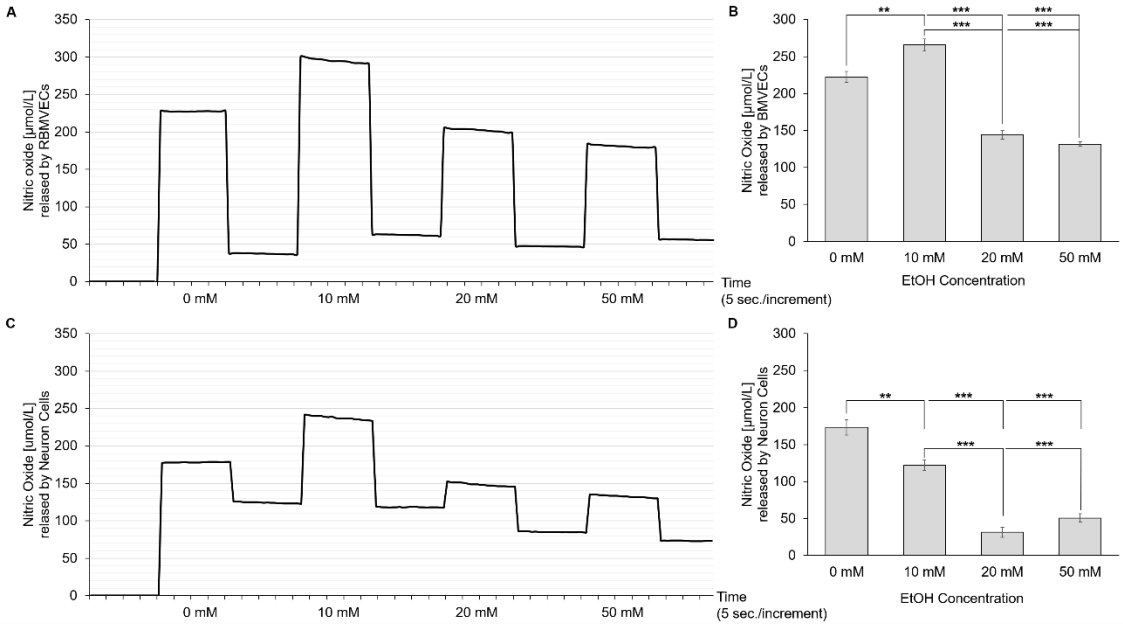

Figure 2.8 Measurement of NO production in cells exposed to ethanol. A and C) Representative graph of NO detection in endothelial and neuronal cells exposed to 0, 10, 20, or 50 mM of ethanol for 24 hrs. 1 increment = 5 sec. Graph represents 20 sec. of signal from treatment followed by 20 sec. of baseline. B and D) Amount of NO produced by endothelial and neuronal cells exposed to increasing concentrations of ethanol for 24 hrs. Results are presented as mean values (±SEM, N = 3 experiments). Significant difference is indicated by ∗∗ $p \leq 0.01$ and ∗∗∗ $p \leq 0.001$.

2.3.5 Neurons undergo structural and behavioral changes with increasing concentrations of TAT

The structural and behavioral nuances of TAT-induced neurodegeneration were also examined. Primary neurons were cultured for 7 days after which time they were treated with 0, 5, 10, or 25 ng/mL of TAT protein. Cells were analyzed for viability with an MTT assay and cell culture morphology by phase contrast and fluorescent microscopy in response to increasing concentrations of TAT. An analysis of variance on neuronal viability revealed significant variation among TAT concentrations ($p<0.001$). A post hoc Tukey's Honest Significance test showed that 5, 10, and 25 ng/mL significantly decreased cell viability (all $p<0.001$). Further analysis showed that 10 and 25 ng/mL TAT showed even

greater decreases in viability than 5 ng/mL ($p<0.01$, $p<0.001$) and 25 ng/mL TAT showed an even greater decrease in viability than 10 ng/mL ($p<0.05$) (**Figure 2.9.A**). These results reveal that neuronal viability decreases with increasing concentrations of TAT.

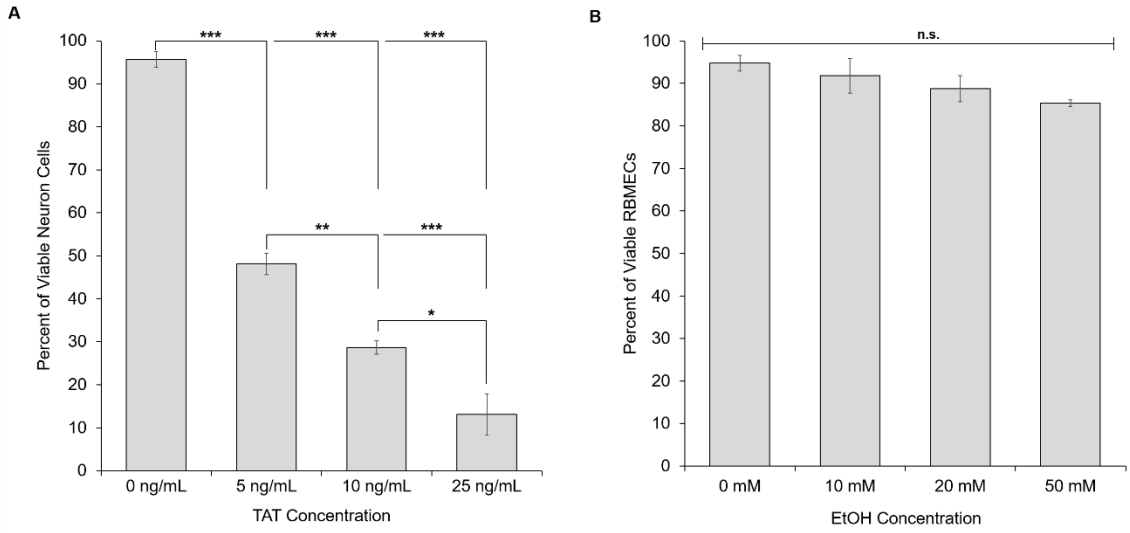

Figure 2.9 Cell viability after treatment with TAT or ethanol. A) Percent of viable neuronal cells after treatment with 0, 5, 10, or 25 ng/mL TAT for 24 hrs. B) Percent of viable rat brain microvascular endothelial cells after treatment with 0, 10, 20, or 50 mM ethanol for 24 hrs. Results are presented as mean values (±SEM, N = 4 experiments). Significant difference is indicated by $* p \leq 0.05$, $** p \leq 0.01$ and $*** p \leq 0.001$, n.s. denotes no significance.

Phase contrast images of neuronal cells exposed to increasing concentrations of TAT explain the decreases in viability observed with the MTT assay. At 5 ng/mL TAT single neurons show significant loss of neuronal projections characterized by fragmenting axons and retracting dendrites. These neurons also move together to form small clusters. With 10 ng/mL TAT, neurons have complete loss of neurites and the largest, most compact clusters begin to dissociate. By 25 ng/mL there is total neuronal death throughout the culture (**Figure 2.10.A**). Fluorescent microscopy confirms this observation for 5 ng/mL treatment (**Figure 2.10.C**). These results suggest a trend to TAT neurotoxicity (**Figure**

2.10.B). Low concentrations of TAT induce stress in the culture and cause neurons to come together to form neuronal clusters. In addition, the chemical structure of TAT allows for it to be easily absorbed by single neuron cells to elicit a toxic response. Single cell toxicity involves fragmentation of long, slender axonal projections and retraction of dendritic branches to a point where only the cell soma remains. Progressively high concentrations of TAT hasten this response as well as cause further damage. The neurons of larger, more robust neuronal clusters die, and clusters become dissociated.

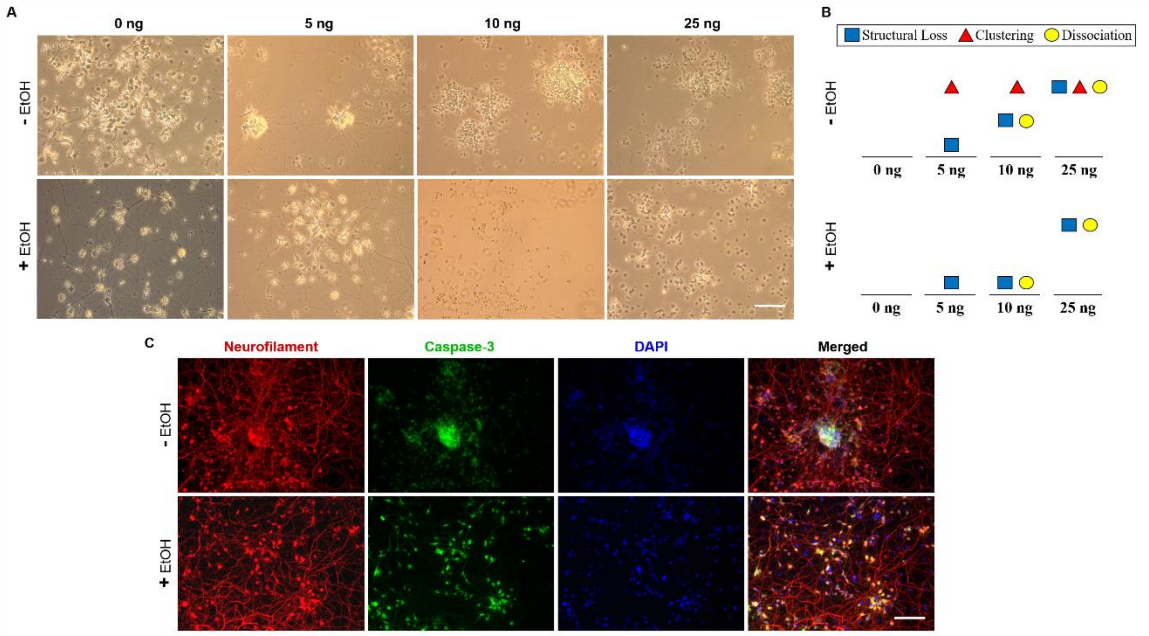

Figure 2.10 Morphology of neuron cultures exposed to TAT concentrations with or without presence of low dose ethanol. A) Representative images of neuron cultures exposed to 0, 5, 10, or 20 ng/mL TAT only (top panels) or in the presence of ≤ 10 mM ethanol (bottom panels). White bar represents 100 μm. B) Cartoon summarizing a trend to TAT toxicity and ethanol attenuation observed in neuronal cultures. Blue square: fragmentation of axons and retraction of dendrites. Red triangle: neuronal movement and formation of compacted clusters. Yellow circle: dissociation of clusters and death of single neurons. C) Representative images of caspase-3 expression in neuronal cultures treated with 5 ng/mL TAT with or without presence of ≤ 10 mM ethanol. Neurofilament staining identifies neurons and their processes. White bar represents 100 μm.

2.3.6 Ethanol delays visible loss of neurite integrity caused by TAT but expedites apoptotic neurodegeneration

The addition of ethanol to a culture of neurons exposed to TAT appears to ameliorate some of its toxic effects. Neurons treated with TAT in the presence of ≤ 10 mM ethanol do not move together to form neuronal clusters. In addition, these single neurons retain neurite integrity for both axons and dendrites up to 10 ng/mL TAT treatment (**Figure 2.10.A**). Fluorescent microscopy confirms this observation for ethanol with 5 ng/mL TAT treatment (**Figure 2.10.C**). Nevertheless, by 25 ng/mL TAT, neurons are all dead in the same way as treatment with TAT alone. These results suggest that low dose ethanol may be delaying the morphological effects of TAT toxicity, but only at low concentrations of TAT (**Figure 2.10.B**). However, upon further examination with caspase-3 staining, it becomes clear that ethanol is not rescuing TAT-injured neurons but instead inducing apoptosis. Caspase-3, also known as the executioner caspase, is activated by initiator caspases, such as caspase-8 and -9, to coordinate the activities required for apoptosis including the destruction of structural proteins as well as cleavage and activation of other enzymes [268]. Once caspase-3 becomes activated, apoptosis is greatly accelerated. Expression of caspase-3 was observed in neurons co-treated with ethanol doses ≤ 10 mM and a 5 ng/mL TAT concentration. (**Figure 2.10.C**) This purports that the ameliorating effects of ethanol treatment observed through neurite preservation are deceptive.

2.4 Discussion

The quad-cultivation of brain endothelial, astrocyte, neuronal, and macrophage cells on a transwell system creates a dynamic model of the BBB. Fluorescent labeling of stimulated macrophage allows for observation of migration through the endothelial/astrocyte cell

coculture. A neuronal culture at the base provides convenience for studying the effects of neurodegeneration on macrophage migration (**Figure 2.1.A**). The two-chamber system achieved by transwell culture permits the division of cells interfacing with the circulation with those of the CNS. In addition, the membrane-base of the transwell insert can produce a chemoattractant gradient when medium from the well contacts the membrane. The endothelial/astrocyte coculture on either of the membrane prevents a collapse in this gradient. Without this coculture, equal amounts of chemoattractant would equilibrate on both sides of the membrane within a few hours.

Evans blue analysis verified the integrity and efficacy of this BBB model by demonstrating a significant reduction in Evans blue penetration to the basolateral side of the insert (**Figure 2.1.C**). Importantly, the addition of cells did not prevent all Evans blue dye from permeating the barrier. In vivo results have shown some Evans blue leakage in control rodents with an intact BBB [269]. Complete dye impermeability would more likely reproduce injury-induced scar tissue formation. After the model was injured with 50 mM ethanol, Evans blue infiltration significantly increased but not to the degree of barrier break down. 50 mM ethanol represents a BAC of 0.23% which is almost three times above the legal limit, manifesting clinically as a decline in motor skills, sluggishness, and mood swings. Driving with this alcohol level can result in criminal penalties. Since this study was examining the effects of low to moderate doses of alcohol, 10 mM and 20 mM ethanol concentrations were chosen. 10 mM ethanol is found with a BAC of 0.05% which is below the legal driving limit of 0.08% BAC. A person with 10 mM ethanol may experience euphoria, loss of inhibition, and stimulation. 20 mM ethanol is found with a BAC of 0.09% which is slightly above the legal driving limit and is characterized by moderate impairment

and feelings of depression in some individuals [262, 270]. Both concentrations may be found in a causal drinker who is not abusing alcohol.

Ethanol doses were always treated on the apical (endothelial) side of the BBB model to replicate ethanol circulation in the blood. Ethanol circulates in the blood when alcohol is consumed in excess and liver enzymes are yet unavailable to degrade it. Ethanol exposure downregulates expression of tight junction proteins in endothelial cells and causes BBB impairment [271]. Our lab has previously shown that ethanol treatment of endothelial cells causes activation of myosin light-chain kinase protein and subsequent phosphorylation of occludin and claudin-5 to disruption the endothelial cell monolayer tight junction and facilitate BBB dysfunction. In addition, leakiness to the barrier is temporary and can be reversed with ethanol withdrawal [272]. Exposure with 10 mM ethanol showed significant macrophage migration only after 48 hrs. while 20 mM ethanol showed significant migration after 24 and 48 hrs (**Figure 2.2.A**). With no significant differences between 10 mM and 20 mM, I conclude that just the presence of ethanol in the circulation, whether it be at low or more moderate doses, is enough to cause pro-inflammatory macrophage to infiltrate the BBB. These low doses may not be affecting BBB integrity, instead ethanol may be causing other biochemical changes to enable this increased migration. Unlike most other drugs, alcohol has a low affinity for its molecular targets, instead readily diffusing through membranes. Nevertheless, there are many molecules, compounds, and systems that are sensitive to even low doses of alcohol. More BBB proteins that are sensitive to low dose alcohol in vivo may yet be discovered and explain alternative impairments to BBB function. The enzymes and by products of alcohol

metabolism may also be play a part in disrupting the BBB. In future, I may examine the effects of acetaldehyde toxicity on macrophage migration in our BBB model.

HIV-TAT protein was always introduced to the basolateral (neuron) side of the BBB model to replicate release of TAT by HIV-1 infected microglia in the CNS. Even in the absence of active HIV-1 viral replication and production, with effective antiretroviral therapy, TAT concentrations can still be found in the CSF [263]. However, those with viral suppression show levels below 6 ng/mL. Exposing the basolateral side of the model with 5 ng/mL TAT showed significant migration after 0, 2, and 4 hrs. while 25 ng/mL ethanol showed significant migration after all time points, still there was no significant difference between 5 ng/mL and 25 ng/mL TAT (**Figure 2.2.B**). These results suggest that a virally suppressed concentration of TAT influences macrophage migration only for a few hours after being introduced. In the neurobiology, TAT protein can be absorbed by non-infected, bystander cells due to several of its properties. Its cell-penetrating peptide allows for easy entry into cells while its nuclear localization signal allows for translocation into cellular nuclei. Therefore, this decline in significant migration after 4 hrs. may be the result of TAT getting absorbed by neurons, astrocytes, or infiltrated macrophage on the basolateral side of the BBB model. Hence, migration under TAT may be more so directed by its presence rather than the toxic response it can elicit. The CC motif of TAT protein can mimic chemokines and enhance cell migration. However, the use of an in vitro model as well as a 48 hrs. time constraint limited the extent of observation. Future research may examine the effects of TAT on macrophage migration into the CNS using an in vivo model over a longer period. There may be latency of migration in response to release of neurotoxic factors by cells under TAT-injury.

The BBB model was also challenged with combined low dose EtOH and TAT protein to examine the effects of casual drinking on macrophage migration under HIV-associated injury. My aim was to study the best clinical outcomes of HIV-1 infection, low viral load, with occasional alcohol consumption. Co-presence of 10 mM ethanol with either 5 ng/mL TAT or 25 ng/mL significantly increase macrophage migration across all time points when compared to those migrating an uninjured model (**Figure 2.4.A**). Therefore, combined ethanol and TAT may be cross amplifying their cellular effects to potentiate toxicity and cause constant macrophage infiltration. No significant difference was found between ethanol with 5 ng/mL TAT and ethanol with 25 ng/mL TAT. This suggests that there may be no true effect of differing TAT concentration, instead the mere presence of some TAT with ethanol can be specifically attributed to macrophage migration through this *in vitro* BBB model.

The results of the EtOH and TAT studies on macrophage migration revealed a dichotomy in migration pattern, low TAT concentrations cause significant migration right after exposure while low dose alcohol causes significant migration at later timepoints. I explored this dichotomy by challenging the model with excessive concentrations of both EtOH and TAT in the respective compartments of the model. 50 ng/mL TAT showed greatest significant migration in the first 4 hrs. but after 6 hrs. 50 mM EtOH produced more significant migration than the TAT (**Figure 2.4.B**). Therefore, with combined ethanol and TAT, there is an effect of TAT first that diminishes over time and is taken over by ethanol to create an environment for continuous infiltration of pro-inflammatory macrophage. To determine which injury produces greatest macrophage migration, I compared number of infiltrated macrophage cells between 10 mM EtOH, 5 ng/mL or 25 ng/mL TAT

concentration, and the combination of both. For both virally suppressed and unsuppressed scenarios, the combination of ethanol with TAT caused greater migration than either ethanol or TAT alone. Also, both TAT concentrations had an overall greater effect on migration compared to low dose ethanol (**Figure 2.7.A and B**). Therefore, even under the best circumstances, HIV-1 suppression and casual drinking, the combination significantly induces macrophage migration across the BBB and causes neuroinflammation. A notable result of all the macrophage migration experiments is that time is the greatest determinant of migration potential (**Figure 2.11**).

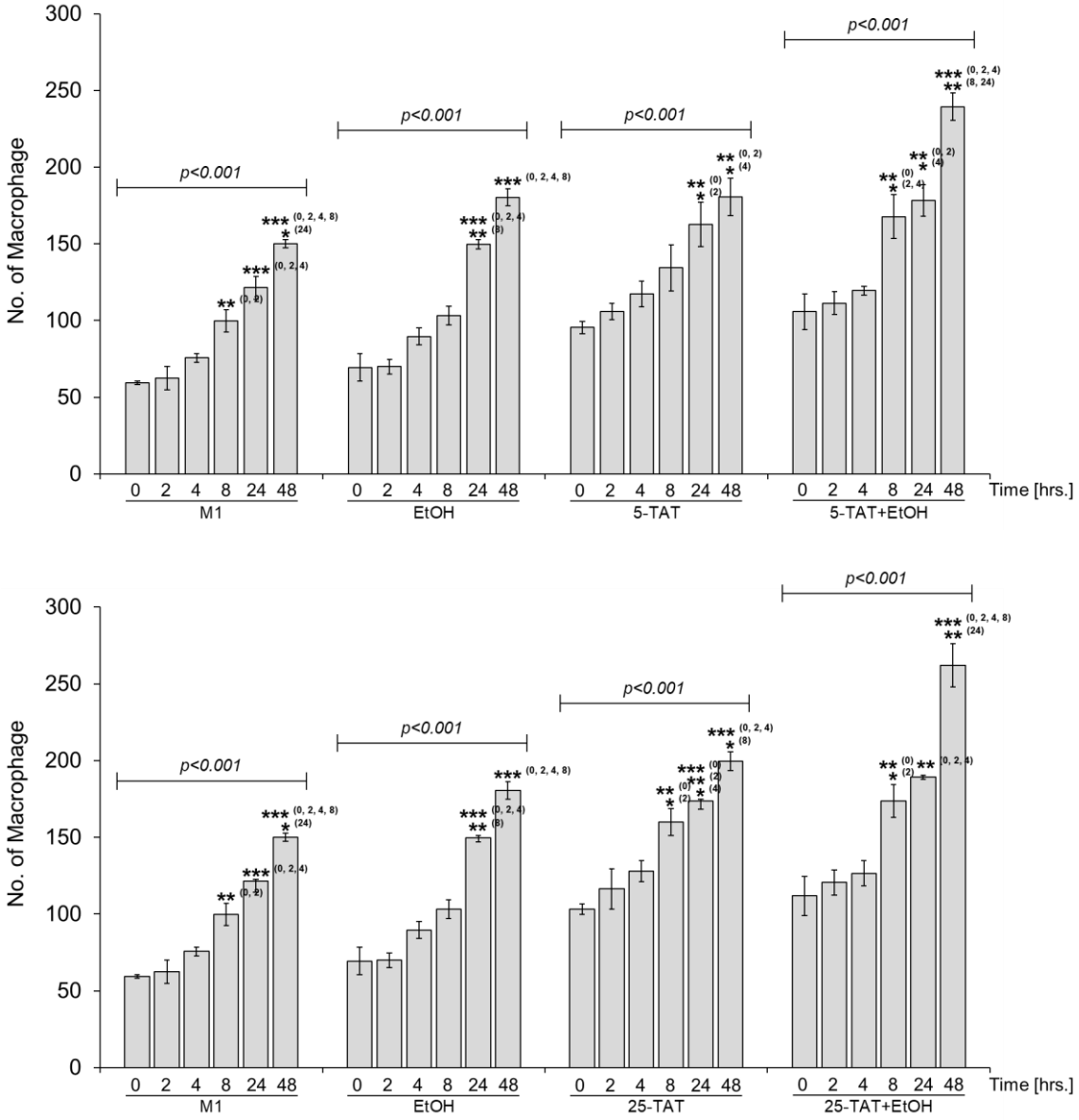

Figure 2.11 Effect of time on macrophage migration. Graphs plot number of infiltrating macrophage cells for each timepoint of a treatment condition. Graphs compliment those found in **Figures 2.7**. Results are presented as mean values (±SEM, N = 3 individual transwell models). Superscript describes timepoint compared. Significant difference is indicated by $* \; p \leq 0.05$, $** \; p \leq 0.01$ and $*** \; p \leq 0.001$.

As a modulator of MCP-1, NO production can affect migration potentials [265, 273]. In the CNS, MCP-1 has shown expression by neurons, astrocytes, and microglia under neuroinflammatory conditions, specifically those caused by neurodegenerative

diseases and insults. Alcohol has been well described to exert local and systemic inflammatory responses, although they may be inconsistent, depending on dose and length of exposure [42]. NO is constantly formed endogenously, but EtOH can affect its production [274]. Effects of EtOH on NO release may be important in regulation of MCP-1 and, in extent, macrophage migration. I measured real time production of NO by endothelial cells exposed to increasing concentration of EtOH for 24 hrs. 10 mM ethanol causes significant NO production while 20 mM and 50 mM ethanol resulted in significant decreases to NO production (**Figure 2.8.A**). This increase in NO by 10 mM ethanol may reduce secretion of MCP-1 in the endothelial cells to prevent a significant macrophage migration at 24 hrs. while the decrease in NO by 20 mM ethanol may encourage secretion of MCP-1 and explain the increase in significant migration observed at 24 hrs. post treatment (**Figure 2.2.A**). Of note, this effect of 10 mM ethanol treatment was also seen at 0, 2, 4, and 8 hrs. treatment (not shown). NO production was also measure in neuronal cells exposed to the same concentrations of ethanol for 24 hrs. Ethanol's lipophilic properties allow for its transfer through the barrier to the neurons on the basolateral side of the model. All ethanol doses decreased release of NO by neurons (**Figure 2.8.B**). This NO inhibition should increase secretion of MCP-1 by neuronal cells and cause significant macrophage migration at 24 hrs. Even though there was significant migration with 20 and 50 mM ethanol, there was none with 10 mM at 24 hrs. (**Figure 2.2.A and Figure 2.4.B**). The consequences of NO production by neurons may be taking effect after macrophage infiltrate the barrier and direct migration of macrophage towards the neuron cells at bottom of the well.

TAT-induced toxicity has been characterized by activation of lipoprotein receptor-related protein-1 (LRP) and N-methyl-D-aspartate receptor (NMDAR) followed by production of glutamate and NO as well as the release of neurotoxic factors by microglia and astrocytes [275]. Marked reductions in cell viability have been observed with less than 5 ng/mL TAT in neurons (**Figure 2.9.A**), 10 ng/mL in astrocytes, and 200 ng/mL TAT in endothelial cells while concentrations as high as 1,000 ng/mL stimulate monocyte/macrophage and microglial cells [275-277]. Therefore, treatment with 5 ng/mL, 25 ng/mL, and 50 ng/mL TAT did cause neuronal death in this model. This suggests that decreases in neuronal viability may dictate the outcome of macrophage migration. However, ethanol treatment of endothelial cells produced similar results and co-presence with TAT exacerbated migration. Consequently, macrophage migration depends on the outcome of the entire BBB system, chiefly neuronal, astrocyte, and endothelial cell integrity. Future studies of immune cell infiltration into the CNS under HIV-associated injury should focus on this dynamic interaction.

There have been numerous studies on the neurotoxicity of TAT to varying results [278-281]. I mapped the subtle structural and behavioral changes of neurons exposed to progressively higher levels of TAT (**Figure 2.10.B**). Low concentrations of TAT caused neuronal clustering and loss of neurites in single cells. Moderate to high concentrations began killing neurons and dissociating these clusters. I found that large clusters of neurons were more resistant to TAT damage (**Figure 2.10.A**). This can be evidence that loss of neurites is the result of forced neuronal pruning by TAT toxicity. As dense populations of neurons show less neurite loss, TAT may not be interacting directly with axons and dendrites but getting absorbed by neuron bodies to initiate apoptosis. Caspase-3 staining

showed expression of this apoptosis executioner in the nodes of neuronal clusters in cultures treated with 5 ng/mL TAT (**Figure 2.10.C**). Conversely, this apoptosis may be the result of a sequestration in receptors and lack of nutrients and oxygen by cells at the center of these clusters.

There exists a strong consensus that ethanol potentiates TAT-induced neuronal death [247]. However, several studies of ethanol treatment under gp120 exposure have shown that ethanol blocks the retroviral protein's toxic effects [282-284]. I treated neurons with TAT in the presence of low dose ethanol to determine if this may also be true of TAT protein. Initially I found that low-dose alcohol may attenuate the structural damages caused by TAT toxicity. Co-treatment inhibited cluster formation and loss of neurites up to 10 ng/mL TAT (**Figure 2.10.A**). MCP-1/CCL2 has been shown to protect cells against damage done by TAT [275]. Therefore, decreases in NO production by ethanol exposure can result in increases in MCP-1/CCL2 expression and reductions in TAT-induced toxicity. However, caspase-3 staining showed that these neurons are undergoing apoptosis and low dose alcohol is not correcting the damage done by TAT (**Figure 2.10.C**) [285, 286]. Such results imply that instead of attenuating TAT toxicity, ethanol may just be masking or temporarily delaying visible injury (**Figure 2.10.B**).

2.5 Conclusion

This work has shown that alcohol is a catalyst for macrophage migration under HIV-associated injury. Even under the best clinical outcomes a person living with HIV-1 may experience, macrophage infiltration into the CNS significantly increases after small consumptions of alcohol. These infiltrating macrophage cells can cause neuroinflammation

by increasing release of inflammatory cytokines. Furthermore, macrophage also infected with HIV-1 may deposit viral components or establish viral reservoirs in the CNS [287]. These results highlight the need for therapeutic interventions against HIV-TAT protein.

CHAPTER 3

ANTIRETROVIRAL DRUG-S FOR A POSSIBLE HIV ELIMINATION

In this chapter, and for my second aim, I challenge a novel compound, called Drug-S, against HIV-1 to observe whether it can inhibit infection. The results presented here are an introductory to the additional experiments that must be done to establish efficacy as well as understand the mechanism(s) of action. However, these results suggest that Drug-S is worth exploring in future. This chapter is a truncated version of the work that was published in the *International Journal of Physiology, Pathophysiology, and Pharmacology* volume 11 on August 2019. James Haorah and I designed the study, analyzed the data, and prepared the manuscript while co-authors Heather Schuetz, Vikas Mishra, and Adam M Szlachetka, coordinated the hands-on work at the University of Nebraska Medical Center, Omaha, NE.

3.1 Introduction

Over the past decade, human immunodeficiency virus type-1 (HIV-1) has been one of the leading causes of death worldwide. With the emergence of combination antiretroviral therapy (HAART), HIV-1 has become manageable and has transformed from a life-threatening to a life-long disease. Nevertheless, the Centers for Disease Control and Prevention shows an epidemic rise of new HIV/AIDS diagnoses in the United States among people living in urban areas (Centers for Disease Control and Prevention and [288]). Recent advances in HAART have visibly reduced the level of replication, HIV-infection and HIV/AIDS progression [289]. This includes a better understanding of viral invasion in the brain, persistence, and neuropathogenesis [290-292]. Yet, HIV/AIDS disease remains

without a cure even with this highly active HAART. Additionally, the adverse side effects of HAART are also known to cause neurological complications in HIV/AIDS patients such as dementia, neuropathy, and various psychological conditions [293]. The efficacy of HAART is further worsened by adverse drug interactions [294], co-infection [295], and malnutrition in HIV/AIDS patients because of inhibition of glucose/lipid metabolism known as lipodystrophy [296, 297]. HIV-1 infected cells are highly energy demanding due to enormous energy wasting while HAART promotes malnutrition, which exacerbates the metabolic imbalance in HIV/AIDS patients [298].

An equally important concern is the multi-faceted complications of HIV/AIDS progression in neuroAIDS patients with chronic substance abuse, where damage of the blood-brain barrier (BBB) enhances infiltration of infected cells into the brain that promotes neuroAIDS progression [201, 299, 300]. Thus, substance use is a risk factor for HIV-infection [301] resulting in the reduction of CD4+ T cells in HIV/AIDS patients. Credence of neuroAIDS in substance use shows depressive symptoms [302], loss of memory, increase neuropathy [303, 304], and excess mortality rates [305] among HIV/AIDS patients as well as increased predisposition to other health problems [306, 307]. Induction of oxidative stress, release of cytokines/glutamate in glial cells, and disruption of the blood-brain barrier (BBB) underlie the mechanisms of HIV-1 encephalitis, increased viremia, and neurotoxicity in the brain, which may contribute to the progression of HIV/AIDS disease [308].

Multi-drug HAART regimens are difficult to manage, but a three-drug combinational HAART is needed to create a genetic barrier against drug resistance and viral mutations [68]. The development of fixed-dose, single tablet medications have

reduced the complexity [309], but daily adherence can still be demanding [310]. Current HAART research is focused on creating long-acting drugs that only require periodic injections [311], sustained release drugs with the use of nanoparticles [312], broadly neutralizing antibodies [313], and a safer less expensive alternative to those already available [314]. It is evident that HAARTs can control viral replication, but a cure for HIV/AIDS is limited by less penetration of HAARTs across the restricted anatomical features such as the BBB and enclosure within the restricted skull cavity [315-319]. Drugs that do cross the BBB are often thrown back out by way of saturable efflux systems such as the multi-drug resistant genes of endothelial cells [320]. Thus, a direct correlation of HAART concentrations and HIV-1 viral load in the brain was observed [321]. Further, the BBB is a bidirectional barrier, accumulated virions in the brain can re-enter the blood circulation for resurgence of HIV-1 infection [322]. This viral resurgence and inability of drugs to freely pass the BBB makes HIV/AIDS progression a constant threat.

The cure for HIV/AIDS disease is further diminished by the persistence of a viral reservoir in latently infected CD4+ T cell genotypes [323]. The stability of this latently infected HIV-1 reservoir is harbored in the central memory CD4+ T cell genotype while the integrated HIV DNA is harbored in the transitional memory CD4+ T cell genotype [324]. This was also observed in intravenous injection of HIV-1 proteins into the brain of rats/mice [325]. Persistence of HIV-1 latency and the CNS reservoir are responsible for the recurrence of HIV-1 self-renewal and reinfection upon withdrawal of HAART in proliferating cells [326]. The ability of HIV-1 self-renewal and reinfection creates a life-long dependency on HAARTs and demonstrates that the body cannot completely clear itself of the virus. Longitudinal studies have shown that it would take someone on HAARTs

their lifetime to eliminate the virus [327]. However, with the continued successful outcome of the Berlin patient [328], there is new hope that a functional cure may be possible; where an infected person can suppress the virus to such low levels that taking HAARTs is no longer a necessity. The Berlin patient showed mutations to the CCR5 gene from his hematopoietic stem cell transplant donor that effectively inhibited further infection [329].

Recently, several non-HAART alternatives have been formulated for eliminating HIV-infection. Some of these non-HAART alternatives are, gene editing to mutate the CCR5 gene [329], “shock-and-kill” approach to activate cells with latent reservoirs for immune cells to locate and kill [330], “block-and-lock” approach to length latency [331], immune modulation to boost the physiological immune system [332], viral-decay accelerators to increase mutation frequency towards catastrophe [333], hematopoietic stem cell transplants from infection resistant donors [329], pharmacological agents like microbicides to prevent transfer through sexual intercourse [334], microRNAs [335], and vaccine developmental approaches [336, 337]. The shortcomings of these strategies include their non-feasibility for clinical applications [338], failure to reach the CNS [339], risks of inducing neurotoxicity [340] and other diseases, in addition these approaches cannot adjust for drug-resistant mutants [341]. Importantly, these strategies cannot eliminate all components of the viral life cycle as latent reservoirs hold replication incompetent HIV-1 that may contain provirus DNA, viral mRNA, viral protein, or any combination of these components [342]. Another major problem are viral mutations. Development of conformational changes in envelope glycoproteins due to viral mutations can mask or lose epitopes to evade immune attack [182]. With as many as 10 different

mutants after one cycle of infection [343, 344], developing a comprehensive vaccine remains a great challenge.

With all of these promising discoveries, a critical need for a cure of HIV/AIDS disease will be to find a safe antiretroviral drug capable of inhibiting HIV-1 replication and eliminating self-renewal of residual HIV-1 in the CNS reservoir and peripheral latency. This study reports that Drug-S has a potential to interfere with HIV-1 viral components, prevent rebound effect of HIV-1 self-renewal, and arrest HIV/AIDS progression. Drug-S is a natural substance derived from the roots of a plant that has not been tested or documented in the literature of ethnopharmacology. The plant extracts were used by indigenous people for mass poisoning by using large quantities of the extract to spike drinks. Today, this same plant extract is used by the indigenous people for poisoning river fish for consumption. Consumption of the whole fish does not cause poisoning, perhaps due to low levels of toxin. Such dichotomy prompted the idea of whether this low concentration of toxin can inhibit HIV-1 infection.

3.2 Methods and Materials

3.2.1 Reagents

The Drug-S extract was obtained by liquid-liquid extraction (water-methanol) of a plant root. The silica Bond Elut C18 extraction column and Vac Elut SPS 24 cartridge manifold used in solid phase extraction were purchased from Varian Medical Systems of Harbor City, CA. The Alltech C18 (4.6 × 100 mm, 5 µm) column and 25 mm VanGuard pre-column used in reverse-phase chromatographic separation was purchased from Waters Corporation of Milford, MA. Other common chemicals, reagents, and solvents used in the

purification of Drug-S were purchased from Sigma-Aldrich of St. Louis, MO and were of the highest grade and purity.

3.2.3 Monocyte/macrophage culture

Human monocytes were isolated by leukapheresis from HIV and hepatitis seronegative donors and purified by counter-current centrifugal elutriation as previously described [325]. Monocytes, cultured at a density of 10^6 cells/mL, were differentiated to macrophage in DMEM (Sigma Chemical Company) supplemented with 10% heat-inactivated pooled human serum, 50 µg/mL gentamicin, 10 µg/mL ciprofloxacin, and 20 ng/mL of macrophage colony stimulating factor (0.2% using a 10 µg/mL stock, Cell Signaling Technology, Cat. #8929) for 7 days to ensure adequate biological responses. Purity of macrophage was assessed by CD68 antibody (Abcam, 1:100) and showed 100% enrichment of macrophage.

3.2.4 MTT assay

Cells cultured on 96-well plates were washed in PBS and incubated with tetrazolium dye MTT 3-(4,5-dimethylthiazol-2-yl)-2,5-diphenyltetrazolium bromide solution (5 mg/mL MTT solution in 10% fetal bovine serum in PBS) for 45 mins at 37°C. After MTT solution was aspirated, plates were incubated with 100 µL dimethyl sulfoxide (DMSO) for 15 mins at room temperature. Conversion of water soluble 3-(4,5-dimethylthiazol-2-yl)-2,5-diphenyltetrazolium bromide to insoluble formazan was read spectrophotometrically at 490 nm absorbance.

3.2.5 Immunocytochemistry

Cells cultured on glass cover slips were washed with PBS, fixed in 4% paraformaldehyde for 15 mins, permeabilized with 0.1% Triton X-100 for 5 mins, blocked for unspecific binding with 3% bovine serum albumin for 1 hr. at room temperature, and incubated with respective primary antibodies, including rabbit anti-CD68 (1:100 dilution) and mouse anti-HIV1 p24 (1:1000 dilution), diluted in antibody buffer consisting of PBS, 1% BSA, and 0.4% Triton X-100 overnight at 4°C. After washing with PBS, cells were incubated for 1 hr. at room temperature with respective secondary antibodies: anti-rabbit-IgG Alexa fluor 594 for CD68 and anti-mouse-IgG Alexa fluor 488 for HIV1 p24. Cover slips were mounted onto glass slides with Immuno Mount containing DAPI (Invitrogen). Images were captured by fluorescent microscopy (Eclipse TE2000-U, Nikon microscope, Melville, NY) using NIS elements (Nikon, Melville, NY) software.

3.2.6 Reverse transcriptase assay

Reverse transcriptase (RT) converts the single-stranded RNA genome to a cDNA molecule during active HIV-1 infection of host cells. HIV-1 virions were lysed with a lysis buffer solution (Bio-Rad Laboratories) to release RT. Supernatants from cell cultures were collected, clarified by low speed centrifugation, and pelleted by centrifugation at 100,000 g for 45 mins at 4°C to collect RT. Pellets were resuspended in 0.01 M Tris-HCl (pH 7.5) and sonicated for 40 sec. 10 µL of RT suspension was combined with a reaction mixture containing 0.05 M Tris-HC1 buffer (pH 8.3), 0.06 M NaCl, 6 mM MnCl2, 0.02 M dithiothreitol, 1 µg poly(rA), 0.5 µg oligo(dT), 0.05% Nonidet P-40, and 10-5 M [3H]dTTP

(52 Ci/mmol) [345-347]. This reaction was incubated at 37°C for 20 mins, then stopped and analyzed for radioactivity by autoradiography (counts per million).

3.2.7 Purification of Drug-S

Methanol and water were used to extract the bioactive metabolite, Drug-S, from the bark of a plant root. This extract was evaporated by a rotary evaporator, re-dissolved in methanol, and subjected to solid phase extraction using a silica Bond Elut C18 extraction column (Varian Medical Systems) with a Vac Elut SPS 24 cartridge manifold (Varian Medical Systems) for sample preparation. Impurity was washed away with hexane with remnant nonpolar impurities being removed by dichloromethane (DCM) eluent. DCM extract was concentrated by distillation and evaluated for recovery, cell toxicity, and antiretroviral activity. After observing high antiretroviral activity, this highly water-soluble DCM analyte was semi-purified by reverse-phase chromatographic separation using an Alltech C18 (4.6 × 100 mm, 5 µm) column (Waters Corporation) fitted with a 25 mm VanGuard pre-column (Waters Corporation). Mobile phase consisted of A: water and B: acetonitrile, both with 0.1% trifluoracetic acid (TFA) (v/v). Separation was done using an isocratic elution of 20% B with a flow rate of 1 mL/min at 220 nm UV detection. A volume of 500 µL (1.0 mg/mL in 0.1% TFA) sample per injection was run for 80 minutes to collect five different fractions, F1 (2-8 mins), F2 (17-31 mins), F3 (31-50 mins), F4 (50-60 mins), and F5 (60-80 mins) in multiple runs (see Figure 1).

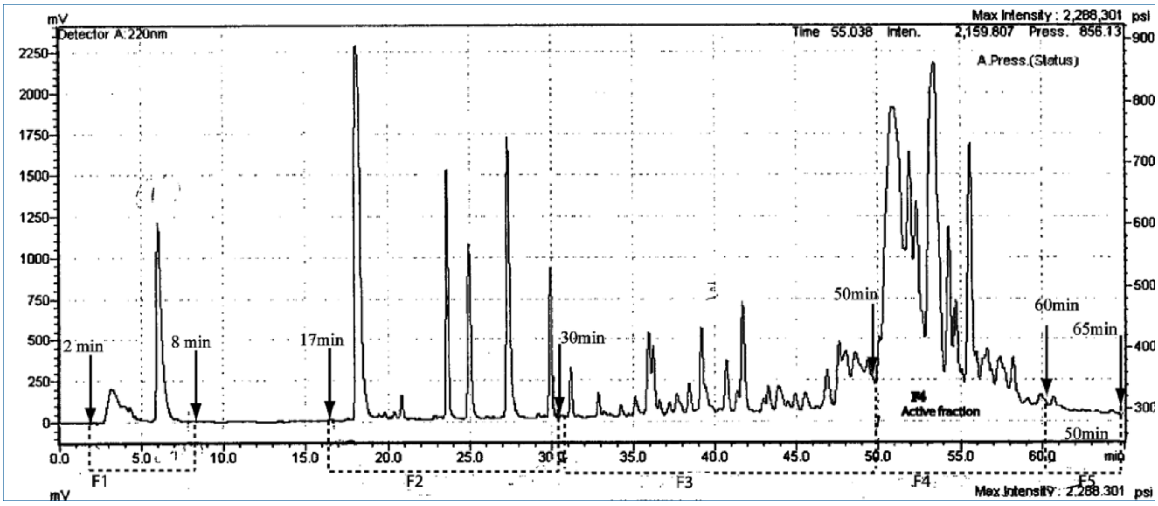

Figure 3.1 Representative graph of reverse-phase chromatographic separation fractions. Resulting peaks were collected into 4 fractions (F1-F5) each containing multiple peaks. Fractions are defined by two arrows and outlined by dotted lines and correspond to F1 being collect 2-8 mins into the run, F2 being collected 17-31 mins into the run, F3 being collected 31-50 mins into the run, F4 being collected 50-60 mins into the run, and F5 being collected 60-80 mins into the run, each in multiple runs. F5 was not analyzed because it did not contain peaks. F4 was found to contain the active antiretroviral activity termed Drug-S.

3.2.8 Determination of fractions containing antiretroviral activity

Each pooled fraction was evaporated to dryness under an argon gas stream, dissolved in saline to a concentration of 0.5 mg/mL, and assessed for antiviral activity with M-strain HIV-1 infected human macrophage in culture. Briefly, media from infected with/without drug fraction and uninfected control cultures of macrophage were collected at days 1, 3, 5, and 7 post-infection and assayed for radiolabeled reverse transcriptase (RT) activity to determine which fraction was most successful at inhibiting viral replication. To confirm assay results, cells were stained for CD68 and P24-Ag and it was found that fraction 4 (F4) contained the active antiretroviral activity. Thus, in this work I termed the antiviral activity of fraction 4, as Drug-S.

3.2.9 Statistical analysis

Results obtained from all experiments were quantified and compared using ANOVA via StatView. For comparisons between multiple conditions, the initial statistical analyses were performed using one-way ANOVA, followed by Bonferroni's test for multiple comparisons. The difference was considered significant if the adjusted p-value was less than 0.05. To power the sample size appropriately, all preliminary data was combined with subsequent experimental data for statistical analyses. Data in graphs are shown as means ± SEM with N = 4, indicating actual number of samples or experiments performed and not the number of replicates per experimental condition.

3.3 Results

3.3.1 Dose-response of Drug-S

Since fraction 4 (Drug-S) was observed to contain highly active antiviral property, the dose-dependent cytotoxicity of Drug-S in primary human macrophages cells culture was determined. Firstly, the effects of Drug-S from 0.25-100 µg/mL on cell viability was determined by an MTT assay in a 96 well plate (1×10^4 cells/well). It was established that Drug-S concentrations of 0.25-20 µg/mL were non-toxic to macrophage cells, while concentrations of Drug-S higher than 20 µg/mL were toxic (**Figure 3.2**). The same level of inhibition of HIV-1 infection in macrophages was observed down to 0.5 µg/mL of Drug-S, as such 0.5 µg/mL became the working concentration.

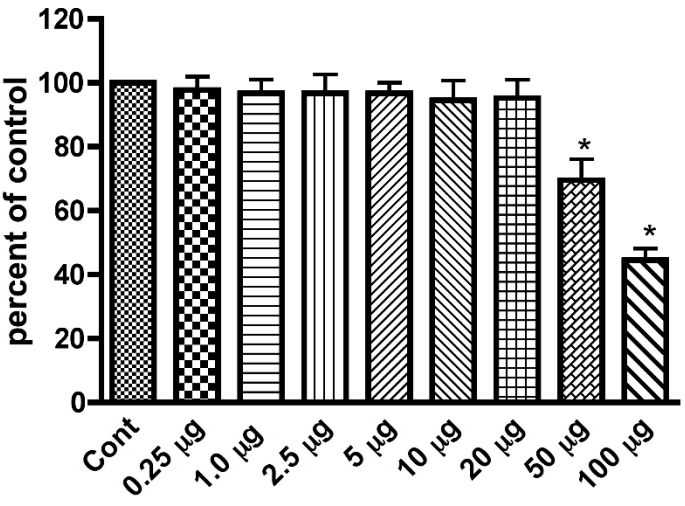

Figure 3.2 Dose-dependent toxicity of Drug-S in macrophage culture. Toxicity was assessed by MTT assay. Similar results were obtained for other primary cell types (data not shown). Drug-S caused significant cell death at concentrations higher than 20 µg/mL. However, concentrations below 20 µg/mL did not show toxicity. Significant difference is indicated by $* \; p \leq 0.05$.

3.3.2 Drug-S inhibited most HIV-1 infection

Cultured macrophage cells were infected with M-tropic strain HIV-1ada inoculum for 16 hrs. After washing out the viral inoculum, infected cells were exposed to 0.5 µg/mL of Drug-S in fresh DMEM media (without MCSF) at 24 hr, 72 hr, day 5, and day 7 post infection. Cell culture media from HIV-1 infected with/without Drug-S, and uninfected control were collected at every 48 hrs before replacing with fresh media. Media supernatants were used for assessment of viral replication by RT assay, while cell culture on cover slips were stained for CD68 and HIV-1/P24-Ag, and observed for multinucleated giant cells (MGC). HIV-1 infection in the absence of Drug-S showed several MGCs and a massive HIV-1 P24-Ag positive staining (**Figure 3.3.B and 3.3.E**) compared with infected cells in the presence of Drug-S (**Figure 3.3.C and 3.3.F**) or uninfected cells (**Figure 3.3.A and 3.3.D**). These results were further validated by RT activity to indicate that HIV-1

replication was reduced by Drug-S. Indeed, RT activity at different time points in post infection showed an increase in HIV-1 replication in the absence of Drug-S compared with HIV-1 infection in the presence of Drug-S (**Figure 3.3.G**). The significant decreases of MGCs, HIV-1/P24-Ag staining, and HIV-1 RT activity in the presence of Drug-S indicated some inhibition of HIV-1 infection. The increased RT activity at 5 and 7 days in Drug-S treated macrophage indicates that these cells may be metabolizing Drug-S or the inhibitory effects of Drug-S may be wearing off while any remaining infected cells begin spreading infection. Supplementing the culture with additional Drug-S at day 5 may result in continued decreases of RT activity and infection. P24-Ag staining after 7 days treatment with Drug-S reveals that Drug-S does not eliminate infection within 7 days and may require longer incubation or redosing for better inhibition.

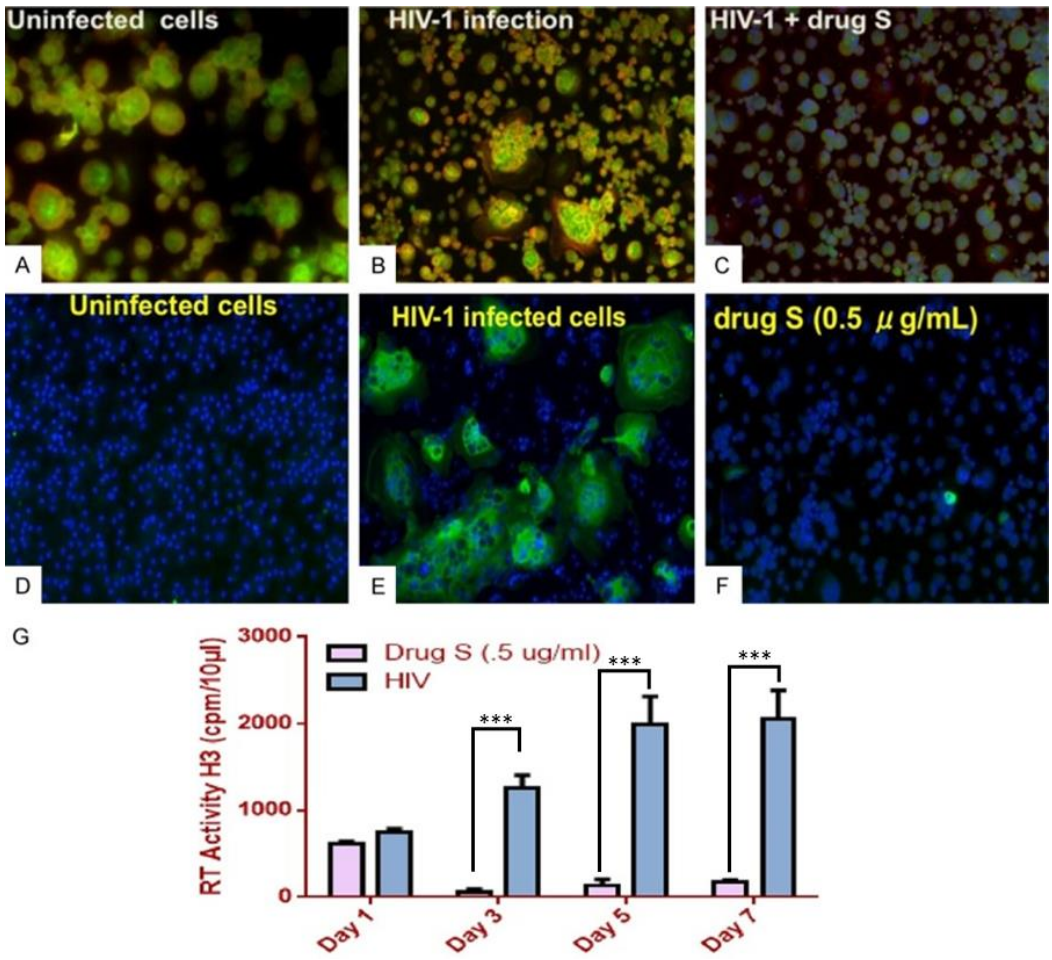

Figure 3.3 Drug-S inhibits HIV-1 infection in primary human macrophage. Upper panels = HIV infection (multinucleated giant cell clusters), middle panels = P24 staining, bottom bar graph= RT activity. One hallmark of HIV-1 infection in macrophage are the formation of multinucleated giant cells (upper panel, middle image) compared to uninfected control (upper panel, left image). In the presence of 0.5 µg/mL Drug-S, infected macrophage formed fewer multinucleated giant cells (upper panel, right image). Another indicator of HIV-1 infection is HIV-1/P24-Ag staining (middle panel, middle image) compared to uninfected control (middle panel, left image). P24 protein was detected by immunocytochemistry and fluorescent microscopy using specific antibody to P24 7 days post HIV infection. In the presence of 0.5 µg/mL Drug-S, few infected macrophage cells stained for P24 (middle panel, right image). An RT activity assay (bottom bar graph) was conducted to determine HIV-1 replication in the presence (pink bar) and absence (dark shaded bar) of Drug-S. Media from infected with/without Drug-S and uninfected control cultures of macrophage were collected at days 1, 3, 5, and 7 post-infection and analyzed for presence of reverse transcriptase. Drug-S progressively lowered RT activity as compared to Drug-S untreated cultures that progressively increased activity. RT activity is expressed as cpms/10 µl of sample. Images are representative; original magnification was 20X (except A which is 40X). Data in the bar graph are presented as mean values ± SD (N = 4). Significant difference is indicated by $*** p \leq 0.001$.

3.3.3 Drug-S pre-treated virions failed to infect macrophage

To assess if Drug-S can act directly on the virion structure, cell free M-tropic strain of HIV-1ada (0.01 MOI) was pre-incubated with/without 0.5 μg/mL of Drug-S at 37°C for 1 hr prior to infecting macrophages for 16 hrs. Supernatants collected in alternate days at post infection were assessed for RT activity. Results showed that pre-treatment of HIV-1 virions with Drug-S did not infect human macrophages (**Figure 3.4.C**) as they appear to be the same as the uninfected control (**Figure 3.4.A**) and different from HIV-1 infection without Drug-S (**Figure 3.4.B**). Assessment of viral replication further revealed a significant decreased in RT activity in Drug-S pre-treated HIV-1 virions (blue/black stripped bars) compared with HIV-1 virions without Drug-S (pink/white stripped bars) (**Figure 3.4** bottom). Thus, pre-treatment of HIV-1 virions with 0.5 μg/mL of Drug-S may prevent HIV-1 infection, suggesting that Drug-S may act directly on HIV-1 viral structure. The initial large RT activity at 1 day post-Drug-S treatment may indicate that Drug-S does not directly inhibit RT. However, subsequent decreases in activity suggests that Drug-S another critical viral component that prevents the virion from infecting. Consequently, dysfunctional virions begin to die.

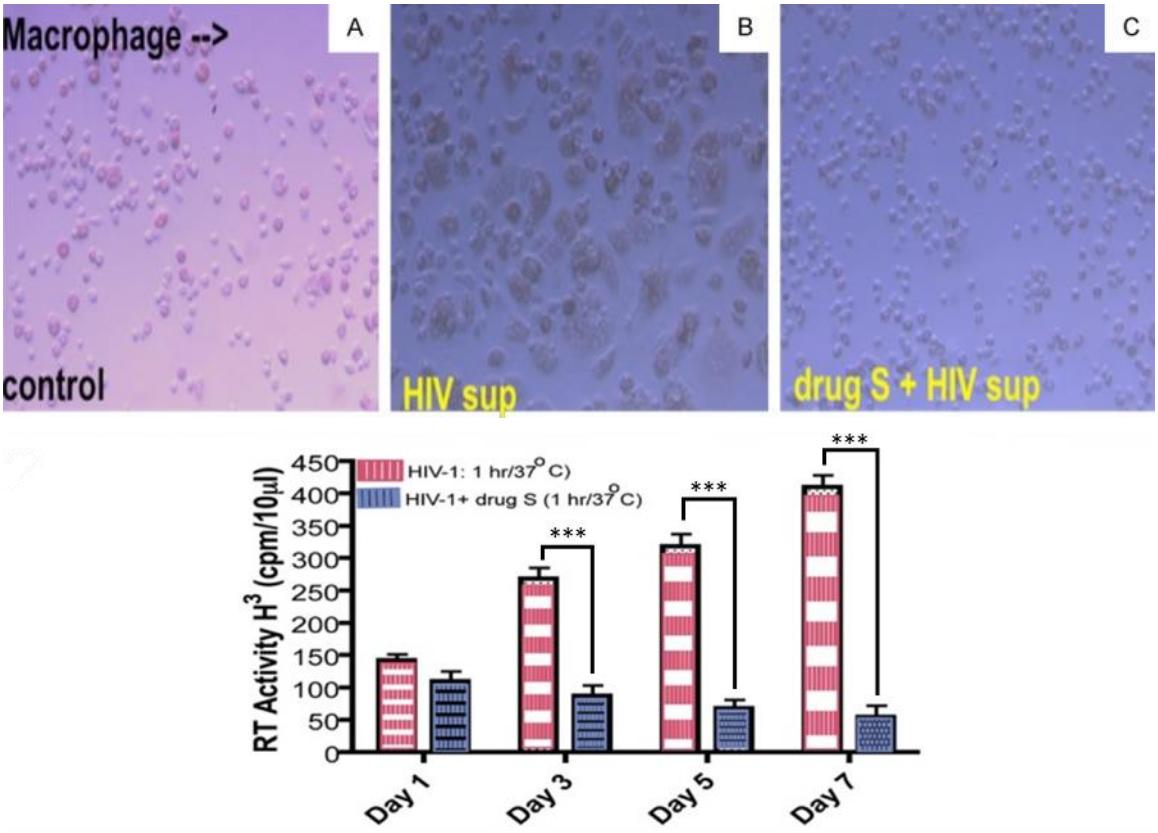

Figure 3.4 Drug-S pre-treated virions did not infect primary human macrophages. Upper panels = HIV infection (multinucleated giant cell clusters), bottom bar graph = RT activity. Macrophage cultures were infected with HIV-1 virions pre-treated with/without 0.5 µg/mL Drug-S for 1 hr. at 37°C prior to infection. Virion pre-treatment with Drug-S caused a lack of formation of multinucleated giant cell clusters (upper panel, right image) as compared to cultures infected with Drug-S un-pre-treated virions (upper panel, middle image). Media from cultures of macrophage supplemented with (pink bars)/without (black stripped bars) Drug-S pre-treated virions were collected at days 1, 3, 5, and 7 post-infection and analyzed for presence of reverse transcriptase. Macrophage cultures supplemented with Drug-S treated virions showed decreasing activity in macrophages, while virions without Drug-S treatment showed reinfection. RT activity is expressed as cpms/10 µl of sample. Images are representative; original magnification was 20X. Data in the bar graph are presented as mean values ± SD (N = 4). Significant difference is indicated by $*** p \leq 0.001$.

3.3.4 Drug-S inhibits HIV-1 reinfection

In two separate experiments, macrophage cultured in one plate were infected with HIV-1 in the absence of Drug-S, while the cells in a second plate were infected with HIV-1 in the presence of 0.5 µg/mL of Drug-S. At day 3 post-infection, Drug-S was withdrawn from the

second plate and continued culturing in normal media. Thereafter, supernatants collected at day 1, 3, 5 and 7 were analyzed for viral replication by RT assay. Results showed that withdrawal of Drug-S continued to prevent HIV-1 rebound infection (**Figure 3.5**). These results demonstrate that Drug-S may inhibit the recurrence of HIV-1 reinfection.

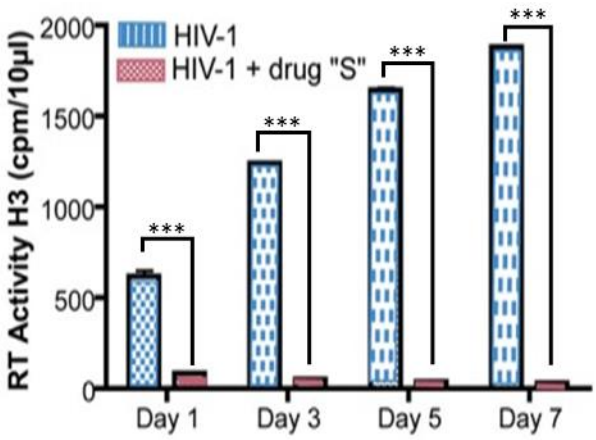

Figure 3.5 Drug-S inhibits HIV-1 reinfection. Withdrawal of Drug-S at day 3 did not see a resurgence of RT activity (pink bars) in macophage unlike those infected without presence of Drug-S (checkered bars). RT activity is expressed as cpms/10 µl of sample. Data are presented as mean values ± SD (N = 4). Significant difference is indicated by *** $p \leq 0.001$.

3.4 Discussion

The rationale for this undertaking is that there is no ART capable of eradicating HIV-1 persistency and purging of the CNS-based latent HIV-1 reservoirs to-date. The goal here is to explore Drug-S as a potential candidate drug for a possible cure for HIV/AIDS disease, which possibility is in part substantiated by our data even though this wishful assumption is still pre-matured. As such, the success of Drug-S as a viable antiviral drug requires more detailed investigation. However, the use of primary human macrophages for testing the cytotoxicity of Drug-S in the present studies is appropriate since Drug-S appeared to be a neurotoxin. The ability of Drug-S to inhibit HIV-1 infection and reinfection in human

macrophage at the non-cytotoxic level has a significant scientific premise towards HIV/AIDS disease. Since lymphocytes are a target of HIV-1 infection, testing the antiviral activity of Drug-S in HIV-1 infected human lymphocytes may be done in the future prior to pre-clinical testing.

Even though Drug-S (F4) contains high antiretroviral activity, Drug-S is still a pooled of multiple compounds in the present form, likely containing several impurities that will make the identification of Drug-S structure difficult. As such, further purification of the Drug-S active fraction is needed for better evaluation of its antiviral activity, structure-activity relationships, and bio-distribution to bring it a step closer to pre-clinical studies. Characterization of Drug-S is expected to enrich antiretroviral activity, decrease cytotoxicity, and unravel its chemical structure/mass. Elucidating the molecular structure of Drug-S is also expected to unlock the ability to synthesize Drug-S that will no longer depend on harvesting plant products. It will also provide the possibility to fluorescently tag Drug-S and trace its movements inside a cell or animal.

With this challenging idea, the establishment of non-cytotoxic low concentrations of Drug-S (0.25-20 μg/mL) in human primary macrophage cells so far tested is an important finding. Further, the effective inhibition of HIV-1 infection/reinfection by these non-cytotoxic low concentrations makes Drug S a potential antiviral drug candidate for a possible elimination of HIV/AIDS. This argument is supported by the data presented in this study. Yet, a comprehensive investigation on the mechanism(s) of HIV-1 inhibition is needed, which would include evaluating the effects of Drug-S on HIV-1 virion structure, HIV-1 production during active infection, and host cellular signaling pathways.

3.5 Conclusion

The ultimate goal of Drug-S would be to compare or to work with already available ART drugs for a possible cure for HIV/AIDS disease. Persistence of HIV-1 latency in CNS reservoirs is the reason for reappearance of virus after withdrawal of ART, which compromises the possibility of HIV/AIDS eradication. A sterilizing cure for HIV-1 with clinical applicability, ability to penetrate the highly protected CNS without causing neurotoxicity while retaining high antiretroviral activity has not yet been achieved. The innovation of this study lies in presenting a new antiretroviral drug derived from a naturally occurring substance that is capable of inhibiting infection without causing toxicity. It is expected to impact a good oral absorption and bio-distribution because Drug-S is highly stable hydrophilic compound. Above all, we have shown that Drug-S may effectively inhibit viral infection, replication, and self-renewal. This will be the first antiretroviral drug to act directly on the HIV-1 virion and eliminate the virus alone.

CHAPTER 4

ALCOHOL DYSREGULATES IRON MANAGEMENT FOLLOWING TBI

This chapter represents my third aim where I looked at the effects of alcohol and TBI-induced injury on iron management in the brain. This work is under review in the TBD as of July 2021. My co-authors, Arun Reddy Ravula, Xiaotang Ma, Yiming Cheng, Kevin D. Belfield, James Haorah, assisted me with either the experiments or data acquisition.

4.1 Introduction

Traumatic brain injury (TBI) is commonly associated with intracranial bleeding and subsequent cerebral hemorrhage such as epidural/subdural hemorrhage, subarachnoid hemorrhage, intraventricular hemorrhage, and hematoma [348, 349]. These intracranial hemorrhages are constantly being detected in TBI patients by fast magnetic resonance imaging (MRI) and computerized tomography (CT) scanning [350]. Since these hemorrhages are observed in conjunction with anemia, coagulopathy, and sepsis, current treatment practices include anticoagulant or red blood cell (RBC) transfusion [351, 352]. However, these therapies do not improve neurological function, rather, RBC transfusions have been shown to significantly exacerbate trauma complications [353]. Since RBCs contain much of the iron found in the body, a possible reason for unresolved, persistent cognitive function deficits may be neurotoxicity caused by iron overload [354]. Massive RBC aggregations at the site of hemorrhage have been observed in our lab's rat model of blunt TBI [355]. This TBI model uses lateral fluid percussion injury (FPI) delivered at a moderate pressure to reproduce TBI without skull fracture and generate hemorrhage,

subdural hematoma, edema, and shearing/stretching of tissue in gray matter, most often seen in athletic sports injuries. FPI reproducibly recapitulates the pathophysiological signatures of human TBI and thus, can be used to examine the fate of RBC clearance and associated iron release at post-TBI [356].

Lacking mitochondria, accumulated RBCs begin undergoing lysis upon energy depletion following blood vessel rupture and removal from the circulation at post-TBI [357]. Hemolysis of RBCs releases iron, carbon monoxide, and biliverdin into the central nervous system (CNS) [358]. The hemolytic product iron is managed by several different proteins to prevent possible iron toxicity that may develop from iron accumulation. Proteins that have already been considered chief iron regulators include: heme oxygenase-1 (HO-1) for associated iron release; lipocalin 2 (LCN2) for intracellular iron transport; ferritin light chain (F-LC), a component of the ferritin complex, for intracellular iron storage; transferrin for extracellular iron transport; and hemosiderin for extracellular iron storage and sequestration [359, 360]. These proteins combine to form two distinct pathways for iron management, the LCN2/HO-1/F-LC system for intracellular iron and transferrin/hemosiderin binding for extracellular iron. These pathways have been studied following TBI alone, but there has been no research on iron management in combining TBI with a secondary stressor such as prior chronic alcohol consumption.

Alcohol use has been shown to prolong neuroinflammation and neurodegeneration at post-TBI by impairing neurological recovery and exacerbating localized neuroinflammation [361, 362]. In addition, as an antiplatelet and anticoagulant, alcohol can thin blood and lead to more profuse bleeding [363]. Together, this suggests that prior alcohol use may increase iron accumulation as well as dysregulate its regular management

following TBI. This chapter examines the time dependent manner of iron regulation by LCN2, HO-1, F-LC, and hemosiderin under combined chronic alcohol exposure and FPI. Although no obvious signs of iron toxicity were present, alcohol did alter the expected FPI-induced iron regulatory pattern. In addition, microglia were observed to also play a role in iron management, in this way microglia may contribute another pathway for iron regulation.

4.2 Methods and Materials

4.2.1 Reagents

The OCT compound was purchased from Fisher Healthcare (#4585). Prussian blue soluble was purchased from Santa Cruz (sc-215757), eosin 5% from Sigma (#R03040-74), and hematoxylin solution from Merck (#HX69851575). Primary antibodies were purchased from Santa Cruz, Thermo Fisher, proteintech, and Abcam (**Table 4.1**). Secondary antibodies were purchased from Thermo Fisher (#32230 and #32260) for western blots and Abcam (ab64255 and ab97049) for immunohistochemistry. The streptavidin protein was purchased from Abcam (ab7403), Pierce DAB substrate kit from Thermo Fisher (#34002), and Cytoseal XYL from Thermo Scientific (#8312-4). The bicinchoninic acid kit for protein determination was purchased from Thermo Fisher (#23227) and the 4–20% precast protein gel (4561094) and trans-blot PVDF transfer kit (#1704272) were purchased from Bio-Rad. The chemiluminescent substrate was purchased from Advansta (#K-12045-D50).

Table 4.1 Source, Catalogue Number, and Dilution Factors of Antibodies Used in Immunohistochemistry and Western Blot Analyses.

Antibody	Marker for	Company	Catalog No.	Dilution for IHC	Dilution for WB
Anti-heme oxygenase 1	heme oxygenase 1	Santa Cruz	sc-390991	1:50	1:1000
Anti-NGAL	lipocalin 2	Thermo Fisher	PA5-79590	1:500	1:1000
Anti-ferritin light chain	ferritin light chain	proteintech	10727-1-AP	1:25	1:1000
Anti-Iba1	microglia	Abcam	ab178847	1:200	-
Anti-CD68	macrophage	Abcam	ab31630	-	1:1000
Anti-transferrin	transferrin	Abcam	ab82411	-	1:1000
Anti-β-actin	beta-actin	Abcam	ab8226	-	1:1000

4.2.2 Animals

Sprague-Dawley rats were purchased from Charles River Laboratory (Wilmington, MA), they were approximately 8 weeks old and weighed about 240-270 grams at the beginning of the experiment. Rats were kept in reversed 12 hrs. light/dark cycle and housed in controlled temperature and humidity conditions. All experiments were conducted in accordance with the National Institutes of Health institutional ethical guidelines for care of laboratory animals and approved by the Institutional Animal Care Use Committee of Rutgers University (Newark, NJ).

4.2.3 Alcohol feeding

Ethanol liquid-diet pair-feeding was employed according to our lab's previously described procedure [364, 365]. Briefly, equal pairs of weight-match rats were acclimated to Lieber-DeCarli control or 29% calorie (5% v/v) ethanol liquid-diets (Dyets Inc., Bethlehem, PA) for 1 week followed by pair feeding regimens for 12-14 weeks. Feeding of the control group was based on the amount of ethanol-liquid diet consumed by the ethanol group. The control-liquid diet was composed of 47% carbohydrate, 35% fat, and 18% protein while the ethanol-liquid diet was composed of 19% carbohydrate, 35% fat, 18% protein, and 29%

ethanol as percent of total caloric intake. Daily food intake was monitored, and weekly body weights were recorded. By the end of the experiment, the average body weight was 410-420 grams for the control group and 460-490 grams for the ethanol group. Prior to sacrifice, the blood alcohol concentration of all the rats on the ethanol-liquid diet was measured, and it was found to be 9.1-28.8 mM with an average of 15.6 mM which is consistent with our previous findings.

4.2.4 Fluid percussion injury

After alcohol feeding, traumatic brain injury was performed using a fluid percussion injury (FPI) model (Amscien Instruments, Richmond, VA) according to our lab's previously described procedure [254, 355, 366]. Briefly, rats were anesthetized with ketamine (100 mg/kg body weight) and xylazine (10 mg/kg body weight) through intraperitoneal injection and positioned on a stereotaxis frame. Craniotomy was performed by drilling a 3.0 mm size hole on the left parietal skull (2.5 mm lateral of the sagittal suture, 3.0 mm caudal of the coronal suture) leaving the dura intact. A Luer Lock hub was glued to the skull over the exposed dura with cyanoacrylate glue and secured with methyl-methacrylate resin (Henry Schein, Melville, NY). The next day, animals were anesthetized by isoflurane and received lateral FPI. Briefly, the Luer Lock hub of the animal was filled with fluid and fitted into the nozzle of the FPI device. Injury was induced by a pendulum weight striking the piston of a fluid filled cylinder and delivering a fluid pressure pulse to the exposed dura. Severity of the injury was controlled by the position of the weight on the pendulum, all animals received moderate injury or around 2.0 atm pressure [356]. After injury, the

hub was removed, the head was sutured, and the rat was returned to it cage. Control animals did not undergo surgery, sham animals underwent surgery but did not receive an injury.

4.2.5 Tissue processing

Animals were sacrificed at time points between several hours to 7-days post-injury. Blood samples were collected from the injury site or the carotid artery if no injury was administered and used in western blot analysis. Brains were removed from the skull and thoroughly washed in PBS. Cryopreservation was performed by subsequent overnight incubations in 4% paraformaldehyde, 10% sucrose, and 30% sucrose, respectively. Brains were then snap-frozen in Tissue-Tek OCT compound (Thermo Fisher, Waltham, MA) and stored at -80^{o}C until slicing. Coronal sections (10-20 μm) were cut on a Leica CM3050 cryostat and collected on Fisherbrand Superfrost Plus slides. Slides were air-dried overnight and then stored at -80^{o}C until staining.

4.2.6 Prussian blue

This reaction detects ferric iron (Fe^{3+}) in tissue sections. Treatment with acidic solutions of ferrocyanides causes any ferric ions (+3) in the tissue to combine with ferrocyanide and form blue pigments of ferric ferrocyanide. Sections were fixed in ice cold methanol for 10 mins., dried for 20 mins, and rehydrated in PBS for 10 mins. Sections were incubated in a working solution of 5% potassium ferrocyanide with 5% hydrochloric acid for 30 mins. after which they were thoroughly washed in distilled water before being counterstained with eosin for 1 min. The working solution was prepared fresh every time and discarded

after use. Results show iron (hemosiderin) as blue, red blood cells as bright pink, and tissue as light pink.

4.2.7 Turnbull's blue

This reaction detects ferrous iron (Fe^{2+}) in tissue. The crystalline structures of Prussian blue and Turnbull's blue compounds are identical but the method by which they are formed is different. Treatment with an acidic solution of potassium ferricyanide causes any ferrous ions (+2) in the tissue to react and form blue pigments of ferrous ferricyanide [367]. Sections were fixed in ice cold methanol for 10 mins., dried for 20 mins, and rehydrated in PBS for 10 mins. Sections were incubated in a working solution of 0.4 mg potassium ferrocyanide with 40 mL 0.006 N hydrochloric acid for 1 hr. after which they were thoroughly washed in 1% acetic acid before being counterstained with eosin for 1 min. The working solution was prepared fresh every time and discarded after use. Results show ferrous iron as blue, red blood cells as bright pink, and tissue as light pink.

4.2.8 Immunohistochemistry

Prussian and Turnbull's blue were combined with immunohistochemistry in a modified technique previously described by Blomster et al. [368]. Following Prussian or Turnbull's blue staining, sections were incubated with 0.3% H_2O_2 for 10 mins. to quench any endogenous activity. After washing, slides were permeabilized with buffer containing 1% bovine serum albumin and 0.4% Triton X-100 in phosphate buffered saline (PBS) then incubated with 10% bovine serum albumin and 0.4% Triton X-100 in PBS to block non-specific antibody binding. The sections were incubated overnight in a humidified chamber

at 4^{o}C with diluted primary antibody: mouse anti-heme oxygenase 1 (1:50, Santa Cruz), rabbit anti-Iba1 (1:200, Abcam), rabbit anti-NGAL (1:500, Thermo Fisher), or rabbit anti-ferritin light chain (1:25, proteintech) (**Table 4.1**). The following day, slides were thoroughly washed in PBS and incubated with the appropriate secondary antibody, biotinylated goat anti-rabbit (1:500, Abcam) for 1 hr. or biotinylated goat anti-mouse (ready-to-use, Abcam) for 20 mins. After washing, slides were incubated with streptavidin-HRP (1:10,000, Abcam) for 30 mins. After a final washing, staining was developed with 3,3'-diaminobenzidine tetrahydrochloride (DAB, Thermo Fisher) for 20 mins., immersed in distilled water to stop the reaction, and counterstained with eosin for 1 min. Alternatively, slides were counterstained with hematoxylin for 10 mins. and washed in running tap water for 10 mins. Sections were dehydrated through 4, 2 min. changes of alcohol (95%, 95%, 100%, and 100%) and mounted with Cytoseal XYL (Thermo Fisher) solution. Results show stained protein as brown, iron as blue, red blood cells as bright pink, and tissue as light pink. Images were captured with a Leica DMi1 or Aperio Versa 200 microscope and slide scanner.

4.2.9 Western blot

Collected blood was centrifuged at 2,100 x g for 10 mins. to separate the plasma for analysis. Protein concentration was estimated using the bicinchoninic acid (BCA) method (Thermo Fisher). 20 μg/lane of protein was loaded into the wells of 4–20% precast polyacrylamide gels (Bio-Rad, Hercules, CA) for separation. Separated proteins were transferred onto PVDF membranes, blocked with 5% non-fat milk, and incubated at 4^{o}C overnight with the respective antibody (1:1,000 dilution) (**Table 4.1**). The following day,

slides were thoroughly washed in tris-buffered saline with 0.1% Tween 20 and incubated with the appropriate secondary antibody, horse-radish peroxidase conjugated goat anti-mouse or horse-radish peroxidase conjugated goat anti-rabbit for 1 hr. (both 1:10,000, Thermo Fisher). After a final washing, immunoreactive bands were detected with WesternBright ECL chemiluminescent substrate (Advansta). Data was quantified as arbitrary intensity units with densitometry analysis using Image J software.

4.2.10 Statistical analysis

Statistical analysis was performed to determine a significant difference in the amount of protein expression between sham and injury. Results were analyzed with independent samples t-tests using the Rcmdr package of R software. Shapiro-Wilk tests were used to validate that the data was normally distributed and Levene's test to check groups did not significantly deviate from variance. Data are presented as mean ± standard error from the mean (SEM). The threshold for statistical significance was $p \leq 0.05$ ($* p \leq 0.05$, $** p \leq 0.01$ and $*** p \leq 0.001$).

4.3 Results

4.3.1 FPI indirectly causes iron accumulation in the CNS

One result of a fluid percussion injury (FPI) and, in general, any type of traumatic brain injury, is the accumulation of red blood cells (RBCs) [369]. These RBCs come from blood vessels ruptured by the transient mechanical forces produced by the impact. Hemorrhage can last up to several days consequently resulting in a substantial aggregation of RBCs especially in the epidural, subarachnoid, and ventricular spaces [370]. Due to their low

resistance and viscoelastic properties, with time, RBC aggregates can penetrate neighboring tissue (**Figure 4.1**) [371]. Interestingly, the most penetration was observed by RBCs at subarachnoid spaces as opposed to any other area. Since the subarachnoid space facilitates fluid flow into the brain, RBCs may be using this current to enter brain tissue [372].

Once removed from circulation, RBCs lose contact with this repository nutrient supply and undergo degeneration. Destruction of RBCs involves severe hemolysis and release of RBC constituents, including hemoglobin, heme, and iron, into the extracellular space. Immediately following injury, this released iron is in a free, ferrous (Fe^{2+}) form and can be stained using Turnbull's blue method [367]. Over time, this iron is oxidized to the insoluble ferric (Fe^{3+}) species and can be stained using Prussian blue. Large bleeding in the ventricular systems showed presence of ferrous iron 0-days post-FPI but by 7-days, all iron was converted to the ferric form (**Figure 4.1**). Understandably, large bleed sites accumulated large deposits of iron while small sites contained considerably less iron. Therefore, the amount of excess iron aggregation depends on the number of RBCs released by FPI.

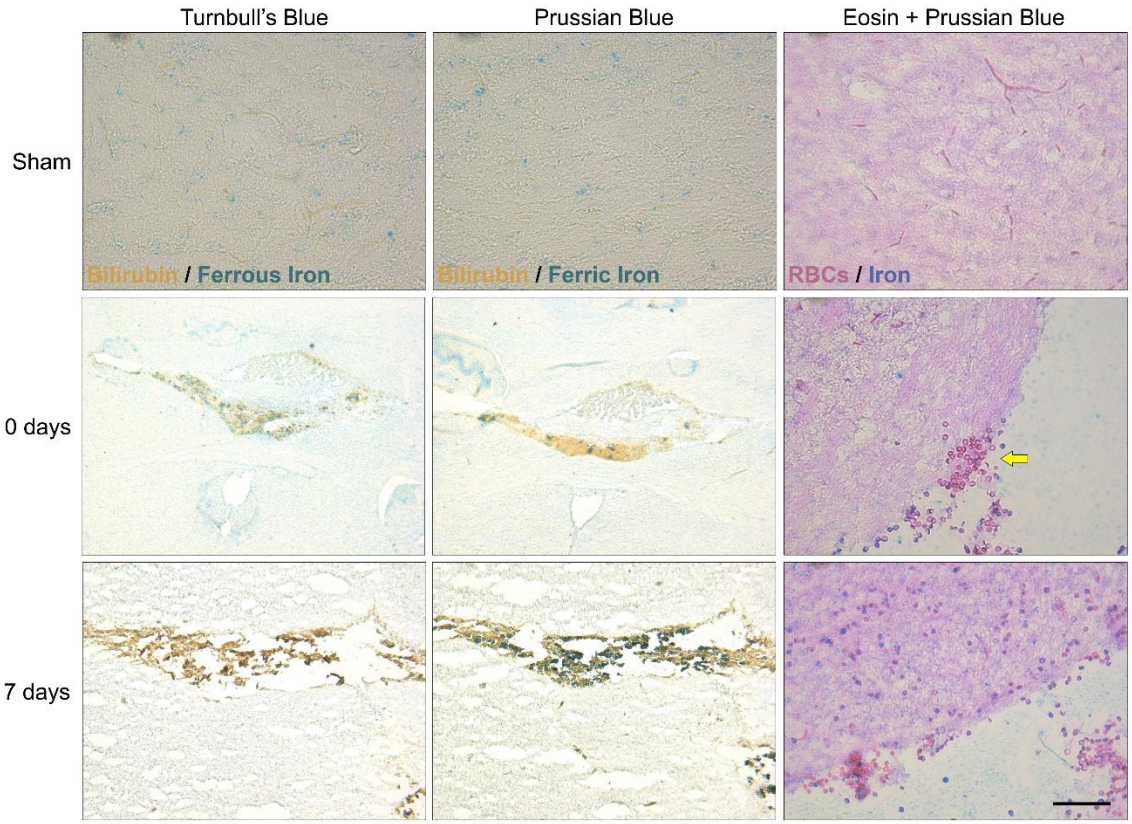

Figure 4.1 Ferrous and ferric iron expression following FPI. The left and middle column are representative images of presence of both ferrous (Fe^{+2}) and ferric (Fe^{+3}) iron at sham injury (Sham), and 0- and 7-days following moderate fluid percussion injury. Turnbull's blue method stains for free or ferrous iron while Prussian blue stains for ferric iron bound as hemosiderin. Both ferrous and ferric iron are stained dark blue while blood is distinguished by the yellow-brown bilirubin pigment. The right column are representative images of red blood cell penetration into the tissue over time. The yellow arrow points to an accumulation of red blood cells. Red blood cells are stained dark pink, iron is blue, and tissue is light pink. All images are focused near the ventricular systems or subarachnoid spaces, sites for major blood accumulation post-injury. The black bar represents 100 μm (N = 5 rats).

4.3.2 Ethanol exposure alters peak LCN2, HO-1, and F-LC expression following FPI

4.3.2.1 Moderate lateral fluid percussion injury

In their paper, Russell et al. describe a time-dependent induction of the iron regulatory proteins lipocalin 2 (LCN2), heme oxygenase 1 (HO-1), and ferritin light chain (F-LC) following an FPI-induced traumatic brain injury [360]. I have observed similar

results in rats that have undergone FPI alone. LCN2 presence was most notable directly at the site of impact. Expression peaked 1-day post-FPI, returning to Sham levels by 3- and 7-days (**Figure 4.2**). At 1-day post-FPI, LCN2 was found in individual cells throughout the tissue, most significantly in cells surrounding both ruptured and intact vessels. This early expression post-injury is attributable to LCN2 involvement in the innate immune response. By immediately trafficking and sequestering iron, LCN2 stimulates anticipation for possible incoming or excess iron to prevent its congestion. In this way, LCN2 may act as a master switch for the induction of subsequent iron regulatory proteins.

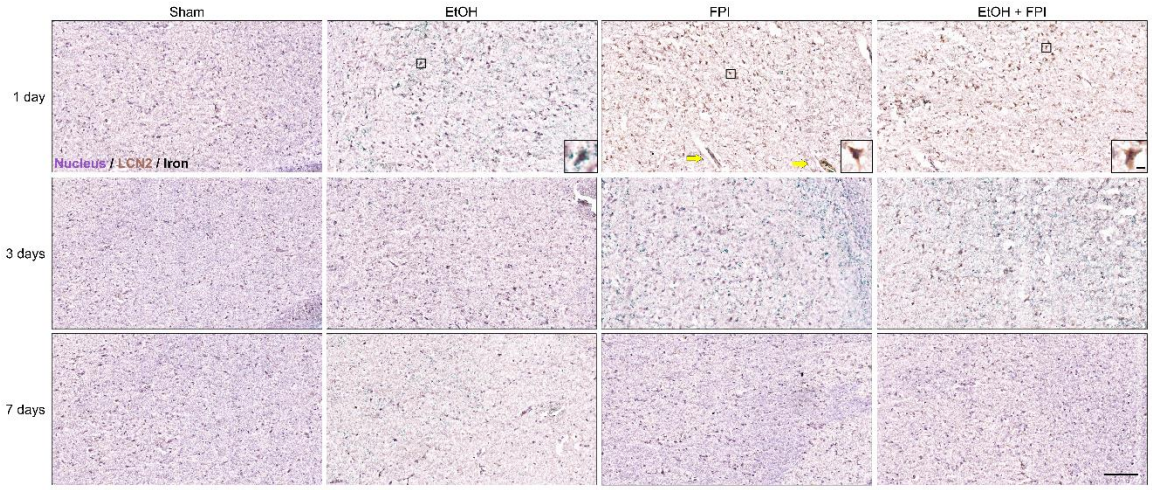

Figure 4.2 LCN2 induction by alcohol, FPI, and the combination. Representative images of lipocalin 2 expression in rats under sham injury (Sham), ethanol feeding (EtOH), fluid percussion injury (FPI), and injury following ethanol feeding (EtOH + FPI) 1-, 3-, and 7-days post-injury. Images focus on the neocortex at the site of impact. LCN2 is stained brown, nuclei purple, and positive ferric iron staining appears as black. The yellow arrows point to LCN2 expression around both longitudinal and cross-section vessels. The insets are higher magnifications of cells within the black box and demonstrate LCN2 generation by a single cell. The black bar represents 100 μm and inset bar represents 25 μm (N = 5 rats).

HO-1 expression was observed in the hippocampus and neocortex, prominently around the site of impact. HO-1 was evident 1-day post-FPI, peaking at 3-days, but by 7-

days post-FPI HO-1 was greatly reduced (**Figure 4.3**). Following peak expression, HO-1 became localized around vessels. Although, like LCN2, HO-1 is stress-responsive, its role is to catabolize free heme into iron, carbon monoxide, and biliverdin; therefore, HO-1 expression is expected to significantly rise upon RBC degeneration, occurring 3-days post-FPI. Although not quantified, the density and intensity of expression was similar between LCN2 and HO-1 staining around the impact site. Unlike immunofluorescence staining, immunoenzymatic methods allow for these descriptive assessments of expression because they are unaffected by manipulation from contrast adjustments. However, western blot analysis showed significantly increased expression of HO-1 ($p<0.001$) when compared to sham while LCN2 ($p=0.181$) did not (**Figure 4.6.D**). This discrepancy can be explained by LCN2 being primarily localized to the impact site and HO-1 being much more dispersed, while western blotting was only performed on plasma samples.

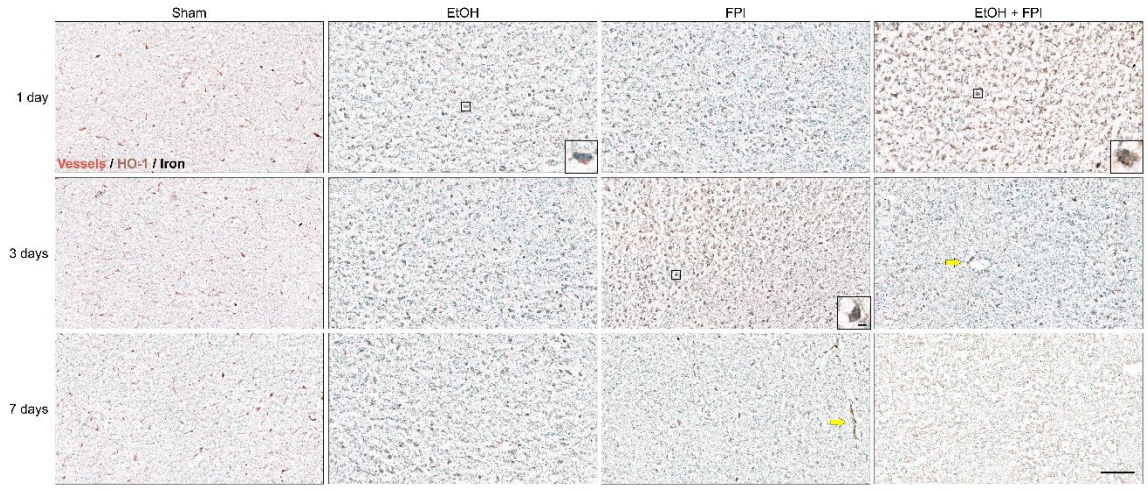

Figure 4.3 HO-1 induction by alcohol, FPI, and the combination. Representative images of heme oxygenase 1 expression in rats under sham injury (Sham), ethanol feeding (EtOH), fluid percussion injury (FPI), and injury following ethanol feeding (EtOH + FPI) 1-, 3-, and 7-days post-injury. Images focus on the neocortex at the site of impact. HO-1 is stained brown and positive ferric iron staining appears as black. Sham sections also stain for vessels as red. The yellow arrows point to HO-1 expression around both longitudinal and cross-section vessels. The insets are higher magnifications of cells within the black box and demonstrate HO-1 generation by a single cell. The black bar represents 100 μm and inset bar represents 25 μm (N = 5 rats).

Unlike LCN2 and HO-1, F-LC expression was more perilesional, found in the hypothalamic and basal forebrain regions of the brain. However, clusters of F-LC were found surrounding the RBCs and iron deposits in these areas. Minimal clusters were found 1-day post-FPI with gradual increases at 3-days and peak amounts 7-days post-FPI with clusters ranging from <1 μm to 50 μm in size (**Figure 4.4**). Increased F-CL ($p<0.001$) expression compared to sham was confirmed with western blot analysis (**Figure 4.6.D**). F-LC clustering may be the result of a partial unfolding of the protein shell in preparation for iron binding [373]. Unlike ferritin heavy chain (F-HC), F-LC has no ferroxidase activity, instead it is involved in the transfer of electrons across its protein cage which allows F-LC staining to mark unfolded shells [374]. This delayed expression of F-LC demonstrates ferritin as the final iron regulatory protein. It acts as a reservoir, collecting any remaining

iron and detoxifying the CNS. This may explain the decreased magnitude of F-LC expression compared to LCN2 or HO-1.

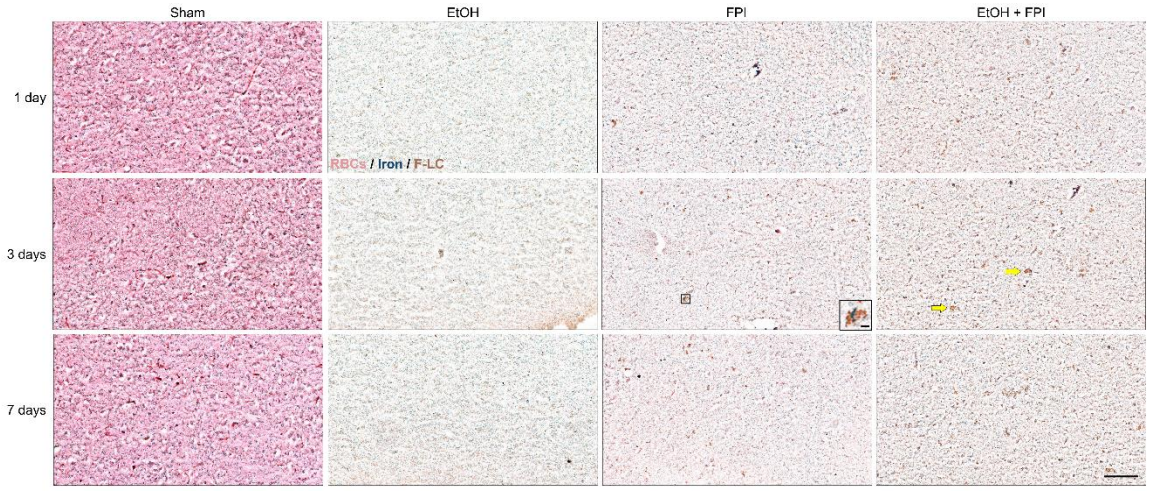

Figure 4.4 F-LC induction by alcohol, FPI, and the combination. Representative images of ferritin light chain expression in rats under sham injury (Sham), ethanol feeding (EtOH), fluid percussion injury (FPI), and injury following ethanol feeding (EtOH + FPI) 1-, 3-, and 7-days post-injury. Images focus on the hypothalamic and basal forebrain regions. F-LC is stained brown, red blood cells/vessels are red, ferric iron is dark navy, and tissue is light pink. The yellow arrows point to a cluster of F-LC expression. The inset is a higher magnification of cells within the black box and demonstrates F-LC generation at sites of red blood cell and iron accumulation. The black bar represents 100 μm and inset bar represents 25 μm (N = 5 rats).

4.3.2.2 Chronic alcohol consumption

In the CNS, one result of chronic alcohol consumption is increased and sustained basal presence of LCN2 (**Figure 4.2**), HO-1 (**Figure 4.3**), and F-LC (**Figure 4.4**). As a physiological stressor, ethanol can induce expression of these stress-responsive proteins. Expression was generally ubiquitous for all three proteins, however, some areas along the edge of the neocortex, did show greater expression (**Figure 4.4**). Being soluble in water, alcohol distributes into fluid spaces, as a result, higher concentrations of ethanol can be found in blood, or cerebral spinal fluid (CSF) surround the brain [375]. More ethanol infers

greater stress and more protein expression at areas in contact with blood or the CSF such as the neocortex. The magnitude of expression was also similar for all three proteins. Background staining may be due to low levels of LCN2, HO-1, and F-LC released by cells. These iron regulatory proteins may be actively secreted into the exterior of the cell in response to inflammation caused by alcohol presence.

4.3.2.3 FPI following alcohol consumption

Alcohol consumption dynamically changed the iron management timetable. LCN2 expression peaked at 1-day post-EtOH + FPI, like FPI alone, however, expression did not disappear 3- or 7-days later (**Figure 4.2**). Ethanol exposure did not alter the location or magnitude of FPI-induced LCN2. LCN2 has recently emerged as an iron regulatory protein by reason of its binding to siderophores and suppressing catalytic iron from accumulating in the cytoplasm [376]. Thus, LCN2's role is to facilitate iron transport or trafficking more so than direct chelation [377]. This may explain the similar peak LCN2 expressions between FPI and EtOH-FPI. This unchanged expression profile may also be due to LCN2's close association with the inflammatory response. This result demonstrates that combined, alcohol and FPI injuries do not necessarily exacerbate the degree of inflammation, but rather prolong its persistence. However, failure to resolve this inflammation can lead to a chronic inflammatory state in the CNS and manifest debilitations in attention and cognition [378]. Therefore, by maintaining LCN2 expression, alcohol consumption may transform FPI-induced inflammatory properties.

HO-1 induction occurred 1-day post-EtOH + FPI, earlier than with FPI alone (**Figure 4.3**). In addition, cellular expression density and intensity appeared greater than

that of LCN2. Like FPI, EtOH + FPI-induced HO-1 presence was prominent at the hippocampus, neocortex, and around vessels near the site of impact. This expression profile may be the consequence of increased bleeding caused by ethanol circulation in the blood stream [379]. Chronic alcohol consumption lengthens bleeding times of injured soft tissue by reducing platelet aggregation. Ethanol may interact with platelet cyclooxygenase-1 to inhibit its function and prevent subsequent development of pro-aggregatory proteins. Other haemodynamic changes in blood pressure and vessel integrity can also contribute to increased bleeding with alcohol. This augmented hemorrhage will result in greater and even faster accumulations of RBCs in the CNS (**Figure 4.6.B**). Therefore, HO-1 is expected to express promptly and regulate this RBC influx. Ethanol-induced increases in basal levels of HO-1 make early expression possible.

The most change in its expression profile after combined alcohol consumption and FPI injuries was observed for F-LC. F-LC greatly increased 1-day post-EtOH + FPI but peaked at 3-days and sustained these levels up to 7-days (**Figure 4.4**). Alcohol alone can increase ferritin and, with FPI, appears to exacerbate its presence [380]. Ferritin is not only involved in iron sequestration, through partial digestion and formation with lysosomes, ferritin creates the iron storing complex hemosiderin. Therefore, ferritin both directly and indirectly manages iron by chelating the metal ion and generating hemosiderin respectfully. For this reason, fold increases in ferritin are needed to contain the excessive numbers of RBCs released by FPI following alcohol consumption, so pronounced expression of F-LC here is expected. In fact, the CNS may become heavily reliant on ferritin if transferrin levels become saturated by rapid iron overabundance. Western blot analysis showed greater F-LC levels in plasma than transferrin (**Figure 4.6.D**). When this main iron binding

protein in the blood is so far extended that it cannot bind any more iron, excess catalytic iron must be stored by ferritin or hemosiderin to prevent iron toxicity. Such increased hemosiderin deposits were observed under EtOH + FPI (**Figure 4.6.B**).

4.3.3 Activated microglia are also involved in iron management

4.3.3.1 Activation

Many studies have already shown that traumatic brain injury activates microglia [381]. Microglia become activated after transitioning through a series of activation states [382]. During this time, microglia undergo changes in both morphology and function. I have also observed such changes in microglia following FPI. Sham injuries did not stimulate microglial activation and so microglia appeared resting with dynamic branching of their processes. However, fully activated microglia in round ameboid shapes were observed as early as 1-day post-FPI. This morphology was sustained at 3-days but by 7-days post-FPI microglia returned to their homeostatic state (**Figure 4.5**). In addition, the number of monocyte lineage cells, marked by CD68 expression, also significantly increased compared to sham controls ($p<0.001$) (**Figure 4.6.D**).

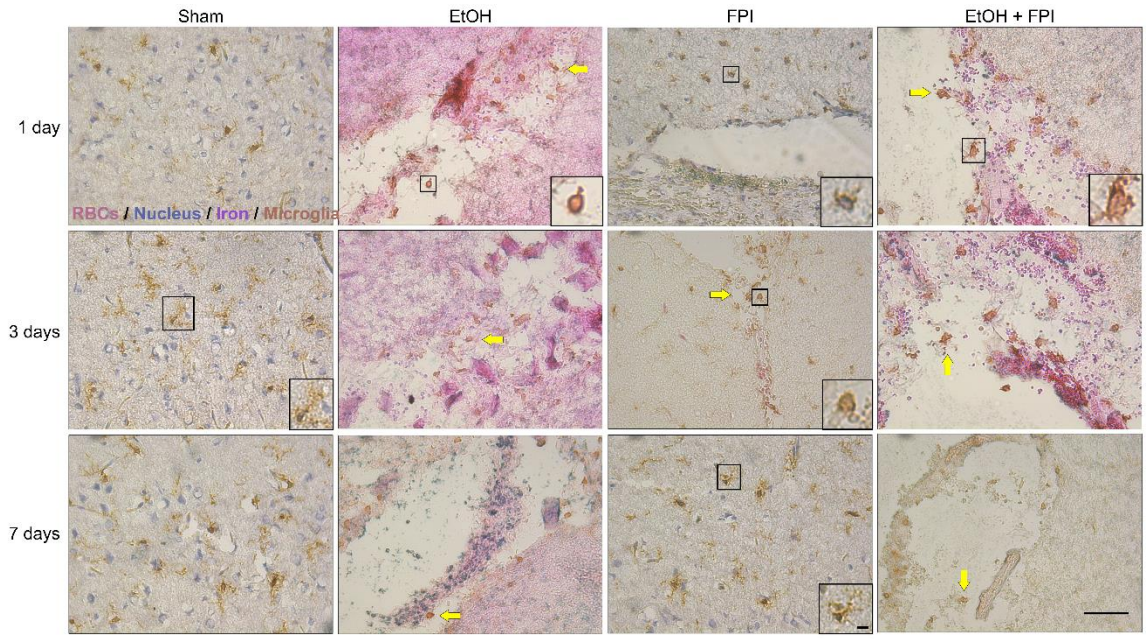

Figure 4.5 Microglial recruitment and activation by alcohol, FPI, and the combination. Representative images of the microglia-specific calcium-binding protein, Iba1, expression in rats under sham injury (Sham), ethanol feeding (EtOH), fluid percussion injury (FPI), and injury following ethanol feeding (EtOH + FPI) 1-, 3-, and 7-days post-injury. Sham images focus on the neocortex at the site of impact while EtOH, FPI, and EtOH + FPI images are focused near the ventricular systems and inferior colliculus at sites with major blood accumulation. Microglia are stained brown, cell nuclei are blue, red blood cells/vessels are red, ferric iron is purple, and tissue is light pink. The yellow arrows point to microglial recruitment to ventricular cavities and sites of red blood cell accumulation. The insets are higher magnifications of cells within the black box and demonstrate changes in microglial morphology following injury. Homeostatic, resting microglia exhibit dynamic branching while activated microglia take on an amoeboid form. Microglia in transition to the ameboid form have shortener, thicker processes. The black bar represents 100 μm and inset bar represents 25 μm (N = 5 rats).

Two important functions performed by activated microglia are motility and phagocytosis. Interestingly, many of these activated microglia remained in the tissue at 1-day, only being present around RBCs and bleed sites 3-days post-FPI. These results demonstrate that morphology precedes function and, although reacting quickly to an injury, microglia may have a delayed immune response to invading RBCs. However, microglia may be responding to only atypical RBCs such as those dying from nutrient deprivation

after being confined in tissue for 3-days post-FPI. Interestingly, a morphological gradient 3-days post-FPI was also observed (**Figure 4.6.C**). At the site of blood accumulation, the gathering microglia were in the active ameboid shape but, several micrometers away from this site resident microglia appeared stress-primed with short, thick processes. In this intermediary state, microglia are very reactive and can easily change to any other of the activation states. Microglia furthest away from bleed sites remained in a homeostatic, surveillance-inclined state.

Alcohol consumption resulted in sustained presence of activated microglia in and around the ventricular systems and inferior colliculus (**Figure 4.5**). Other studies also demonstrating this microglial response found that ethanol induces microglia activation by stimulating their toll-like receptor 4 (TLR4) [383, 384]. Our lab has previously shown that alcohol can induce neuroinflammation by upregulating expression of programmed death-1 receptor and its ligands in neuroimmune cells [42]. Therefore, as a sensing receptor, TLR4 may be recognizing released proinflammatory mediators and controlling microglial activation [228, 385]. Ultimately, as a prominent stressor, alcohol itself can mobilize microglial changes.

In FPI following chronic alcohol exposure, microglia also appeared activated at 1-day, invading cavities near the inferior colliculus. However, unlike in FPI or EtOH alone, there were greater numbers of microglia present (**Figure 4.5**). Since combined alcohol and FPI injuries generate the largest amount of bleeding and RBC aggregation, more microglia are necessary for proper regulation, repair, and recovery to homeostasis. High microglial numbers were sustained 3-days post-EtOH + FPI, but by 7-days, with considerably less RBC presence, there were fewer of these immune cells. However, microglia sustained an

activated form 1-, 3-, and 7-days under EtOH + FPI. Under alcohol alone, microglia remained activated for all days, therefore, the addition of FPI only reinforces continuation in this form. Interestingly, several of these microglia also appeared bigger in size. Further investigation revealed that microglia may be phagocytosing moribund RBCs.

4.3.3.2 Autophagy

One role of macrophage is to phagocytose senescent RBCs [386]. Therefore, in behaving like macrophage, activated microglia have been observed to also phagocytose RBC aggregations and, in so doing, regulate excess iron presence in the CNS. At 3-days post-FPI, sites with microglia and RBCs show these microglia ingesting individual, intact RBCs (**Figure 4.6.A**). In that same area, a neighboring microglia cell that has earlier phagocytosed an RBC is found with free, ferrous iron inside its cell body. The lack of surrounding free iron suggests that this cytoplasmic iron must come from the ingestion and breakdown of an RBC. However, microglia may also be phagocytosing iron-containing complexes seeing as bound, ferric iron was also found in microglia, otherwise, the iron released from ingested RBCs is quick sequestered as hemosiderin (**Figure 4.6.B**). With FPI following chronic alcohol consumption at 1-day, microglia appeared more reactive, ingesting more than one RBC or iron-containing complex at a time, and increasing tremendously in size. Conversely, the abundance of RBCs may simply force single microglia to ingest more. Phagocytosis was also observed under EtOH alone at sites with some RBC presence (**Figure 4.5**). Low CD68-positive staining confirm that these immune cells were not macrophage.

These results reveal a pathway for iron management by microglial cells (**Figure 4.8**). Activated microglia appear to be ingesting RBCs accumulating from ruptured vessels following FPI (**Figure 4.6.A**). Subsequently, heme is released and processed in the cell cytoplasm (**Figure 4.6.B**). Excess iron increases the labile iron pool (**Figure 4.6.A**) but is quickly sequestered and stored as ferritin (**Figure 4.4**) or hemosiderin (**Figure 4.6.C**). Free iron released by extracellular heme oxygenase 1 and surrounding the cells (**Figure 4.2**) is also efficiently managed with iron being removed by transferrin (**Figure 4.6.D**) or, when saturated, bound as hemosiderin with extracellular ferritin-lysosome complexes (**Figure 4.6.C**). Chronic alcohol use increases RBC aggregation and iron as well as iron storage (**Figure 4.6.B**), however no abnormal increases in free, ferrous iron were observed in the extracellular spaces. These results demonstrate microglial involvement as another efficient means of iron regulation in the CNS. Although alcohol consumption exacerbates iron accumulation, the iron management system can adjust to accommodate this increased influx. However, continued alcohol use may lead to further iron deposition or even release of iron stores and hasten the onset of alcohol related diseases in the CNS or other complications.

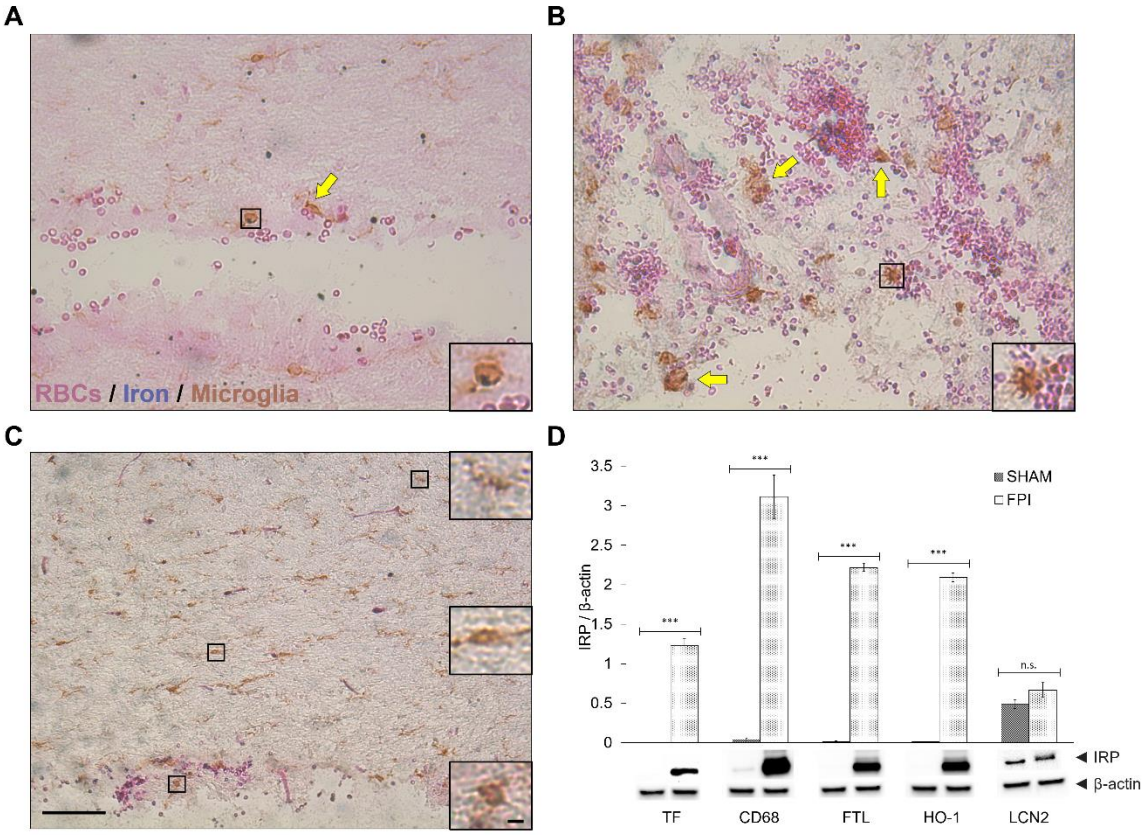

Figure 4.6 Microglial phagocytosis of accumulated red blood cells. (A) Representative image of microglial phagocytosis of red blood cells near the ventricular systems 3-days post-FPI. The iron stained is in the free, ferrous form. (B) Representative image of microglial phagocytosis of red blood cells in the cavities next to the inferior colliculus 1-day post-EtOH + FPI. The iron stained is in the bound, ferric form. (C) Representative image of a morphological gradient 3-days post-FPI. Microglia next to red blood cells have an ameboid form, those near bleed sites are primed with shorter, thicker processes, and microglia even further away remain in a resting, ramified state. For all images, microglia are stained brown, iron is blue, red blood cells are dark pink, and tissue is light pink. The yellow arrows point to active or completed phagocytosis. The insets are higher magnifications of cells within the black box and demonstrate (A and B) presence of iron and red blood cells inside the microglia or (C) changes in microglial morphology near bleed sites. The black bar represents 100 μm and inset bar represents 25 μm. (D) Bar graph showing western blot analysis of transferrin (TF), monocyte/macrophage marker (CD68), ferritin light chain (FTL), heme oxygenase 1 (HO-1), and lipocalin 2 (LCN2) levels in plasma following sham and FPI injuries. Data were analyzed using ImageJ to obtain arbitrary densitometry intensities and quantified as the ratio of iron regulatory protein (IRP) to β-actin. Results are presented as mean values (±SEM, N = 5 rats). FPI is compared to Sham injury for each protein. Significant difference is indicated by *** $p \leq 0.001$, n.s. denotes no significance.

4.4 Discussion

FPI causes the rupture of blood vessels through various transient mechanical forces caused by the impact [356]. Tensile and compressive forces stretch and compact vessels respectfully so that they become structurally weakened, while shear forces from blood and CSF fluid rush cause additional damage. Increases in magnitude and repetition of these forces causes eventual vessel breakage and hemorrhage. The opening of blood vessels is necessary to allow oxygen, nutrients, and immune cells to reach the affected area and accelerate healing. In fact, vasodilation occurs to allow even more entry of these beneficial factors [387]. Unfortunately, the consequence of this increased blood flow is hemorrhage and accumulation of RBCs in the brain. Failure to clear RBC aggregates can cause the formation of an impacted blood mass and result in an enduring mass effect. Since hemorrhage can last several days, the accumulation may become staggering. In addition, the many crevices and cavities provided by the structure of the brain can collect and trap blood. Directly, this blood mass can increase pressure in the CNS and interfere with brain function [388]. Overtime, the incompressible, viscoelastic properties of RBCs allow them to easily deform and penetrate surrounding tissue [389]. However, removed from the nutrient supply provided by the circulation, RBCs begin to die, hemolyze, and release hemoglobin solution and iron into the CNS (**Figure 4.1**). Therefore, proper iron management is an important process to repair and restore homeostasis.

4.4.1 Excess iron is regulated by three distinct pathways

4.4.1.1 Hemosiderin and transferrin binding. Resident iron levels and hemosiderin deposits in the brain are very small and inapparent with general stains. Therefore, the Prussian and Turnbull's blue methods could only stain for iron and hemosiderin originating from RBCs. In this way, excess iron can be easily identified and distinguished from inherent iron. In fact, these methods were sensitive enough to stain for iron produced by just one RBC (**Figure 4.1**). In addition, both Prussian and Turnbull's blue were able to penetrate cells and stain for iron present inside intact vessels (**Figure 4.3**) as well as iron trapped by microglia (**Figure 4.6**). Finally, these methods did not interfere with other chromogens, such as the naturally occurring bilirubin (**Figure 4.1**), however the overlay of multiple stains did cause positive iron to appear different shades of dark blue.

In agreement with others, I have found that iron remains ferrous for only a few hours following injury as ferric iron was observed as early as 1-day post-FPI (**Figure 4.4**). In its ferric form, iron can be bound to transferrin for transport, ferritin for immediate storage, or hemosiderin for long-term storage (**Figure 4.8**). Free iron, whether as a ferrous cation or an unbound ferric species, is readily absorbed by cells and can be very toxic [390]. The unpaired electrons make free iron highly chemically reactive and, through the Fenton-Haber-Weiss reaction, catalyze the formation of free radicals (**Figure 4.8**). This may be a reason for iron's rapid transformation from the ferrous, to the ferric, and finally to the bound form by the body.

Transferrin is an iron carrier and its binding results in the transport of iron through the circulation and subsequent removal from the CNS [391]. As the only protein capable of transporting iron, transferrin binding becomes the ultimate pathway for excess iron

detoxification. Although increased following injury (**Figure 4.6.D**), transferrin becomes saturated when ~70% is bound with iron [392]. Instead, ferritin and hemosiderin, a complex formed from combining partially degraded ferritin with lysosomes, are involved in sequestering excess iron. Since, in its ferric form, iron is quickly processed, with excessive iron being bound as hemosiderin, Prussian blue staining exposes deposits of these iron-containing complexes (**Figure 4.1**). Significant amounts of hemosiderin collections, ranging in size, were found at all bleed sites. These results reveal hemosiderin binding as a pathway in iron management specially reserved for superfluous excesses of iron. Iron as hemosiderin is not readily available for release thereby making this binding very stable. Like ferritin binding, iron release from hemosiderin may possibly be achieved by lysosomes. Extracellular hemosiderin complexes may also follow suit and be degraded by strong digestive enzymes. More research is needed on the fate of iron following hemosiderin binding and on understanding the circumstances and elements involved in its release; it is likely lysosomes are involved.

4.4.1.2 Sequestration by iron regulatory proteins. The lipocalin 2/heme oxygenase 1/ferritin system is the chief regulatory mechanism for processing intracellular excesses of iron. As the first responding iron managing protein, LCN2 organizes existing iron for chelation, by binding to siderophores, or transport to ensure incoming iron does not accumulate in the cytoplasm. Important to the innate immune response, LCN2 expression may also correspond to insult severity and help mobilize the appropriate response. Currently, LCN2 levels are being used to diagnose several inflammatory diseases such as acute kidney injury **[51]**. I have seen in both FPI and EtOH + FPI situations a similar

expression pattern, that is, early, rapid increase, peaking at 1-day post-injury but decreasing to its lowest levels at 3-days (**Figure 7**). This result demonstrates that LCN2 induction may not depend on the type of injury but rather by the inflammation associated with the injury. Therefore, if the injury causes any release of inflammatory stimuli, LCN2 will be expressed. Moreover, the magnitude and length of LCN2 expression may indicate the degree of inflammation. LCN2 may occupy a greater role in iron regulation than has been so far suggested.

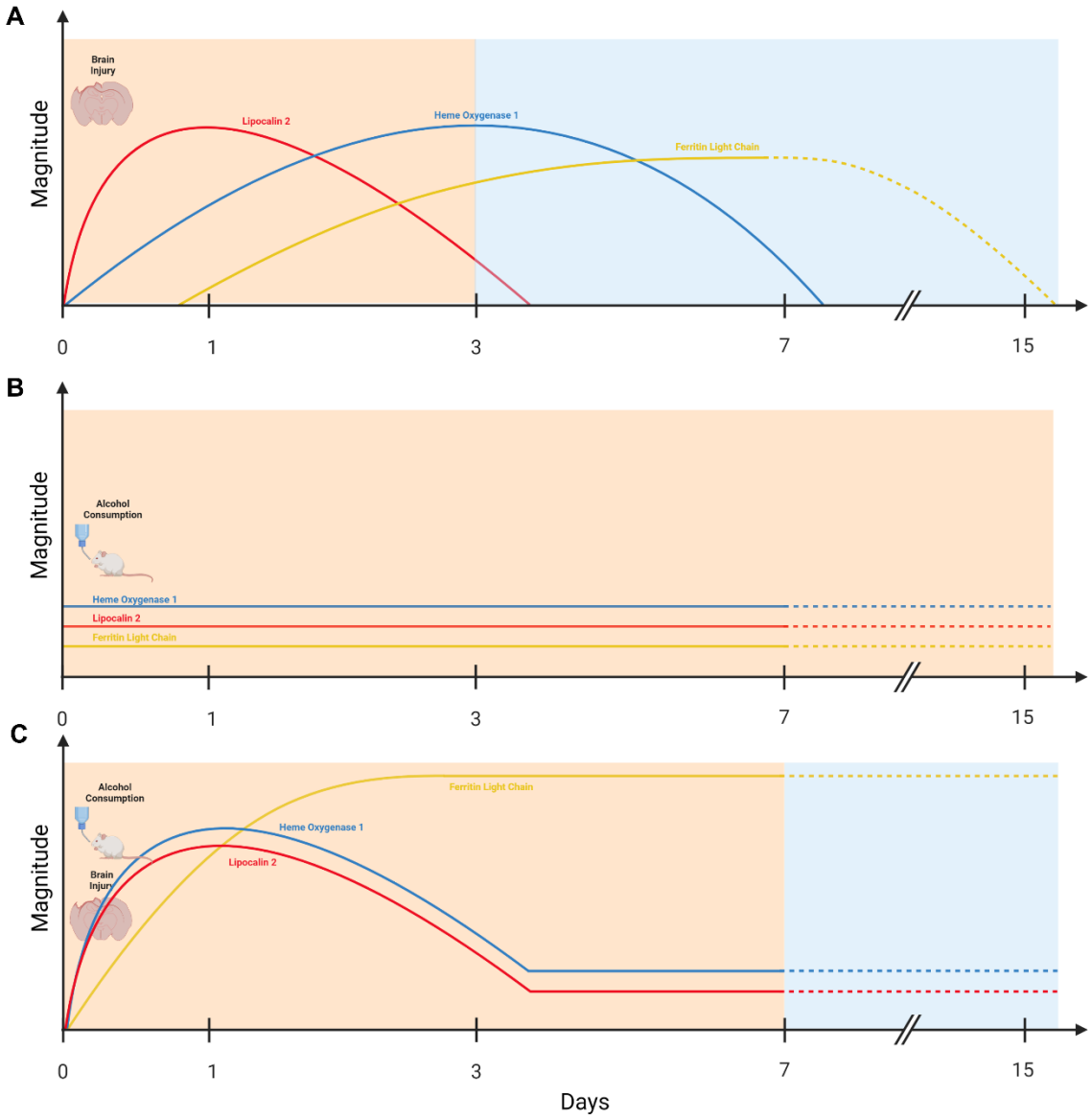

Figure 4.7 Summary of LCN2, HO-1, and F-LC presence over time. Cartoon graphs depict the expression length and magnitude of each iron regulatory protein after its induction by (A) brain injury, (B) alcohol consumption, or (C) the combination. The magnitude units are arbitrary, time is expressed in days with Day 0 representing injury initiation. The red, blue, and yellow lines denote LNC2, HO-1, and F-LC respectfully. The dashed lines speculate expression after 7-days post-injury. The light orange shading signifies hemorrhage/a pro-inflammatory response while the light blue shading signifies repair/an anti-inflammatory response. All cartoons were created with BioRender.com.

This study has demonstrated that excess iron comes from RBC accumulation following FPI, specifically the heme compound released by dying RBCs. This heme can trigger the synthesis of HO-1. HO-1 degrades heme by opening its porphyrin ring to release free iron [393]. One important regulator of HO-1 expression is the nuclear transcription factor Nrf2. Nrf2 also controls production of the antioxidant proteins that protect against the oxidative damage caused by an insult. Therefore, HO-1 is directly related to the presence and extent of oxidative damage. Our lab has previously shown that inflammation, from both FPI and the resulting hemorrhage, can trigger oxidative damage. Since LCN2 expression is determined by inflammation and HO-1 is mediated by oxidative stress, HO-1 induction is expected to occur after LCN2 under FPI (**Figure 4.7**). However, alcohol presence causes HO-1 to express concurrent with LCN2 (**Figure 4.7**). EtOH + FPI must exacerbate oxidative damage enough to deregulate the inflammatory response and cause this shift to earlier protein expression.

Ferritin, as the primary iron-storage protein of the cell, is paramount to the success of iron management. Insufficient levels, and eventual transferrin saturation, would cause free, toxic forms of iron to circulate in the body which, over time and more iron accumulation, would lead to iron overload. In fact, ferritin levels are used as a measure to infer iron concentrations in the body [394]. Individuals with hemochromatosis, an inherited mutation in the genes that causes increased iron absorption, show high levels of ferritin while those with anemia, a reduction in RBCs, show low levels and indicate an iron deficiency. Like others, I have seen a delayed ferritin response following FPI, peaking at 7-days (**Figure 4.7**). In addition, I qualitatively observed that the intensity of expression was less than either LCN2 or HO-1. These results demonstrate that ferritin is the final

regulatory protein involved in iron management, sequestering any remaining unbound iron for accessible storage. Even hemosiderin, observed 1-day post-FPI, precedes significant ferritin expression (**Figure 4.4**). Furthermore, this delay shows ferritin to be induced primarily by iron release and secondarily by heme presence. Low ferritin levels under EtOH alone suggest that ferritin is nominally induced by stress. However, EtOH + FPI caused early, increased, and sustained ferritin expression. Due to the excess RBC accumulation following these combined injuries, much of this ferritin may be being excreted and transformed to hemosiderin for more stable storage. These increased ferritin levels also imply high iron concentrations in the CNS.

Interestingly, LCN2, HO-1, and F-LC were also expressed directly atop bleed sites, interacting with RBCs (**Figure 4.4**). This presence may be explained by the mechanical forces caused by the impact bursting cells and releasing intracellular proteins into the extracellular space. As demonstrated, alcohol may also help facilitate secretion of these proteins by increasing their basal levels. There is evidence of LCN2, HO-1, and F-LC secretion in other organ systems. Hepatic cells have been shown to secrete ferritin, while HO-1 has been found in various extracellular, fluid filled compartments and LCN2, as a mediator of inflammation, is routinely released by various cell types, most notably immune cells [395-397]. Extrapolating these findings and relating then to the CNS space, HO-1 may be in the CSF while LCN2 gets secreted by astrocytes and microglia, and ferritin released by neurons. Then protein targeting mechanisms may explain their localization at sites of RBC aggregation. More research on the default expression levels and locations of LCN2, HO-1, and F-LC in the CNS as well as their intrinsic signaling sequences may help to explain this phenomenon.

To curb the scope of this study I did not stain for colocalization of these proteins with themselves or specific cell markers. In their paper, Russell et al. did perform colocalization and found overlap in LCN2, HO-1, and F-LC with GFAP, a marker for astrocytes, as well as LCN2 with HO-1 and LCN2 with F-LC between 1- to 7-days post-FPI. LCN2/HO-1 colocalization can indicate that even HO-1 may not be constrained to expression following FPI, instead it can be induced by the oxidative stress accompanying inflammation [398]. Meanwhile, LCN2/F-LC colocalization suggests LCN2 expression may recruit F-LC generation in preparation for iron sequestration. The lack of microglial expression of these iron regulatory proteins suggests microglia may not be involved in the lipocalin 2/heme oxygenase 1/ferritin system of iron management. Another limitation of this study was confining it to 7-days. However, previous studies have shown that beyond 7-days, LCN2, HO-1, and F-LC levels comparatively return, or being to return, to basal levels in most cells of the CNS [360]. A notable exception are microglia which have shown elevated HO-1 expression as late as 30-days relative to controls under a moderate cortical impact [399]. In this effect, I argue that microglial involvement may create a separate pathway for iron management, removed from that created by the iron regulatory proteins of the remaining CNS cells.

4.4.1.3 Microglial phagocytosis. To my knowledge, this is the first demonstration of RBC phagocytosis by microglia and subsequent cytosolic iron deposition following injury. Previous studies revealing iron presence in microglia have only considered this accumulation as iron retention and a signature of microglial activation [400]. The idea of a link between iron management, by extent metabolism, and activated microglia has been

contemplated for some time [401]. Moreover, the capacity for RBC autophagy by microglial cells has already been well established as an important corrective response to CNS hemorrhage [402]. In agreement with previous studies, I have observed microglial activation following FPI alone [403]. In addition, chronic alcohol exposure also provoked activation (**Figure 4.5**) [404]. Expectedly, the combination likewise caused microglia activation and greater numbers to gather at sites with RBC aggregation. Interestingly, this was found as early as 1-day post-EtOH + FPI with many microglia already swollen with RBCs and iron deposits (**Figure 4.6.B**). Chronic alcohol use prior to FPI may be sensitizing microglia to stress and, in this manner, preconditioning the brain to future injuries. In other words, the CNS stays in 'high alert' for possible stress so that when stress does appear an appropriate response is rapidly mobilized. This state of hypervigilance may dysregulate inflammatory and immune responses to cause inappropriate and even exaggerated reactions. In this respect we observed multiple RBCs within activated microglia following EtOH + FPI. This excessive phagoptosis may either be due to chronic phagocytic activity or the engulfment of multiple RBCs at once. Similarly, the increased number of microglia present may either be the result of migration, division, or some degree of both. Future work will include studies exploring these fundamental possibilities. A recent study has shown that microglia can assume a range of phenotypes under alcohol dependency and much remains to be understood in regard to their activation [405].

Collectively, these results begin to distinguish a pathway for iron maintenance by microglial cells. Activated microglia phagoptose and hemolyze RBCs, catabolize heme, and release free iron. Immediately, this iron gets bound to ferritin or hemosiderin. Any extracellular free iron becomes bound to apotransferrin or hemosiderin to form iron-

containing complexes. Knowledge of macrophage iron management can be used to infer other details of the microglial-centric pathway. Heme transporters may also be involved in transporting heme into the cell or release it from plasma membrane-derived vacuoles following phagocytosis. Increases in the labile iron pool may cause excess iron to catalyze production of reactive oxygen species. Iron release may be inhibited by hepcidin hormone binding to and degrading ferroportin transporters. As iron can only bind when in the ferric form, membrane bound ferroxidases may be oxidizing the ferrous form. As an additional idea, the debris following RBC hemolysis and heme release may be shuffled to lysosomes for degradation (**Figure 4.8**). Any lysosomal iron may be combined with partially degraded ferritin protein to create hemosiderin. Finally, additional stressors may free iron and evoke toxicity such as ferroptosis, an iron-dependent programmed cell death [406]. Many directions remain to be studied in an effort to understand iron management by microglial cells. I have only begun to discover this alternative pathway of iron regulation.

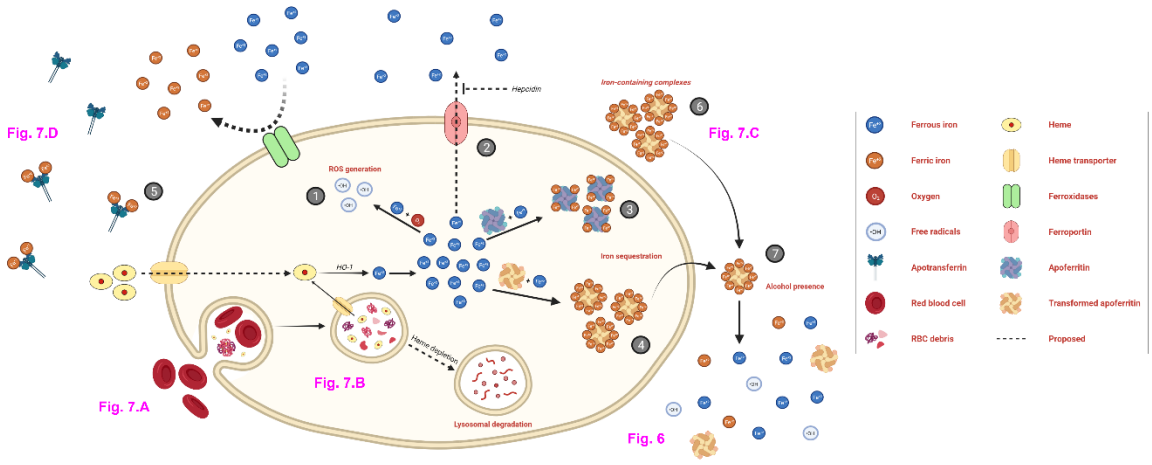

Figure 4.8 Schematic of iron regulation by activated microglia. Cartoon depicts pathways for microglial management of excess iron following traumatic brain injury. Activated microglia phagocytose red blood cells whereupon heme becomes released. Following heme depletion, any remaining debris may be transported to lysosomes for degradation. Alternatively, extracellular heme may be transferred into the microglia via a heme transporter. Cytosolic heme can be lysed by heme oxygenase 1 to release free iron and increase the labile iron pool. Excessive intracellular iron can be: (1) oxidized to produce reactive oxygen species, (2) released by ferroportin transporters, (3) stored by ferritin, or (4) bound as hemosiderin for long term storage. Excessive extracellular iron can be converted to the more stable, ferric form by ferroxidases and (5) bind to apotransferrin for transportation or, when apotransferin becomes saturated, (6) be stored in iron-containing vesicles. (7) However, in the presence of alcohol, stored iron may be released, converted to its toxic, ferrous form by ferrireductase, and, as a result, generate oxidative stress. The pink text indicates a representative image that depicts this event. The cartoon was created with BioRender.com.

4.4.2 Alcohol's influence extends to iron management

As the major alcohol filtrating and metabolizing organ of the body, the liver becomes an obvious site for alcohol-induced iron build-up [407]. In fact, this iron accumulation has been shown to contribute to the onset of alcoholic liver disease. This then develops into hepatitis and, over time, liver cirrhosis and destruction. In these same respects, generation of iron deposits in the brain may also lead to a form of inflammation and, if not corrected, neurodegeneration. This study has shown that alcohol consumption increases bleeding and consequent iron deposition in the CNS (**Figure 4.6.B**). In addition, alcohol abuse has also

been shown to frequent rebleeding incidents and, in so doing, can augment deposition numbers even more [408]. Despite this, I did not observe noticeable amounts of ferrous iron under EtOH + FPI. Therefore, although alcohol consumption significantly increases iron load in the CNS, the iron regulatory mechanisms adapted to accommodate this upsurge and prevent free iron accumulation and iron toxicity. To this effect, this study has shown that prior chronic alcohol exposure changes the response of all three iron management pathways following FPI (**Figure 7**). Specifically, alcohol galvanized LCN2, HO-1, and F-LC into early expression and, for F-LC, maintained this level. Even though LCN2 and HO-1 expression did greatly recede over time, low levels were still found. It may be that continued chronic alcohol consumption following FPI is required to release hemosiderin bound iron. This persistent stress would prevent inflammation from resolving and deregulate CNS functions. One affected system may be iron storage wherein the hemosiderin protein complex becomes destabilized and releases iron. Future research should examine iron aggregation and regulation when chronic alcohol consumption is continued following FPI (an EtOH + FPI + ETOH model).

4.5 Conclusion

The iron management system in the body is very efficient, especially so in the CNS. This becomes most evident when examining iron regulation under FPI following chronic alcohol consumption. In effect, three distinct pathways coordinate to ensure iron is only ever briefly unbound. The LCN2/HO-1/F-LC arrangement serves to identify, extract, and sort excess iron coming from its primary source, hemorrhage. Meanwhile, transferrin and hemosiderin binding control the overflow. I have shown that microglia play a role as well

in clearing away some of the RBCs and iron deposits. Even with these processes, the CNS has additional chelators and neuromelanin to trap more iron. There may also be even more iron regulatory pathways and iron toxicity safeguards yet undiscovered. These results contribute to and expound upon the impressive iron management system.

CHAPTER 5

SUMMARY CONCLUSION

In Chapter 1 I conduct a literary search and describe alcohol use and HIV-1 infection as having a pervasive impact on brain function, which extends to the requirement, distribution, and utilization of energy within the central nervous system. This effect on neuroenergetics may explain, in part, the exacerbation of HIV-1 disease under the influence of alcohol, particularly the persistence of HIV-associated neurological complications. I wanted to highlight the possible mechanisms of HIV/AIDS progression in alcohol users from the perspective of oxidative stress, neuroinflammation, and interruption of energy metabolism. These include the hallmark of sustained immune cell activation and high metabolic energy demand by HIV-1-infected cells in the central nervous system, with at-risk alcohol use. The increase in energy supply requirement by HIV-1-infected neuroimmune cells as well as the deterrence of nutrient uptake across the blood-brain barrier significantly depletes the energy source and neuro-environment homeostasis in the CNS. Finally, I described the mechanistic idea that comorbidity of HIV-1 infection and alcohol use can cause a metabolic shift and redistribution of energy usage toward HIV-1-infected neuroimmune cells. Under such an imbalanced neuro-environment, meaningless energy waste is expected in infected cells, along with unnecessary malnutrition in non-infected neuronal cells, which is likely to accelerate HIV neuro-infection progression in alcohol use. Thus, it will be important to consider the factor of nutrients/energy imbalance in formulating treatment strategies to help impede the progression of HIV-1 disease and associated neurological disorders in alcohol use.

In Chapter 2 I explored alcohol and HIV-1 protein trans-activator of transcription (TAT) on macrophage migration. TAT is an HIV-1 regulatory protein that is actively sloughed by infected cells. Once released, TAT can injure bystander cells and bring about their dysfunction. In the presence of ethanol, TAT-induced toxicity potentiates and, in so doing, exacerbates inflammation. One key aspect of neuroinflammation involves the infiltration of peripheral macrophage to the central nervous system. I used an interactive neuroimmune cell coculture of brain endothelial, astrocyte, neuron, and macrophage cells to model the blood-brain barrier and evaluate macrophage migration upon challenge with ethanol and TAT concentrations. I have limited this study to examine TAT concentrations found in people living with HIV-1 with (5 ng/mL) or without (25 ng/mL) viral suppression and ethanol doses below the legal driving limit (10 mM). In so doing, I study the effects of casual drinking on people living with HIV-1 but experiencing the best possible clinical outcome. Results showed that TAT alone increases macrophage migration immediately (before 4 hrs.) while ethanol alone increases migration in a delayed manner (occurring at 48 hrs.). Ethanol-induced NO production by endothelial cells and TAT's chemoattractant properties may explain this dichotomy in migration pattern. Combined low dose ethanol significantly increased migration under both 5 ng/mL and 25 ng/mL TAT injuries across all timepoints. These findings suggest that co-presence of ethanol and TAT may be the combination of an initial TAT effect followed by subsequent ethanol injury. I also examined the structural and behavioral changes of neurons treated with TAT and ethanol to understand their contribution to neurotoxicity.

Chapter 3 examined a possible antiretroviral compound called Drug-S. Although the combination of highly active antiretroviral therapy (cART) can remarkably control

human immunodeficiency virus type-1 (HIV-1) replication, it fails to cure HIV/AIDS disease. It is attributed to the incapability of cART to eliminate persistent HIV-1 contained in latent reservoirs in the central nervous system (CNS) and other tissue organs. Thus, withdrawal of cART causes rebound viral replication and resurgent of HIV/AIDS. The lack of success on non-ART approaches for elimination of HIV-1 include the targeted molecules not reaching the CNS, not adjusting well with drug-resistant mutants, or unable to eliminate all components of viral life cycle. I show that our lab's newly discovered Drug-S can effectively inhibit most HIV-1 infection at the low concentration without causing any toxicity to neuroimmune cells.

Finally, Chapter 4 explored the effects of combined chronic alcohol use and traumatic brain injury on iron management. Hemorrhage is often a major component of traumatic brain injury. However, without a defined clearance system, red blood cells (RBCs) are forced to accumulate at the hemorrhagic site. Upon energy depletion, RBCs undergo hemolysis and release free iron into the central nervous system (CNS) that must be efficiently managed to prevent accumulation associated toxicities. Prior chronic alcohol consumption, as a secondary stressor, may increase iron aggregation and alter its management. Using an animal model of chronic alcohol exposure and fluid percussion injury (FPI), I examined iron regulation under this combined injury. Results showed that excess iron can be managed by three distinct pathways, transferrin and hemosiderin binding, a lipocalin 2/heme oxygenase 1/ferritin system, and microglial phagocytosis. Previous studies have shown that in the CNS iron is regulated in a time-dependent manner following FPI. With alcohol exposure, more iron deposition was found as well as a time shift to regulation. In addition, I provide evidence that microglia also play a role in iron

management through RBC phagocytosis. These results reveal the intricacy and plasticity of iron management and highlight the importance of proper iron regulation in the CNS.

REFERENCES

1. Joint United Nations Programme on HIV/AIDS *Global HIV & AIDS statistics — 2020 fact sheet*. 2020. Accessed 02-20-2021. Retrieved from https://www.unaids.org/en/resources/fact-sheet.

2. HIV.gov *Global statistics*. 2020. Accessed 02-20-2021 Retrieved from https://www.hiv.gov/hiv-basics/overview/data-and-trends/global-statistics.

3. CDC, *Estimated HIV incidence and prevalence in the United States, 2014–2018.* Centers for Disease Control and Prevention, 2020: p. Acessed 02-20-2021 Retrieved from https://www.cdc.gov/hiv/pdf/library/reports/surveillance/cdc-hiv-surveillance-supplemental-report-vol-25-1.pdf.

4. CDC, *Human immunodeficiency virus (HIV) diagnoses, by year of diagnosis and selected characteristics: United States, 2012–2017.* Centers for Disease Control and Prevention, 2018: p. Acessed 02-20-2021 Retrieved from https://www.ncbi.nlm.nih.gov/books/NBK551099/table/ch3.tab11/?report=objectonly.

5. CDC, *Monitoring selected national HIV prevention and care objectives by using HIV surveillance data—United States and 6 dependent areas, 2018.* Centers for Disease Control and Prevention, 2020: p. Accessed 02-20-2021 Retrieved from https://www.cdc.gov/hiv/pdf/library/reports/surveillance/cdc-hiv-surveillance-supplemental-report-vol-25-2.pdf.

6. Nance, R., Delaney, J.A., Simoni, J., Wilson, I., Mayer, K., Whitney, B., Aunon, F., Safren, S., Mugavero, M., Mathews, W., Christopoulos, K., Eron, J., Napravnik, S., Moore, R., Rodriguez, B., Lau, B., Fredericksen, R., Saag, M., Kitahata, M., Crane, H., *HIV viral suppression trends over time among HIV-infected patients receiving care in the United States, 1997 to 2015.* Annals of Internal Medicine, 2018. **169**(6): p. 376-384.

7. Crepaz, N., T. Tang, G. Marks, M.J. Mugavero, L. Espinoza, and H.I. Hall, *Durable viral suppression and transmission risk potential among persons with diagnosed HIV infection: United States, 2012-2013.* Clinical Infectious Diseases, 2016. **63**(7): p. 976-83.

8. Yehia, B.R., J.A. Fleishman, J.P. Metlay, R.D. Moore, and K.A. Gebo, *Sustained viral suppression in HIV-infected patients receiving antiretroviral therapy.* Jama, 2012. **308**(4): p. 339-42.

9. Chander, G., B. Lau, and R.D. Moore, *Hazardous alcohol use: a risk factor for non-adherence and lack of suppression in HIV infection.* Journal of Acquired Immune Deficiency Syndromes, 2006. **43**(4): p. 411-7.

10. Kalichman, S.C., T. Grebler, C.M. Amaral, M. McNerney, D. White, M.O. Kalichman, C. Cherry, and L. Eaton, *Viral suppression and antiretroviral medication adherence among alcohol using HIV-positive adults.* International Journal of Behavioral Medicine, 2014. **21**(5): p. 811-20.

11. Hahn, J.A. and J.H. Samet, *Alcohol and HIV disease progression: weighing the evidence.* Current HIV/AIDS Report, 2010. **7**(4): p. 226-33.

12. Greenwood, B.N. and R. Agarwal, *Matching platforms and HIV incidence: an empirical investigation of race, gender, and socioeconomic status.* Management Science, 2016. **62**(8): p. 2281-2303.

13. Seabrook, J.A. and W.R. Avison, *Socioeconomic status and cumulative disadvantage processes across the life course: implications for health outcomes.* Canadian Review of Sociology, 2012. **49**(1): p. 50-68.

14. Kalichman, S.C. and D. Rompa, *Functional health literacy is associated with health status and health-related knowledge in people living with HIV-AIDS.* Journal of Acquired Immune Deficiency Syndromes, 2000. **25**(4): p. 337-44.

15. Buot, M.L., J.P. Docena, B.K. Ratemo, M.J. Bittner, J.T. Burlew, A.R. Nuritdinov, and J.R. Robbins, *Beyond race and place: distal sociological determinants of HIV disparities.* PLoS One, 2014. **9**(4): p. e91711.

16. Collins, S.E., *Associations between socioeconomic factors and alcohol outcomes.* Alcohol Research, 2016. **38**(1): p. 83-94.

17. Probst, C., C.D.H. Parry, and J. Rehm, *HIV/AIDS mortality attributable to alcohol use in South Africa: a comparative risk assessment by socioeconomic status.* BMJ Open, 2018. **8**(2): p. e017955.

18. Probst, C., L.C. Simbayi, C.D.H. Parry, P.A. Shuper, and J. Rehm, *Alcohol use, socioeconomic status and risk of HIV infections.* AIDS and Behavior, 2017. **21**(7): p. 1926-1937.

19. Shuper, P.A., N. Joharchi, P.M. Monti, M. Loutfy, and J. Rehm, *Acute alcohol consumption directly increases HIV transmission risk: a randomized controlled experiment.* Journal of Acquired Immune Deficiency Syndromes, 2017. **76**(5): p. 493-500.

20. Choudhry, V., A. Agardh, M. Stafström, and P.O. Östergren, *Patterns of alcohol consumption and risky sexual behavior: a cross-sectional study among Ugandan university students.* BMC Public Health, 2014. **14**: p. 128.

21. Petruželka, B., M. Barták, V. Rogalewicz, J. Rosina, P. Popov, B. Gavurová, M. Čierna, L. Vaska, M. Šavrnochová, and M. Dlouhý, *Problematic and risky sexual behaviour under the influence of alcohol among university students.* Central European Journal of Public Health, 2018. **26**(4): p. 289-297.

22. Samet, J.H., N.J. Horton, S. Meli, K.A. Freedberg, and A. Palepu, *Alcohol consumption and antiretroviral adherence among HIV-infected persons with alcohol problems.* Alcoholism: Clinical and Experimental Research, 2004. **28**(4): p. 572-7.

23. Sarna, A., R.J. Singh, J.J. Schensul, S.S. Gaikwad, K. Joshi, R. Malye, B. Mahapatra, T. Ha, and S. Schensul, *Viral load outcomes in a cohort of alcohol-consuming people living with HIV receiving antiretroviral therapy in Mumbai, India.* International Journal of STD and AIDS, 2020. **31**(8): p. 763-772.

24. Suttajit, S., P. Kittirattanapaiboon, B. Junsirimongkol, S. Likhitsathian, and M. Srisurapanont, *Risks of major depressive disorder and anxiety disorders among Thais with alcohol use disorders and illicit drug use: findings from the 2008 Thai National Mental Health survey.* Addictive Behaviors, 2012. **37**(12): p. 1395-9.

25. Wang, M., J. Shen, Y. Deng, X. Liu, J. Li, K. Wolff, and E. Finch, *Association of higher-risk alcohol consumption with injecting paraphernalia sharing behaviours in intravenous drug users.* American Journal of Drug and Alcohol Abuse, 2014. **40**(2): p. 137-42.

26. Bernhardt, N., S. Nebe, S. Pooseh, M. Sebold, C. Sommer, J. Birkenstock, U.S. Zimmermann, A. Heinz, and M.N. Smolka, *Impulsive decision making in young adult social drinkers and detoxified alcohol-dependent patients: a cross-sectional and longitudinal study.* Alcoholism: Clinical and Experimental Research, 2017. **41**(10): p. 1794-1807.

27. Grønkjaer, M., T. Flensborg-Madsen, M. Osler, H.J. Sørensen, U. Becker, and E.L. Mortensen, *Intelligence test scores before and after alcohol-related disorders-a longitudinal study of danish male conscripts.* Alcoholism: Clinical and Experimental Research, 2019. **43**(10): p. 2187-2195.

28. Tolomeo, S., J.A. McFarlane, A. Baldacchino, G.F. Koob, and J.D. Steele, *Alcohol binge drinking: negative and positive valence system abnormalitier.* Biological Psychiatry: Cognitive Neuroscience and Neuroimaging, 2020.

29. Comley, R.E. and M.J. Dry, *Acute tolerance to alcohol-induced impairment in cognitive performance.* Experimental and Clinical Psychopharmacology, 2020.

30. Zhang, R., L. Shen, T. Miles, Y. Shen, J. Cordero, Y. Qi, L. Liang, and C. Li, *Association of low to moderate alcohol drinking with cognitive functions from middle to older age among US adults.* JAMA Network Open, 2020. **3**(6): p. e207922.

31. Felker-Kantor, E.A., M.E. Wallace, A.S. Madkour, D.T. Duncan, K. Andrinopoulos, and K. Theall, *HIV stigma, mental health, and alcohol use disorders among people living with HIV/AIDS in new orleans.* Journal of Urban Health, 2019. **96**(6): p. 878-888.

32. Liu, X., J. Zha, J. Nishitani, H. Chen, and J.A. Zack, *HIV-1 infection in peripheral blood lymphocytes (PBLs) exposed to alcohol.* Virology, 2003. **307**(1): p. 37-44.

33. Long, J.E., B.A. Richardson, G. Wanje, K.S. Wilson, J. Shafi, K. Mandaliya, J.M. Simoni, J. Kinuthia, W. Jaoko, and R.S. McClelland, *Alcohol use and viral suppression in HIV-positive Kenyan female sex workers on antiretroviral therapy.* PLoS One, 2020. **15**(11): p. e0242817.

34. Wagman, J.A., A. Wynn, M. Matsuzaki, N. Gnatienko, L.R. Metsch, C. Del Rio, D.J. Feaster, R.M. Nance, B.M. Whitney, J.A.C. Delaney, S.Y. Kahana, H.M. Crane, R.K. Chandler, J.C. Elliott, F. Altice, G.M. Lucas, S.H. Mehta, Y. Hirsch-Moverman, W.M. El-Sadr, Q. Vu, B. Nguyen Thanh, S.A. Springer, J.I. Tsui, and J.H. Samet, *Hazardous alcohol use, antiretroviral therapy receipt, and viral suppression in people living with HIV who inject drugs in the United States, India, Russia, and Vietnam.* Aids, 2020. **34**(15): p. 2285-2294.

35. Wang, P., B.Y. Liu, M.M. Wu, X.Y. Wei, S. Sheng, S.W. You, L.X. Shang, and F. Kuang, *Moderate prenatal alcohol exposure suppresses the TLR4-mediated innate immune response in the hippocampus of young rats.* Neuroscience Letters, 2019. **699**: p. 77-83.

36. Sharma, A.R., R. Venkatadri, V. Sabapathy, S. Mohammad, and R. Sharma, *Sub-lethal dose of alcohol modulates innate immune-mediated regulatory T-Cell differentiation.* The Journal of Immunology, 2020. **204**(1 Supplement): p. 228.14-228.14.

37. Sureshchandra, S., A. Raus, A. Jankeel, B.J.K. Ligh, N.A.R. Walter, N. Newman, K.A. Grant, and I. Messaoudi, *Dose-dependent effects of chronic alcohol drinking on peripheral immune responses.* Scientific Report, 2019. **9**(1): p. 7847.

38. Romeo, J., J. Wärnberg, E. Nova, L.E. Díaz, S. Gómez-Martinez, and A. Marcos, *Moderate alcohol consumption and the immune system: A review.* British Journal of Nutrition, 2007. **98**(S1): p. S111-S115.

39. Mandrekar, P., D. Catalano, A. Dolganiuc, K. Kodys, and G. Szabo, *Inhibition of myeloid dendritic cell accessory cell function and induction of T cell anergy by alcohol correlates with decreased IL-12 production.* Journal of Immunology, 2004. **173**(5): p. 3398-407.

40. Pothlichet, J., T. Rose, F. Bugault, L. Jeammet, A. Meola, A. Haouz, F. Saul, D. Geny, J. Alcami, E. Ruiz-Mateos, L. Teyton, G. Lambeau, and J. Thèze, *PLA2G1B is involved in CD4 anergy and CD4 lymphopenia in HIV-infected patients.* Journal of Clinical Investigation, 2020. **130**(6): p. 2872-2887.

41. Eken, A., V. Ortiz, and J.R. Wands, *Ethanol inhibits antigen presentation by dendritic cells.* Clinical and Vaccine Immunology, 2011. **18**(7): p. 1157-66.

42. Mishra, V., A. Agas, H. Schuetz, J. Kalluru, and J. Haorah, *Alcohol induces programmed death receptor-1 and programmed death-ligand-1 differentially in neuroimmune cells.* Alcohol, 2020. **86**: p. 65-74.

43. Ye, L., S. Wang, X. Wang, Y. Zhou, J. Li, Y. Persidsky, and W. Ho, *Alcohol impairs interferon signaling and enhances full cycle hepatitis C virus JFH-1 infection of human hepatocytes.* Drug and Alcohol Dependence, 2010. **112**(1-2): p. 107-16.

44. Zhang, T., C.J. Guo, S.D. Douglas, D.S. Metzger, C.P. O'Brien, Y. Li, Y.J. Wang, X. Wang, and W.Z. Ho, *Alcohol suppresses IL-2-induced CC chemokine production by natural killer cells.* Alcoholism: Clinical and Experimental Research, 2005. **29**(9): p. 1559-67.

45. Yolitz, J., C. Schwing, J. Chang, D. Van Ryk, F. Nawaz, D. Wei, C. Cicala, J. Arthos, and A.S. Fauci, *Signal peptide of HIV envelope protein impacts glycosylation and antigenicity of gp120.* Proceedings of the National Academy of Sciences of the United States of America, 2018. **115**(10): p. 2443-2448.

46. Bagby, G.J., A.M. Amedee, R.W. Siggins, P.E. Molina, S. Nelson, and R.S. Veazey, *Alcohol and HIV effects on the immune system.* Alcohol Research, 2015. **37**(2): p. 287-97.

47. McGinnis, K.A., D.A. Fiellin, J.P. Tate, R.L. Cook, R.S. Braithwaite, K.J. Bryant, E.J. Edelman, A.J. Gordon, K.L. Kraemer, S.A. Maisto, and A.C. Justice, *Number of drinks to "feel a buzz" by HIV status and viral load in men.* AIDS and Behavior, 2016. **20**(3): p. 504-11.

48. McCance-Katz, E.F., P.J. Lum, G. Beatty, V.A. Gruber, M. Peters, and P.M. Rainey, *Untreated HIV infection is associated with higher blood alcohol levels.* Journal of Acquired Immune Deficiency Syndromes, 2012. **60**(3): p. 282-8.

49. Wei, J., L. Qin, Y. Fu, Y. Dai, Y. Wen, and S. Xu, *Long-term consumption of alcohol exacerbates neural lesions by destroying the functional integrity of the blood-brain barrier.* Drug and Chemical Toxicology, 2019: p. 1-8.

50. Cederbaum, A.I., *Alcohol metabolism.* Clinics in Liver Disease, 2012. **16**(4): p. 667-85.

51. Floreani, N.A., T.J. Rump, P.M. Abdul Muneer, S. Alikunju, B.M. Morsey, M.R. Brodie, Y. Persidsky, and J. Haorah, *Alcohol-induced interactive phosphorylation of Src and toll-like receptor regulates the secretion of inflammatory mediators by human astrocytes.* Journal of Neuroimmune Pharmacology, 2010. **5**(4): p. 533-45.

52. Zakhari, S., *Overview: how is alcohol metabolized by the body?* Alcohol Research and Health, 2006. **29**(4): p. 245-54.

53. Zimatkin, S.M. and R.A. Deitrich, *Ethanol metabolism in the brain.* Addiction Biology, 1997. **2**(4): p. 387-400.

54. Jin, M., P. Arya, K. Patel, B. Singh, P.S. Silverstein, H.K. Bhat, A. Kumar, and S. Kumar, *Effect of alcohol on drug efflux protein and drug metabolic enzymes in U937 macrophages.* Alcoholism: Clinical and Experimental Research, 2011. **35**(1): p. 132-9.

55. Ganesan, M., L.Y. Poluektova, K.K. Kharbanda, and N.A. Osna, *Liver as a target of human immunodeficiency virus infection.* World Journal of Gastroenterology, 2018. **24**(42): p. 4728-4737.

56. Ganesan, M., R.S. Dagur, E. Makarov, L.I. Poluektova, S. Kidambi, and N.A. Osna, *Matrix stiffness regulate apoptotic cell death in HIV-HCV co-infected hepatocytes: Importance for liver fibrosis progression.* Biochemical and Biophysical Research Communications, 2018. **500**(3): p. 717-722.

57. Xiao, P., O. Usami, Y. Suzuki, H. Ling, N. Shimizu, H. Hoshino, M. Zhuang, Y. Ashino, H. Gu, and T. Hattori, *Characterization of a CD4-independent clinical HIV-1 that can efficiently infect human hepatocytes through chemokine (C-X-C motif) receptor 4.* Aids, 2008. **22**(14): p. 1749-57.

58. Gong, Y., P.S.S. Rao, N. Sinha, S. Ranjit, T.J. Cory, and S. Kumar, *The role of cytochrome P450 2E1 on ethanol-mediated oxidative stress and HIV replication in human monocyte-derived macrophages.* Biochemistry and Biophysics Reports, 2019. **17**: p. 65-70.

59. Pardo, M., A.J. Betz, N. San Miguel, L. López-Cruz, J.D. Salamone, and M. Correa, *Acetate as an active metabolite of ethanol: studies of locomotion, loss of righting reflex, and anxiety in rodents.* Frontiers in Behavioral Neuroscience, 2013. **7**: p. 81.

60. Werner, J., M. Saghir, A.L. Warshaw, K.B. Lewandrowski, M. Laposata, R.V. Iozzo, E.A. Carter, R.J. Schatz, and C. Fernández-Del Castillo, *Alcoholic pancreatitis in rats: injury from nonoxidative metabolites of ethanol.* American Journal of Physiology-Gastrointestinal and Liver Physiology, 2002. **283**(1): p. G65-73.

61. Bora, P.S. and L.G. Lange, *Molecular mechanism of ethanol metabolism by human brain to fatty acid ethyl esters.* Alcoholism: Clinical and Experimental Research, 1993. **17**(1): p. 28-30.

62. Laposata, E.A., D.E. Scherrer, C. Mazow, and L.G. Lange, *Metabolism of ethanol by human brain to fatty acid ethyl esters.* Journal of Biological Chemistry, 1987. **262**(10): p. 4653-7.

63. Haorah, J., S.H. Ramirez, N. Floreani, S. Gorantla, B. Morsey, and Y. Persidsky, *Mechanism of alcohol-induced oxidative stress and neuronal injury.* Free Radical Biology and Medicine, 2008. **45**(11): p. 1542-50.

64. Rao, P.S. and S. Kumar, *Chronic effects of ethanol and/or darunavir/ritonavir on U937 monocytic cells: regulation of cytochrome P450 and antioxidant enzymes, oxidative stress, and cytotoxicity.* Alcoholism: Clinical and Experimental Research, 2016. **40**(1): p. 73-82.

65. Auger, C., J. Lemire, D. Cecchini, A. Bignucolo, and V.D. Appanna, *The metabolic reprogramming evoked by nitrosative stress triggers the anaerobic utilization of citrate in Pseudomonas fluorescens.* PLoS One, 2011. **6**(12): p. e28469.

66. Galley, J.C. and A.C. Straub, *Redox control of vascular function.* Arteriosclerosis, Thrombosis, and Vascular Biology, 2017. **37**(12): p. e178-e184.

67. Haorah, J., B. Knipe, S. Gorantla, J. Zheng, and Y. Persidsky, *Alcohol-induced blood-brain barrier dysfunction is mediated via inositol 1,4,5-triphosphate receptor (IP3R)-gated intracellular calcium release.* Journal of Neurochemistry, 2007. **100**(2): p. 324-36.

68. Haorah, J., B. Knipe, J. Leibhart, A. Ghorpade, and Y. Persidsky, *Alcohol-induced oxidative stress in brain endothelial cells causes blood-brain barrier dysfunction.* Journal of Leukocyte Biology, 2005. **78**(6): p. 1223-32.

69. Boven, L.A., J. Middel, J. Verhoef, C.J. De Groot, and H.S. Nottet, *Monocyte infiltration is highly associated with loss of the tight junction protein zonula occludens in HIV-1-associated dementia.* Neuropathology and Applied Neurobiology, 2000. **26**(4): p. 356-60.

70. Singh, V.B., M.V. Singh, D. Piekna-Przybylska, S. Gorantla, L.Y. Poluektova, and S.B. Maggirwar, *Sonic Hedgehog mimetic prevents leukocyte infiltration into the CNS during acute HIV infection.* Scientific Report, 2017. **7**(1): p. 9578.

71. Phillips, D.E., S.K. Krueger, K.A. Wall, L.H. Smoyer-Dearing, and A.K. Sikora, *The development of the blood-brain barrier in alcohol-exposed rats.* Alcohol, 1997. **14**(4): p. 333-43.

72. Leibrand, C.R., J.J. Paris, M.S. Ghandour, P.E. Knapp, W.K. Kim, K.F. Hauser, and M. McRae, *HIV-1 Tat disrupts blood-brain barrier integrity and increases phagocytic perivascular macrophages and microglia in the dorsal striatum of transgenic mice.* Neuroscience Letters, 2017. **640**: p. 136-143.

73. Shiu, C., E. Barbier, F. Di Cello, H.J. Choi, and M. Stins, *HIV-1 gp120 as well as alcohol affect blood-brain barrier permeability and stress fiber formation: involvement of reactive oxygen species.* Alcoholism: Clinical and Experimental Research, 2007. **31**(1): p. 130-7.

74. Castro, V., L. Bertrand, M. Luethen, S. Dabrowski, J. Lombardi, L. Morgan, N. Sharova, M. Stevenson, I.E. Blasig, and M. Toborek, *Occludin controls HIV transcription in brain pericytes via regulation of SIRT-1 activation.* FASEB Journal, 2016. **30**(3): p. 1234-46.

75. Quertemont, E. and S. Tambour, *Is ethanol a pro-drug? The role of acetaldehyde in the central effects of ethanol.* Trends in Pharmacological Sciences, 2004. **25**(3): p. 130-4.

76. Phillips, S.C. and B.G. Cragg, *Weakening of the blood-brain barrier by alcohol-related stresses in the rat.* Journal of the Neurological Sciences, 1982. **54**(2): p. 271-8.

77. Singh, A.K., Y. Jiang, S. Gupta, and E. Benlhabib, *Effects of chronic ethanol drinking on the blood brain barrier and ensuing neuronal toxicity in alcohol-preferring rats subjected to intraperitoneal LPS injection.* Alcohol Alcohol, 2007. **42**(5): p. 385-99.

78. Hazleton, J.E., J.W. Berman, and E.A. Eugenin, *Novel mechanisms of central nervous system damage in HIV infection.* HIV/AIDS (Auckland, N.Z.), 2010. **2**: p. 39-49.

79. Ivan, D.C., S. Walthert, and G. Locatelli, *Monocyte recruitment to the inflamed central nervous system: migration pathways and distinct functional polarization.* bioRxiv, 2020: p. 2020.04.04.025395.

80. Savarin, C., S.A. Stohlman, R. Atkinson, R.M. Ransohoff, and C.C. Bergmann, *Monocytes regulate T cell migration through the glia limitans during acute viral encephalitis.* Journal of Virology, 2010. **84**(10): p. 4878-88.

81. Schneider, C.A., D.X. Figueroa Velez, R. Azevedo, E.M. Hoover, C.J. Tran, C. Lo, O. Vadpey, S.P. Gandhi, and M.B. Lodoen, *Imaging the dynamic recruitment of monocytes to the blood-brain barrier and specific brain regions during Toxoplasma gondii infection.* Proceedings of the National Academy of Sciences of the United States of America, 2019. **116**(49): p. 24796-24807.

82. Kumar, R., A.E. Perez-Casanova, G. Tirado, R.J. Noel, C. Torres, I. Rodriguez, M. Martinez, S. Staprans, E. Kraiselburd, Y. Yamamura, J.D. Higley, and A. Kumar, *Increased viral replication in simian immunodeficiency virus/simian-HIV-infected macaques with self-administering model of chronic alcohol consumption.* Journal of Acquired Immune Deficiency Syndromes, 2005. **39**(4): p. 386-90.

83. Cenker, J.J., R.D. Stultz, and D. McDonald, *Brain microglial cells are highly susceptible to HIV-1 infection and spread.* AIDS Resesearch on Human Retroviruses, 2017. **33**(11): p. 1155-1165.

84. Chaillon, A., S. Gianella, S. Dellicour, S.A. Rawlings, T.E. Schlub, M.F. De Oliveira, C. Ignacio, M. Porrachia, B. Vrancken, and D.M. Smith, *HIV persists throughout deep tissues with repopulation from multiple anatomical sources.* Journal of Clinical Investigation, 2020. **130**(4): p. 1699-1712.

85. Li, G.H., D. Maric, E.O. Major, and A. Nath, *Productive HIV infection in astrocytes can be established via a nonclassical mechanism.* Aids, 2020. **34**(7): p. 963-978.

86. Ghosh, A.K., K.V. Rao, P.R. Nyalapatla, S. Kovela, M. Brindisi, H.L. Osswald, B. Sekhara Reddy, J. Agniswamy, Y.F. Wang, M. Aoki, S.I. Hattori, I.T. Weber, and H. Mitsuya, *Design of highly potent, dual-acting and central-nervous-system-penetrating HIV-1 protease inhibitors with excellent potency against multidrug-resistant HIV-1 variants.* ChemMedChem, 2018. **13**(8): p. 803-815.

87. Gong, Y., P. Chowdhury, P.K.B. Nagesh, M.A. Rahman, K. Zhi, M.M. Yallapu, and S. Kumar, *Novel elvitegravir nanoformulation for drug delivery across the blood-brain barrier to achieve HIV-1 suppression in the CNS macrophages.* Scientific Reports, 2020. **10**(1): p. 3835.

88. Vendel, E., V. Rottschäfer, and E.C.M. de Lange, *The need for mathematical modelling of spatial drug distribution within the brain.* Fluids Barriers CNS, 2019. **16**(1): p. 12.

89. Lingineni, K., V. Belekar, S.R. Tangadpalliwar, and P. Garg, *The role of multidrug resistance protein (MRP-1) as an active efflux transporter on blood-brain barrier (BBB) permeability.* Molecular Diversity, 2017. **21**(2): p. 355-365.

90. Calcagno, A., S. Bonora, M. Simiele, R. Rostagno, M.C. Tettoni, M. Bonasso, A. Romito, D. Imperiale, A. D'Avolio, and G. Di Perri, *Tenofovir and emtricitabine cerebrospinal fluid-to-plasma ratios correlate to the extent of blood-brainbarrier damage.* Aids, 2011. **25**(11): p. 1437-9.

91. Calcagno, A., J. Cusato, M. Simiele, I. Motta, S. Audagnotto, M. Bracchi, A. D'Avolio, G. Di Perri, and S. Bonora, *High interpatient variability of raltegravir CSF concentrations in HIV-positive patients: a pharmacogenetic analysis.* Journal of Antimicrobiol Chemotherapy, 2014. **69**(1): p. 241-5.

92. Calcagno, A., M.C. Alberione, A. Romito, D. Imperiale, V. Ghisetti, S. Audagnotto, F. Lipani, S. Raviolo, G. Di Perri, and S. Bonora, *Prevalence and predictors of blood-brain barrier damage in the HAART era.* Journal of Neurovirology, 2014. **20**(5): p. 521-5.

93. Troya, J. and J. Bascuñana, *Safety and tolerability: current challenges to antiretroviral therapy for the long-term management of HIV infection.* AIDS Reviews, 2016. **18**(3): p. 127-137.

94. Bertrand, L., M. Velichkovska, and M. Toborek, *Cerebral vascular toxicity of antiretroviral therapy.* Journal of Neuroimmune Pharmacology, 2019.

95. Queen, S.E., B.M. Mears, K.M. Kelly, J.L. Dorsey, Z. Liao, J.B. Dinoso, L. Gama, R.J. Adams, M.C. Zink, J.E. Clements, S.J. Kent, and J.L. Mankowski, *Replication-competent simian immunodeficiency virus (SIV) Gag escape mutations archived in latent reservoirs during antiretroviral treatment of SIV-infected macaques.* Journal of Virology, 2011. **85**(17): p. 9167-75.

96. Agas, A., H. Schuetz, V. Mishra, A.M. Szlachetka, and J. Haorah, *Antiretroviral drug-S for a possible HIV elimination.* Interntional Journal of Physiology, Pathophysiology, and Pharmacology, 2019. **11**(4): p. 149-162.

97. Lutgen, V., S.D. Narasipura, H.J. Barbian, M. Richards, J. Wallace, R. Razmpour, T. Buzhdygan, S.H. Ramirez, L. Prevedel, E.A. Eugenin, and L. Al-Harthi, *HIV infects astrocytes in vivo and egresses from the brain to the periphery.* PLoS Pathogens, 2020. **16**(6): p. e1008381.

98. Braithwaite, R.S. and K.J. Bryant, *Influence of alcohol consumption on adherence to and toxicity of antiretroviral therapy and survival.* Alcohol Research and Health, 2010. **33**(3): p. 280-7.

99. Paolillo, E.W., A. Gongvatana, A. Umlauf, S.L. Letendre, and D.J. Moore, *At-risk alcohol use is associated with antiretroviral treatment nonadherence among adults living with HIV/AIDS.* Alcoholism: Clinical and Experimental Research, 2017. **41**(8): p. 1518-1525.

100. Midde, N.M., N. Sinha, P.B. Lukka, B. Meibohm, and S. Kumar, *Alterations in cellular pharmacokinetics and pharmacodynamics of elvitegravir in response to ethanol exposure in HIV-1 infected monocytic (U1) cells.* PLoS One, 2017. **12**(2): p. e0172628.

101. Hong-Brown, L.Q., C.R. Brown, D.S. Huber, and C.H. Lang, *Alcohol and indinavir adversely affect protein synthesis and phosphorylation of MAPK and mTOR signaling pathways in C2C12 myocytes.* Alcoholism: Clinical and Experimental Research, 2006. **30**(8): p. 1297-307.

102. Zhang, K.E., E. Wu, A.K. Patick, B. Kerr, M. Zorbas, A. Lankford, T. Kobayashi, Y. Maeda, B. Shetty, and S. Webber, *Circulating metabolites of the human immunodeficiency virus protease inhibitor nelfinavir in humans: structural identification, levels in plasma, and antiviral activities.* Antimicrobial Agents and Chemotherapy, 2001. **45**(4): p. 1086-93.

103. Gong, Y., S. Haque, P. Chowdhury, T.J. Cory, S. Kodidela, M.M. Yallapu, J.M. Norwood, and S. Kumar, *Pharmacokinetics and pharmacodynamics of cytochrome P450 inhibitors for HIV treatment.* Expert Opinion on Drug Metabolism and Toxicology, 2019. **15**(5): p. 417-427.

104. Zhang, Y., F. Song, Z. Gao, W. Ding, L. Qiao, S. Yang, X. Chen, R. Jin, and D. Chen, *Long-term exposure of mice to nucleoside analogues disrupts mitochondrial DNA maintenance in cortical neurons.* PLoS One, 2014. **9**(1): p. e85637.

105. McCance-Katz, E.F., V.A. Gruber, G. Beatty, P.J. Lum, and P.M. Rainey, *Interactions between alcohol and the antiretroviral medications ritonavir or efavirenz.* Journal of Addiction Medicine, 2013. **7**(4): p. 264-70.

106. Farhadian, N., S. Moradi, M.H. Zamanian, V. Farnia, S. Rezaeian, M. Farhadian, and M. Shahlaei, *Effectiveness of naltrexone treatment for alcohol use disorders in HIV: a systematic review.* Substance Abuse Treatment, Prevention, and Policy, 2020. **15**(1): p. 24.

107. Kumar, S., M. Jin, A. Ande, N. Sinha, P.S. Silverstein, and A. Kumar, *Alcohol consumption effect on antiretroviral therapy and HIV-1 pathogenesis: role of cytochrome P450 isozymes.* Expert Opinion on Drug Metabolism and Toxicology, 2012. **8**(11): p. 1363-75.

108. Ogedengbe, O.O., E.C.S. Naidu, and O.O. Azu, *Antiretroviral therapy and alcohol interactions: X-raying testicular and seminal parameters under the HAART era.* European Journal of Drug Metabolism and Pharmacokinetics, 2018. **43**(2): p. 121-135.

109. Dienel, G.A., *Brain glucose metabolism: integration of energetics with function.* Physiological Reviews, 2019. **99**(1): p. 949-1045.

110. Üner, A.G., O. Keçik, P.G.F. Quaresma, T.M. De Araujo, H. Lee, W. Li, H.J. Kim, M. Chung, C. Bjørbæk, and Y.B. Kim, *Role of POMC and AgRP neuronal activities on glycaemia in mice.* Scientific Report, 2019. **9**(1): p. 13068.

111. Cotto, B., K. Natarajanseenivasan, and D. Langford, *HIV-1 infection alters energy metabolism in the brain: Contributions to HIV-associated neurocognitive disorders.* Progress in Neurobiology, 2019. **181**: p. 101616.

112. Hammoud, D.A., S. Sinharay, S. Steinbach, P.G. Wakim, K. Geannopoulos, K. Traino, A.K. Dey, E. Tramont, S.I. Rapoport, J. Snow, N.N. Mehta, B.R. Smith, and A. Nath, *Global and regional brain hypometabolism on FDG-PET in treated HIV-infected individuals.* Neurology, 2018. **91**(17): p. e1591-e1601.

113. Towgood, K.J., M. Pitkanen, R. Kulasegaram, A. Fradera, S. Soni, N. Sibtain, L.J. Reed, C. Bradbeer, G.J. Barker, J.T. Dunn, F. Zelaya, and M.D. Kopelman, *Regional cerebral blood flow and FDG uptake in asymptomatic HIV-1 men.* Human Brain Mapping, 2013. **34**(10): p. 2484-93.

114. van Gorp, W.G., M.A. Mandelkern, M. Gee, C.H. Hinkin, C.E. Stern, D.K. Paz, W. Dixon, G. Evans, F. Flynn, C.J. Frederick, and et al., *Cerebral metabolic dysfunction in AIDS: findings in a sample with and without dementia.* Journal of Neuropsychiatry and Clinical Neurosciences, 1992. **4**(3): p. 280-7.

115. Clergue-Duval, V., F. Questel, J. Azuar, C. Paquet, E. Cognat, J. Amami, M. Queneau, A. Dereux, T. Barré, F. Bellivier, K. Farid, and F. Vorspan, *Brain 18FDG-PET pattern in patients with alcohol-related cognitive impairment.* European Journal of Nuclear Medicine and Molecular Imaging, 2020. **47**(2): p. 281-291.

116. Abdul Muneer, P.M., S. Alikunju, A.M. Szlachetka, A.J. Mercer, and J. Haorah, *Ethanol impairs glucose uptake by human astrocytes and neurons: protective effects of acetyl-L-carnitine.* Interntional Journal of Physiology, Pathophysiology, and Pharmacology, 2011. **3**(1): p. 48-56.

117. Lindberg, D., A.M.C. Ho, L. Peyton, and D.S. Choi, *Chronic ethanol exposure disrupts lactate and glucose homeostasis and induces dysfunction of the astrocyte-neuron lactate shuttle in the brain.* Alcoholism: Clinical and Experimental Research, 2019. **43**(9): p. 1838-1847.

118. An, J., W.B. Haile, F. Wu, E. Torre, and M. Yepes, *Tissue-type plasminogen activator mediates neuroglial coupling in the central nervous system.* Neuroscience, 2014. **257**: p. 41-8.

119. Muraleedharan, R., M.V. Gawali, D. Tiwari, A. Sukumaran, N. Oatman, J. Anderson, D. Nardini, M.A.N. Bhuiyan, I. Tkáč, A.L. Ward, M. Kundu, R. Waclaw, L.M. Chow, C. Gross, R. Rao, S. Schirmeier, and B. Dasgupta, *AMPK-regulated astrocytic lactate shuttle plays a non-cell-autonomous role in neuronal survival.* Cell Reports, 2020. **32**(9): p. 108092.

120. Pascal, S., L. Resnick, W.W. Barker, D. Loewenstein, F. Yoshii, J.Y. Chang, T. Boothe, J. Sheldon, and R. Duara, *Metabolic asymmetries in asymptomatic HIV-1 seropositive subjects: relationship to disease onset and MRI findings.* The Journal of Nuclear Medicine, 1991. **32**(9): p. 1725-9.

121. Mergenthaler, P., U. Lindauer, G.A. Dienel, and A. Meisel, *Sugar for the brain: the role of glucose in physiological and pathological brain function.* Trends Neuroscience, 2013. **36**(10): p. 587-97.

122. Andersen, A.B., I. Law, K.S. Krabbe, H. Bruunsgaard, S.R. Ostrowski, H. Ullum, L. Højgaard, A. Lebech, J. Gerstoft, and A. Kjaer, *Cerebral FDG-PET scanning abnormalities in optimally treated HIV patients.* Journal of Neuroinflammation, 2010. **7**: p. 13.

123. Warwick, J.M. and M.M. Sathekge, *PET/CT scanning with a high HIV/AIDS prevalence.* Transfusion and Apheresis Science, 2011. **44**(2): p. 167-72.

124. Sathekge, M., I. Goethals, A. Maes, and C. van de Wiele, *Positron emission tomography in patients suffering from HIV-1 infection.* European Journal of Nuclear Medicine and Molecular Imaging, 2009. **36**(7): p. 1176-84.

125. Lewitschnig, S., K. Gedela, M. Toby, R. Kulasegaram, M. Nelson, M. O'Doherty, and G.J. Cook, *^{18}F-FDG PET/CT in HIV-related central nervous system pathology.* European Journal of Nuclear Medicine and Molecular Imaging, 2013. **40**(9): p. 1420-7.

126. Schreiber-Stainthorp, W., S. Sinharay, S. Srinivasula, S. Shah, J. Wang, L. Dodd, H.C. Lane, M. Di Mascio, and D.A. Hammoud, *Brain (18)F-FDG PET of SIV-infected macaques after treatment interruption or initiation.* Journal of Neuroinflammation, 2018. **15**(1): p. 207.

127. Meyerhoff, D.J., S. MacKay, D. Sappey-Marinier, R. Deicken, G. Calabrese, W.P. Dillon, M.W. Weiner, and G. Fein, *Effects of chronic alcohol abuse and HIV infection on brain phosphorus metabolites.* Alcoholism: Clinical and Experimental Research, 1995. **19**(3): p. 685-92.

128. Anderson, A.M., C. Fennema-Notestine, A. Umlauf, M.J. Taylor, D.B. Clifford, C.M. Marra, A.C. Collier, B.B. Gelman, J.C. McArthur, J.A. McCutchan, D.M. Simpson, S. Morgello, I. Grant, and S.L. Letendre, *CSF biomarkers of monocyte activation and chemotaxis correlate with magnetic resonance spectroscopy metabolites during chronic HIV disease.* Journal of Neurovirology, 2015. **21**(5): p. 559-67.

129. Chang, L., T. Ernst, M.D. Witt, N. Ames, M. Gaiefsky, and E. Miller, *Relationships among brain metabolites, cognitive function, and viral loads in antiretroviral-naïve HIV patients.* Neuroimage, 2002. **17**(3): p. 1638-48.

130. Mohamed, M.A., M.R. Lentz, V. Lee, E.F. Halpern, N. Sacktor, O. Selnes, P.B. Barker, and M.G. Pomper, *Factor analysis of proton MR spectroscopic imaging data in HIV infection: metabolite-derived factors help identify infection and dementia.* Radiology, 2010. **254**(2): p. 577-86.

131. Young, A.C., C.T. Yiannoutsos, M. Hegde, E. Lee, J. Peterson, R. Walter, R.W. Price, D.J. Meyerhoff, and S. Spudich, *Cerebral metabolite changes prior to and after antiretroviral therapy in primary HIV infection.* Neurology, 2014. **83**(18): p. 1592-600.

132. Bansal, P., S. Wang, S. Liu, Y.Y. Xiang, W.Y. Lu, and Q. Wang, *GABA coordinates with insulin in regulating secretory function in pancreatic INS-1 β-cells.* PLoS One, 2011. **6**(10): p. e26225.

133. Roberto, M., S.G. Madamba, D.G. Stouffer, L.H. Parsons, and G.R. Siggins, *Increased GABA release in the central amygdala of ethanol-dependent rats.* Journal of Neuroscience, 2004. **24**(45): p. 10159-66.

134. Ford, S.M., Jr., L. Simon, C. Vande Stouwe, T. Allerton, D.E. Mercante, L.O. Byerley, J.P. Dufour, G.J. Bagby, S. Nelson, and P.E. Molina, *Chronic binge alcohol administration impairs glucose-insulin dynamics and decreases adiponectin in asymptomatic simian immunodeficiency virus-infected macaques.* American Journal of Physiology-Regulatory, Integrative and Comparative Physiology, 2016. **311**(5): p. R888-r897.

135. Jiang, L., B.I. Gulanski, H.M. De Feyter, S.A. Weinzimer, B. Pittman, E. Guidone, J. Koretski, S. Harman, I.L. Petrakis, J.H. Krystal, and G.F. Mason, *Increased brain uptake and oxidation of acetate in heavy drinkers.* Journal of Clinical Investigation, 2013. **123**(4): p. 1605-14.

136. Dencker, D., A. Molander, M. Thomsen, C. Schlumberger, G. Wortwein, P. Weikop, H. Benveniste, N.D. Volkow, and A. Fink-Jensen, *Ketogenic diet suppresses alcohol withdrawal syndrome in rats.* Alcoholism: Clinical and Experimental Research, 2018. **42**(2): p. 270-277.

137. Hasselbalch, S.G., G.M. Knudsen, J. Jakobsen, L.P. Hageman, S. Holm, and O.B. Paulson, *Blood-brain barrier permeability of glucose and ketone bodies during short-term starvation in humans.* American Journal of Physiology, 1995. **268**(6 Pt 1): p. E1161-6.

138. Klosinski, L.P., J. Yao, F. Yin, A.N. Fonteh, M.G. Harrington, T.A. Christensen, E. Trushina, and R.D. Brinton, *White matter lipids as a ketogenic fuel supply in aging female brain: implications for Alzheimer's disease.* EBioMedicine, 2015. **2**(12): p. 1888-904.

139. Matsui, T., H. Omuro, Y.F. Liu, M. Soya, T. Shima, B.S. McEwen, and H. Soya, *Astrocytic glycogen-derived lactate fuels the brain during exhaustive exercise to maintain endurance capacity.* Proceedings of the National Academy of Sciences of the United States of America, 2017. **114**(24): p. 6358-6363.

140. Najac, C., M. Radoul, L.M. Le Page, G. Batsios, E. Subramani, P. Viswanath, A.M. Gillespie, and S.M. Ronen, *In vivo investigation of hyperpolarized [1,3-(13)C(2)]acetoacetate as a metabolic probe in normal brain and in glioma.* Scientific Report, 2019. **9**(1): p. 3402.

141. Mitchell, R.W., N.H. On, M.R. Del Bigio, D.W. Miller, and G.M. Hatch, *Fatty acid transport protein expression in human brain and potential role in fatty acid transport across human brain microvessel endothelial cells.* Journal of Neurochemistry, 2011. **117**(4): p. 735-46.

142. Castellano, P., L. Prevedel, S. Valdebenito, and E.A. Eugenin, *HIV infection and latency induce a unique metabolic signature in human macrophages.* Scientific Reports, 2019. **9**(1): p. 3941.

143. Yang, C., B. Ko, C.T. Hensley, L. Jiang, A.T. Wasti, J. Kim, J. Sudderth, M.A. Calvaruso, L. Lumata, M. Mitsche, J. Rutter, M.E. Merritt, and R.J. DeBerardinis, *Glutamine oxidation maintains the TCA cycle and cell survival during impaired mitochondrial pyruvate transport.* Molecular Cell, 2014. **56**(3): p. 414-24.

144. Pellerin, L., *Food for thought: the importance of glucose and other energy substrates for sustaining brain function under varying levels of activity.* Diabetes and Metabolism, 2010. **36 Suppl 3**: p. S59-63.

145. Omeragic, A., O. Kayode, M.T. Hoque, and R. Bendayan, *Potential pharmacological approaches for the treatment of HIV-1 associated neurocognitive disorders.* Fluids and Barriers of the CNS, 2020. **17**(1): p. 42.

146. Dickens, A.M., D.C. Anthony, R. Deutsch, M.M. Mielke, T.D. Claridge, I. Grant, D. Franklin, D. Rosario, T. Marcotte, S. Letendre, J.C. McArthur, and N.J. Haughey, *Cerebrospinal fluid metabolomics implicate bioenergetic adaptation as a neural mechanism regulating shifts in cognitive states of HIV-infected patients.* Aids, 2015. **29**(5): p. 559-69.

147. Schurr, A. and R.S. Payne, *Lactate, not pyruvate, is neuronal aerobic glycolysis end product: an in vitro electrophysiological study.* Neuroscience, 2007. **147**(3): p. 613-9.

148. Boska, M.D., P.K. Dash, J. Knibbe, A.A. Epstein, S.P. Akhter, N. Fields, R. High, E. Makarov, S. Bonasera, H.A. Gelbard, L.Y. Poluektova, H.E. Gendelman, and S. Gorantla, *Associations between brain microstructures, metabolites, and cognitive deficits during chronic HIV-1 infection of humanized mice.* Molecular Neurodegeneration, 2014. **9**: p. 58.

149. Kim, J., G. Yang, Y. Kim, J. Kim, and J. Ha, *AMPK activators: mechanisms of action and physiological activities.* Experimental and Molecular Medicine, 2016. **48**(4): p. e224-e224.

150. You, M., M. Matsumoto, C.M. Pacold, W.K. Cho, and D.W. Crabb, *The role of AMP-activated protein kinase in the action of ethanol in the liver.* Gastroenterology, 2004. **127**(6): p. 1798-808.

151. Saito, M., G. Chakraborty, R.F. Mao, R. Wang, T.B. Cooper, C. Vadasz, and M. Saito, *Ethanol alters lipid profiles and phosphorylation status of AMP-activated protein kinase in the neonatal mouse brain.* Journal of Neurochemistry, 2007. **103**(3): p. 1208-18.

152. Chuquet, J., P. Quilichini, E.A. Nimchinsky, and G. Buzsáki, *Predominant enhancement of glucose uptake in astrocytes versus neurons during activation of the somatosensory cortex.* Journal of Neuroscience, 2010. **30**(45): p. 15298-303.

153. Boulay, A.C., B. Saubaméa, N. Adam, S. Chasseigneaux, N. Mazaré, A. Gilbert, M. Bahin, L. Bastianelli, C. Blugeon, S. Perrin, J. Pouch, B. Ducos, S. Le Crom, A. Genovesio, F. Chrétien, X. Declèves, J.L. Laplanche, and M. Cohen-Salmon, *Translation in astrocyte distal processes sets molecular heterogeneity at the gliovascular interface.* Cell Discovery, 2017. **3**: p. 17005.

154. Mason, S., *Lactate shuttles in neuroenergetics-homeostasis, allostasis and beyond.* Frontiers in Neuroscience, 2017. **11**: p. 43.

155. Gebril, H.M., B. Avula, Y.H. Wang, I.A. Khan, and M.B. Jekabsons, *(13)C metabolic flux analysis in neurons utilizing a model that accounts for hexose phosphate recycling within the pentose phosphate pathway.* Neurochemistry International, 2016. **93**: p. 26-39.

156. Butts, M., S. Singh, J. Haynes, S. Arthur, and U. Sundaram, *Moderate alcohol consumption uniquely regulates sodium-dependent glucose co-transport in rat intestinal epithelial cells in vitro and in vivo.* Journal of Nutrition, 2020. **150**(4): p. 747-755.

157. Coggan, J.S., D. Keller, C. Calì, H. Lehväslaiho, H. Markram, F. Schürmann, and P.J. Magistretti, *Norepinephrine stimulates glycogenolysis in astrocytes to fuel neurons with lactate.* PLoS Computational Biology, 2018. **14**(8): p. e1006392.

158. Dienel, G.A. and N.F. Cruz, *Aerobic glycolysis during brain activation: adrenergic regulation and influence of norepinephrine on astrocytic metabolism.* Journal of Neurochemistry, 2016. **138**(1): p. 14-52.

159. Hertz, L., *The astrocyte-neuron lactate shuttle: a challenge of a challenge.* Journal of Cerebral Blood Flow and Metabolism, 2004. **24**(11): p. 1241-8.

160. Jha, M.K. and B.M. Morrison, *Lactate transporters mediate glia-neuron metabolic crosstalk in homeostasis and disease.* Frontiers in Cellular Neuroscience, 2020. **14**: p. 589582.

161. Chih, C.P. and E.L. Roberts, Jr., *Energy substrates for neurons during neural activity: a critical review of the astrocyte-neuron lactate shuttle hypothesis.* Journal of Cerebral Blood Flow and Metabolism, 2003. **23**(11): p. 1263-81.

162. Dienel, G.A., *Lack of appropriate stoichiometry: Strong evidence against an energetically important astrocyte-neuron lactate shuttle in brain.* Journal of Neuroscience Research, 2017. **95**(11): p. 2103-2125.

163. Barros, L.F., I. Ruminot, A. San Martín, R. Lerchundi, I. Fernández-Moncada, and F. Baeza-Lehnert, *Aerobic glycolysis in the brain: warburg and crabtree contra pasteur.* Neurochemical Research, 2020.

164. Demetrius, L.A., P.J. Magistretti, and L. Pellerin, *Alzheimer's disease: the amyloid hypothesis and the Inverse Warburg effect.* Frontiers in Physiology, 2014. **5**: p. 522.

165. Mangia, S., I.A. Simpson, S.J. Vannucci, and A. Carruthers, *The in vivo neuron-to-astrocyte lactate shuttle in human brain: evidence from modeling of measured lactate levels during visual stimulation.* Journal of Neurochemistry, 2009. **109 Suppl 1**(Suppl 1): p. 55-62.

166. Fonseca, L.L., P.M. Alves, M.J. Carrondo, and H. Santos, *Effect of ethanol on the metabolism of primary astrocytes studied by (13)C- and (31)P-NMR spectroscopy.* Journal of Neuroscience Research, 2001. **66**(5): p. 803-11.

167. Valentín-Guillama, G., S. López, Y.V. Kucheryavykh, N.E. Chorna, J. Pérez, J. Ortiz-Rivera, M. Inyushin, V. Makarov, A. Valentín-Acevedo, A. Quinones-Hinojosa, N. Boukli, and L.Y. Kucheryavykh, *HIV-1 envelope protein gp120 promotes proliferation and the activation of glycolysis in glioma cell.* Cancers (Basel), 2018. **10**(9).

168. Ru, W. and S.J. Tang, *HIV-associated synaptic degeneration.* Molecular Brain, 2017. **10**(1): p. 40.

169. Sokolova, I.V., A. Szucs, and P.P. Sanna, *Reduced intrinsic excitability of CA1 pyramidal neurons in human immunodeficiency virus (HIV) transgenic rats.* Brain Research, 2019. **1724**: p. 146431.

170. Mason, S., A.M. van Furth, L.J. Mienie, U.F. Engelke, R.A. Wevers, R. Solomons, and C.J. Reinecke, *A hypothetical astrocyte-microglia lactate shuttle derived from a (1)H NMR metabolomics analysis of cerebrospinal fluid from a cohort of South African children with tuberculous meningitis.* Metabolomics, 2015. **11**(4): p. 822-837.

171. Mason, S., C.J. Reinecke, W. Kulik, A. van Cruchten, R. Solomons, and A.M. van Furth, *Cerebrospinal fluid in tuberculous meningitis exhibits only the L-enantiomer of lactic acid.* BMC Infectious Diseases, 2016. **16**: p. 251.

172. Demetrius, L.A. and D.K. Simon, *An inverse-Warburg effect and the origin of Alzheimer's disease.* Biogerontology, 2012. **13**(6): p. 583-94.

173. Paris, J.J., S. Zou, Y.K. Hahn, P.E. Knapp, and K.F. Hauser, *5α-reduced progestogens ameliorate mood-related behavioral pathology, neurotoxicity, and microgliosis associated with exposure to HIV-1 Tat.* Brain, Behavior, and Immunity, 2016. **55**: p. 202-214.

174. Urbach, A., J. Brueckner, and O.W. Witte, *Cortical spreading depolarization stimulates gliogenesis in the rat entorhinal cortex.* Journal of Cerebral Blood Flow and Metabolism, 2015. **35**(4): p. 576-82.

175. McGuire, J.L., A.J. Gill, S.D. Douglas, and D.L. Kolson, *Central and peripheral markers of neurodegeneration and monocyte activation in HIV-associated neurocognitive disorders.* Journal of NeuroVirology, 2015. **21**(4): p. 439-48.

176. Ratai, E.M., L. Annamalai, T. Burdo, C.G. Joo, J.P. Bombardier, R. Fell, R. Hakimelahi, J. He, M.R. Lentz, J. Campbell, E. Curran, E.F. Halpern, E. Masliah, S.V. Westmoreland, K.C. Williams, and R.G. González, *Brain creatine elevation and N-Acetylaspartate reduction indicates neuronal dysfunction in the setting of enhanced glial energy metabolism in a macaque model of neuroAIDS.* Magnetic Resonance in Medicine, 2011. **66**(3): p. 625-34.

177. Sokolowski, J.D., C.N. Chabanon-Hicks, C.Z. Han, D.S. Heffron, and J.W. Mandell, *Fractalkine is a "find-me" signal released by neurons undergoing ethanol-induced apoptosis.* Frontiers in Cellular Neuroscience, 2014. **8**: p. 360.

178. Duan, M., H. Yao, Y. Cai, K. Liao, P. Seth, and S. Buch, *HIV-1 Tat disrupts CX3CL1-CX3CR1 axis in microglia via the NF-κBYY1 pathway.* Current HIV Research, 2014. **12**(3): p. 189-200.

179. Aurelian, L. and I. Balan, *GABA(A)R α2-activated neuroimmune signal controls binge drinking and impulsivity through regulation of the CCL2/CX3CL1 balance.* Psychopharmacology (Berlin), 2019. **236**(10): p. 3023-3043.

180. Limatola, C. and R.M. Ransohoff, *Modulating neurotoxicity through CX3CL1/CX3CR1 signaling.* Frontiers in Cellular Neuroscience, 2014. **8**: p. 229.

181. Alvarez-Carbonell, D., F. Ye, N. Ramanath, Y. Garcia-Mesa, P.E. Knapp, K.F. Hauser, and J. Karn, *Cross-talk between microglia and neurons regulates HIV latency.* PLoS Pathogens, 2019. **15**(12): p. e1008249.

182. Castellano, P., L. Prevedel, and E.A. Eugenin, *HIV-infected macrophages and microglia that survive acute infection become viral reservoirs by a mechanism involving Bim.* Scientific Reports, 2017. **7**(1): p. 12866.

183. Díaz, L., M. Martínez-Bonet, J. Sánchez, A. Fernández-Pineda, J.L. Jiménez, E. Muñoz, S. Moreno, S. Álvarez, and M. Muñoz-Fernández, *Bryostatin activates HIV-1 latent expression in human astrocytes through a PKC and NF-κB-dependent mechanism.* Scientific Reports, 2015. **5**: p. 12442.

184. Gorska, A.M. and E.A. Eugenin, *The glutamate system as a crucial regulator of CNS toxicity and survival of HIV reservoirs.* Frontiers in Cellular and Infection Microbiology, 2020. **10**: p. 261.

185. Gao, G., C. Li, J. Zhu, Y. Wang, Y. Huang, S. Zhao, S. Sheng, Y. Song, C. Ji, C. Li, X. Yang, L. Ye, X. Qi, Y. Zhang, X. Xia, and J.C. Zheng, *Glutaminase 1 regulates neuroinflammation after cerebral ischemia through enhancing microglial activation and pro-inflammatory exosome release.* Frontiers in Immunology, 2020. **11**: p. 161.

186. Wu, B., J. Liu, R. Zhao, Y. Li, J. Peer, A.L. Braun, L. Zhao, Y. Wang, Z. Tong, Y. Huang, and J.C. Zheng, *Glutaminase 1 regulates the release of extracellular vesicles during neuroinflammation through key metabolic intermediate alpha-ketoglutarate.* Journal of Neuroinflammation, 2018. **15**(1): p. 79.

187. Datta, P.K., S. Deshmane, K. Khalili, S. Merali, J.C. Gordon, C. Fecchio, and C.A. Barrero, *Glutamate metabolism in HIV-1 infected macrophages: Role of HIV-1 Vpr.* Cell Cycle, 2016. **15**(17): p. 2288-98.

188. Bell-Temin, H., P. Zhang, D. Chaput, M.A. King, M. You, B. Liu, and S.M. Stevens, Jr., *Quantitative proteomic characterization of ethanol-responsive pathways in rat microglial cells.* Journal of Proteome Research, 2013. **12**(5): p. 2067-77.

189. Fernandez-Lizarbe, S., M. Pascual, and C. Guerri, *Critical role of TLR4 response in the activation of microglia induced by ethanol.* Journal of Immunology, 2009. **183**(7): p. 4733-44.

190. Alfonso-Loeches, S., J. Ureña-Peralta, M.J. Morillo-Bargues, U. Gómez-Pinedo, and C. Guerri, *Ethanol-induced TLR4/NLRP3 neuroinflammatory response in microglial cells promotes leukocyte infiltration across the BBB.* Neurochemical Research, 2016. **41**(1-2): p. 193-209.

191. Blankson, J.N. and R.F. Siliciano, *Elite suppression of HIV-1 replication.* Immunity, 2008. **29**(6): p. 845-7.

192. Lang, K.S., N. Honke, N. Shaabani, D. Häussinger, and P.A. Lang, *Enforced viral replication, a mechanism for immune activation.* European Journal of Medical Research, 2014. **19**(Suppl 1): p. S26-S26.

193. Cook, R.L., Z. Zhou, N.E. Kelso-Chichetto, J. Janelle, J.P. Morano, C. Somboonwit, W. Carter, G.E. Ibanez, N. Ennis, C.L. Cook, R.A. Cohen, B. Brumback, and K. Bryant, *Alcohol consumption patterns and HIV viral suppression among persons receiving HIV care in Florida: an observational study.* Addiction Science and Clinical Practice, 2017. **12**(1): p. 22.

194. Guha, D., M.C.E. Wagner, and V. Ayyavoo, *Human immunodeficiency virus type 1 (HIV-1)-mediated neuroinflammation dysregulates neurogranin and induces synaptodendritic injury.* Journal of Neuroinflammation, 2018. **15**(1): p. 126.

195. Perry, S.W., J.P. Norman, A. Litzburg, D. Zhang, S. Dewhurst, and H.A. Gelbard, *HIV-1 transactivator of transcription protein induces mitochondrial hyperpolarization and synaptic stress leading to apoptosis.* Journal of Immunology, 2005. **174**(7): p. 4333-44.

196. Avdoshina, V., J.A. Fields, P. Castellano, S. Dedoni, G. Palchik, M. Trejo, A. Adame, E. Rockenstein, E. Eugenin, E. Masliah, and I. Mocchetti, *The HIV protein gp120 alters mitochondrial dynamics in neurons.* Neurotoxicity Research, 2016. **29**(4): p. 583-593.

197. Stauch, K.L., K. Emanuel, B.G. Lamberty, B. Morsey, and H.S. Fox, *Central nervous system-penetrating antiretrovirals impair energetic reserve in striatal nerve terminals.* Journal of NeuroVirology, 2017. **23**(6): p. 795-807.

198. Singh, K.K., *Mitochondria damage checkpoint in apoptosis and genome stability.* FEMS Yeast Research, 2004. **5**(2): p. 127-32.

199. Duplanty, A.A., L. Simon, and P.E. Molina, *Chronic binge alcohol-induced dysregulation of mitochondrial-related genes in skeletal muscle of simian immunodeficiency virus-infected rhesus macaques at end-stage disease.* Alcohol Alcohol, 2017. **52**(3): p. 298-304.

200. Shefa, U., N.Y. Jeong, I.O. Song, H.J. Chung, D. Kim, J. Jung, and Y. Huh, *Mitophagy links oxidative stress conditions and neurodegenerative diseases.* Neural Regeneration Research, 2019. **14**(5): p. 749-756.

201. Macallan, D.C., C. Noble, C. Baldwin, S.A. Jebb, A.M. Prentice, W.A. Coward, M.B. Sawyer, T.J. McManus, and G.E. Griffin, *Energy expenditure and wasting in human immunodeficiency virus infection.* The New England Journal of Medicine, 1995. **333**(2): p. 83-8.

202. Molina, P.E., M. McNurlan, J. Rathmacher, C.H. Lang, K.L. Zambell, J. Purcell, R.P. Bohm, P. Zhang, G.J. Bagby, and S. Nelson, *Chronic alcohol accentuates nutritional, metabolic, and immune alterations during asymptomatic simian immunodeficiency virus infection.* Alcoholism: Clinical and Experimental Research, 2006. **30**(12): p. 2065-78.

203. Lozupone, C.A., M. Li, T.B. Campbell, S.C. Flores, D. Linderman, M.J. Gebert, R. Knight, A.P. Fontenot, and B.E. Palmer, *Alterations in the gut microbiota associated with HIV-1 infection.* Cell Host and Microbe, 2013. **14**(3): p. 329-39.

204. Pencharz, P., D. Macallan, and A. Tomkins, *Macronutrients and HIV/AIDS: Macronutrients and HIV/AIDS: a review of current evidence a review of current evidence.* World Health Organization, 2005.

205. Molina, P.E., C.H. Lang, M. McNurlan, G.J. Bagby, and S. Nelson, *Chronic alcohol accentuates simian acquired immunodeficiency syndrome-associated wasting.* Alcoholism: Clinical and Experimental Research, 2008. **32**(1): p. 138-47.

206. Thomson, A.D., *Mechanisms of vitamin deficiency in chronic alcohol misusers and the development of the Wernicke-Korsakoff syndrome.* Alcohol and Alcoholism, 2000. **35**(Supplement_1): p. 2-1.

207. Hong-Brown, L.Q., A.A. Kazi, and C.H. Lang, *Mechanisms mediating the effects of alcohol and HIV anti-retroviral agents on mTORC1, mTORC2 and protein synthesis in myocytes.* Journal of Biological Chemistry, 2012. **3**(6): p. 110-20.

208. Tavazzi, E., D. Morrison, P. Sullivan, S. Morgello, and T. Fischer, *Brain inflammation is a common feature of HIV-infected patients without HIV encephalitis or productive brain infection.* Current HIV Research, 2014. **12**(2): p. 97-110.

209. Yadav, A. and R.G. Collman, *CNS inflammation and macrophage/microglial biology associated with HIV-1 infection.* Journal of Neuroimmune Pharmacology, 2009. **4**(4): p. 430-47.

210. Kakanakova, A., S. Popov, and M. Maes, *Immunological disturbances and neuroimaging findings in major depressive disorder (MDD) and alcohol use disorder (AUD) comorbid patients.* Current Topics in Medicinal Chemistry, 2020. **20**(9): p. 759-769.

211. McColl, E.R. and M. Piquette-Miller, *SLC neurotransmitter transporters as therapeutic targets for alcohol use disorder: a narrative review.* Alcoholism: Clinical and Experimental Research, 2020. **44**(10): p. 1965-1976.

212. Cho, Y.E., M.H. Lee, and B.J. Song, *Neuronal cell death and degeneration through increased nitroxidative stress and tau phosphorylation in HIV-1 transgenic rats.* PLoS One, 2017. **12**(1): p. e0169945.

213. Lull, M.E. and M.L. Block, *Microglial activation and chronic neurodegeneration.* Neurotherapeutics, 2010. **7**(4): p. 354-65.

214. Moran, L.M., S. Fitting, R.M. Booze, K.M. Webb, and C.F. Mactutus, *Neonatal intrahippocampal HIV-1 protein Tat(1-86) injection: neurobehavioral alterations in the absence of increased inflammatory cytokine activation.* International Journal of Developmental Neuroscience : the Official Journal of the International Society for Developmental Neuroscience, 2014. **38**: p. 195-203.

215. Zheng, J., A. Ghorpade, D. Niemann, R.L. Cotter, M.R. Thylin, L. Epstein, J.M. Swartz, R.B. Shepard, X. Liu, A. Nukuna, and H.E. Gendelman, *Lymphotropic virions affect chemokine receptor-mediated neural signaling and apoptosis: implications for human immunodeficiency virus type 1-associated dementia.* Journal of Virology, 1999. **73**(10): p. 8256-67.

216. Masiá, M., S. Padilla, M. Fernández, C. Rodríguez, A. Moreno, J.A. Oteo, A. Antela, S. Moreno, J. Del Amo, and F. Gutiérrez, *Oxidative stress predicts all-cause mortality in HIV-infected patients.* PLoS One, 2016. **11**(4): p. e0153456.

217. Pawate, S. and N.R. Bhat, *Role of glia in CNS inflammation*, in *Handbook of Neurochemistry and Molecular Neurobiology: Neuroimmunology*, A. Lajtha, A. Galoyan, and H.O. Besedovsky, Editors. 2008, Springer US: Boston, MA. p. 309-330.

218. Hu, X.T., *HIV-1 Tat-mediated calcium dysregulation and neuronal dysfunction in vulnerable brain regions.* Current Drug Targets, 2016. **17**(1): p. 4-14.

219. Mayne, M., C.P. Holden, A. Nath, and J.D. Geiger, *Release of calcium from inositol 1,4,5-trisphosphate receptor-regulated stores by HIV-1 Tat regulates TNF-alpha production in human macrophages.* Journal of Immunology, 2000. **164**(12): p. 6538-42.

220. Xu, C., J. Liu, L. Chen, S. Liang, N. Fujii, H. Tamamura, and H. Xiong, *HIV-1 gp120 enhances outward potassium current via CXCR4 and cAMP-dependent protein kinase A signaling in cultured rat microglia.* Glia, 2011. **59**(6): p. 997-1007.

221. Zorova, L.D., V.A. Popkov, E.Y. Plotnikov, D.N. Silachev, I.B. Pevzner, S.S. Jankauskas, V.A. Babenko, S.D. Zorov, A.V. Balakireva, M. Juhaszova, S.J. Sollott, and D.B. Zorov, *Mitochondrial membrane potential.* Analytical Biochemistry, 2018. **552**: p. 50-59.

222. Kaul, M. and S.A. Lipton, *Chemokines and activated macrophages in HIV gp120-induced neuronal apoptosis.* Proceedings of the National Academy of Sciences, 1999. **96**(14): p. 8212-8216.

223. Saribal, D., F.S. Hocaoglu-Emre, F. Karaman, H. Mırsal, and M.C. Akyolcu, *Trace element levels and oxidant/antioxidant status in patients with alcohol abuse.* Biological Trace Element Research, 2020. **193**(1): p. 7-13.

224. Haorah, J., D. Heilman, C. Diekmann, N. Osna, T.M. Donohue, Jr., A. Ghorpade, and Y. Persidsky, *Alcohol and HIV decrease proteasome and immunoproteasome function in macrophages: implications for impaired immune function during disease.* Cell Immunology, 2004. **229**(2): p. 139-48.

225. Thangavel, S., C.T. Mulet, V.S.R. Atluri, M. Agudelo, R. Rosenberg, J.G. Devieux, and M.P.N. Nair, *Oxidative stress in HIV infection and alcohol use: role of redox signals in modulation of lipid rafts and ATP-binding cassette transporters.* Antioxidants and Redox Signaling, 2018. **28**(4): p. 324-337.

226. Tang, Y. and W. Le, *Differential Roles of M1 and M2 Microglia in Neurodegenerative Diseases.* Molecular Neurobiology, 2016. **53**(2): p. 1181-1194.

227. Varnum, M.M. and T. Ikezu, *The classification of microglial activation phenotypes on neurodegeneration and regeneration in Alzheimer's disease brain.* Archivum Immunologiae et Therapiae Experimentalis, 2012. **60**(4): p. 251-66.

228. Alfonso-Loeches, S., M. Pascual-Lucas, A.M. Blanco, I. Sanchez-Vera, and C. Guerri, *Pivotal role of TLR4 receptors in alcohol-induced neuroinflammation and brain damage.* Journal of Neuroscience, 2010. **30**(24): p. 8285-95.

229. Pandey, R. and A. Ghorpade, *HIV-1 and alcohol abuse promote astrocyte inflammation: A mechanistic synergy via the cytosolic phospholipase A2 pathway.* Cell Death and Disease, 2015. **6**(12): p. e2017.

230. Pandey, R. and A. Ghorpade, *Cytosolic phospholipase A2 regulates alcohol-mediated astrocyte inflammatory responses in HIV-associated neurocognitive disorders.* Cell Death Discovery, 2015. **1**(1): p. 15045.

231. Potula, R., J. Haorah, B. Knipe, J. Leibhart, J. Chrastil, D. Heilman, H. Dou, R. Reddy, A. Ghorpade, and Y. Persidsky, *Alcohol abuse enhances neuroinflammation and impairs immune responses in an animal model of human immunodeficiency virus-1 encephalitis.* The American Journal of Pathology, 2006. **168**(4): p. 1335-44.

232. DiSabato, D.J., N. Quan, and J.P. Godbout, *Neuroinflammation: the devil is in the details.* Journal of Neurochemistry, 2016. **139 Suppl 2**(Suppl 2): p. 136-153.

233. Boban, J., D. Kozic, V. Turkulov, J. Ostojic, R. Semnic, D. Lendak, and S. Brkic, *HIV-associated neurodegeneration and neuroimmunity: multivoxel MR spectroscopy study in drug-naïve and treated patients.* European Radiology, 2017. **27**(10): p. 4218-4236.

234. Dash, P.K., S. Gorantla, H.E. Gendelman, J. Knibbe, G.P. Casale, E. Makarov, A.A. Epstein, H.A. Gelbard, M.D. Boska, and L.Y. Poluektova, *Loss of neuronal integrity during progressive HIV-1 infection of humanized mice.* The Journal of Neuroscience, 2011. **31**(9): p. 3148-3157.

235. Cysique, L.A., L. Jugé, T. Gates, M. Tobia, K. Moffat, B.J. Brew, and C. Rae, *Covertly active and progressing neurochemical abnormalities in suppressed HIV infection.* Neurology Neuroimmunology and Neuroinflammation, 2018. **5**(1): p. e430.

236. Chabenne, A., C. Moon, C. Ojo, A. Khogali, B. Nepal, and S. Sharma, *Biomarkers in fetal alcohol syndrome.* Biomarkers and Genomic Medicine, 2014. **6**(1): p. 12-22.

237. Miguez, M.J., D. Bueno, L. Espinoza, W. Chan, and C. Perez, *Among adolescents, BDNF and pro-BDNF lasting changes with alcohol use are stage specific.* Neural Plasticity, 2020. **2020**: p. 3937627.

238. Silva-Peña, D., N. García-Marchena, F. Alén, P. Araos, P. Rivera, A. Vargas, M.I. García-Fernández, A.I. Martín-Velasco, M. Villanúa, E. Castilla-Ortega, L. Santín, F.J. Pavón, A. Serrano, G. Rubio, F. Rodríguez de Fonseca, and J. Suárez, *Alcohol-induced cognitive deficits are associated with decreased circulating levels of the neurotrophin BDNF in humans and rats.* Addiction Biology, 2019. **24**(5): p. 1019-1033.

239. Michael, H., T. Mpofana, S. Ramlall, and F. Oosthuizen, *The role of brain derived neurotrophic factor in HIV-associated neurocognitive disorder: from the bench-top to the bedside.* Neuropsychiatric Disease and Treatment, 2020. **16**: p. 355-367.

240. Matza, L.S., K.C. Chung, K.J. Kim, T.M. Paulus, E.W. Davies, K.D. Stewart, G.A. McComsey, and M.W. Fordyce, *Risks associated with antiretroviral treatment for human immunodeficiency virus (HIV): qualitative analysis of social media data and health state utility valuation.* Quality of Life Research, 2017. **26**(7): p. 1785-1798.

241. Watkins, C.C. and G.J. Treisman, *Cognitive impairment in patients with AIDS - prevalence and severity.* HIV AIDS (Auckland, NZ), 2015. **7**: p. 35-47.

242. Tarancon-Diez, L., E. Rodríguez-Gallego, A. Rull, J. Peraire, C. Viladés, I. Portilla, M.R. Jimenez-Leon, V. Alba, P. Herrero, M. Leal, E. Ruiz-Mateos, and F. Vidal, *Immunometabolism is a key factor for the persistent spontaneous elite control of HIV-1 infection.* EBioMedicine, 2019. **42**: p. 86-96.

243. Cains, S., C. Blomeley, M. Kollo, R. Rácz, and D. Burdakov, *Agrp neuron activity is required for alcohol-induced overeating.* Nature Communications, 2017. **8**(1): p. 14014.

244. Luo, J., *Autophagy and ethanol neurotoxicity.* Autophagy, 2014. **10**(12): p. 2099-108.

245. Palmer, C.S., G.A. Duette, M.C.E. Wagner, D.C. Henstridge, S. Saleh, C. Pereira, J. Zhou, D. Simar, S.R. Lewin, M. Ostrowski, J.M. McCune, and S.M. Crowe, *Metabolically active CD4+ T cells expressing Glut1 and OX40 preferentially harbor HIV during in vitro infection.* FEBS Lett, 2017. **591**(20): p. 3319-3332.

246. Louboutin, J.P. and D. Strayer, *Role of oxidative stress in HIV-1-associated neurocognitive disorder and protection by gene delivery of antioxidant enzymes.* Antioxidants (Basel), 2014. **3**(4): p. 770-97.

247. Brailoiu, E., G.C. Brailoiu, G. Mameli, A. Dolei, B.E. Sawaya, and N.J. Dun, *Acute exposure to ethanol potentiates human immunodeficiency virus type 1 Tat-induced Ca2+ overload and neuronal death in cultured rat cortical neurons.* Journal of NeuroVirology, 2006. **12**(1): p. 17-24.

248. Chen, W., Z. Tang, P. Fortina, P. Patel, S. Addya, S. Surrey, E.A. Acheampong, M. Mukhtar, and R.J. Pomerantz, *Ethanol potentiates HIV-1 gp120-induced apoptosis in human neurons via both the death receptor and NMDA receptor pathways.* Virology, 2005. **334**(1): p. 59-73.

249. Flora, G., H. Pu, Y.W. Lee, R. Ravikumar, A. Nath, B. Hennig, and M. Toborek, *Proinflammatory synergism of ethanol and HIV-1 Tat protein in brain tissue.* Experimental Neurology, 2005. **191**(1): p. 2-12.

250. Self, R.L., P.J. Mulholland, B.R. Harris, A. Nath, and M.A. Prendergast, *Cytotoxic effects of exposure to the human immunodeficiency virus type 1 protein Tat in the hippocampus are enhanced by prior ethanol treatment.* Alcoholism: Clinical and Experimental Research, 2004. **28**(12): p. 1916-1924.

251. Molina, P.E., A.M. Amedee, R. Veazey, J. Dufour, J. Volaufova, G.J. Bagby, and S. Nelson, *Chronic binge alcohol consumption does not diminish effectiveness of continuous antiretroviral suppression of viral load in simian immunodeficiency virus-infected macaques.* Alcoholism, clinical and experimental research, 2014. **38**(9): p. 2335-2344.

252. Lowe, P.P., C. Morel, A. Ambade, A. Iracheta-Vellve, E. Kwiatkowski, A. Satishchandran, I. Furi, Y. Cho, B. Gyongyosi, D. Catalano, E. Lefebvre, L. Fischer, S. Seyedkazemi, D.P. Schafer, and G. Szabo, *Chronic alcohol-induced neuroinflammation involves CCR2/5-dependent peripheral macrophage infiltration and microglia alterations.* Journal of Neuroinflammation, 2020. **17**(1): p. 296.

253. Ma, X., A. Agas, Z. Siddiqui, K. Kim, P. Iglesias-Montoro, J. Kalluru, V. Kumar, and J. Haorah, *Angiogenic peptide hydrogels for treatment of traumatic brain injury.* Bioactive Materials, 2020. **5**(1): p. 124-132.

254. Sarkar, B., X. Ma, A. Agas, Z. Siddiqui, P. Iglesias-Montoro, P.K. Nguyen, K.K. Kim, J. Haorah, and V.A. Kumar, *In vivo neuroprotective effect of a self-assembled peptide hydrogel.* Chemical Engineering Journal, 2021. **408**: p. 127295.

255. Weischenfeldt, J. and B. Porse, *Bone marrow-derived macrophages (BMM): isolation and applications.* Cold Spring Harbor Protocols, 2008. **2008**: p. pdb.prot5080.

256. Bartosh, T.J. and J.H. Ylostalo, *Macrophage inflammatory assay.* Biology Methods and Protocols, 2014. **4**(14).

257. Eugenin, E.A. and J.W. Berman, *Chemokine-dependent mechanisms of leukocyte trafficking across a model of the blood–brain barrier.* Methods, 2003. **29**(4): p. 351-361.

258. Hatherell, K., P.O. Couraud, I.A. Romero, B. Weksler, and G.J. Pilkington, *Development of a three-dimensional, all-human in vitro model of the blood-brain barrier using mono-, co-, and tri-cultivation Transwell models.* Journal of Neuroscience Methods, 2011. **199**(2): p. 223-9.

259. Stone, N.L., T.J. England, and S.E. O'Sullivan, *A novel transwell blood brain barrier model using primary human cells.* Frontiers in Cellular Neuroscience, 2019. **13**: p. 230.

260. Wang, H.-L. and T.W. Lai, *Optimization of Evans blue quantitation in limited rat tissue samples.* Scientific Reports, 2014. **4**(1): p. 6588.

261. Fox J, B.-V.M., *R Commander.* . 2020.

262. Cui, C. and G.F. Koob, *Titrating tipsy targets: the neurobiology of low-dose alcohol.* Trends in Pharmacological Sciences, 2017. **38**(6): p. 556-568.

263. Mele, A.R., J. Marino, W. Dampier, B. Wigdahl, and M.R. Nonnemacher, *HIV-1 Tat length: comparative and functional considerations.* Frontiers in Microbiology, 2020. **11**(444).

264. Wayman, W.N., L. Chen, A.L. Persons, and T.C. Napier, *Cortical consequences of HIV-1 Tat exposure in rats are enhanced by chronic cocaine.* Current HIV research, 2015. **13**(1): p. 80-87.

265. Zeiher, A.M., B. Fisslthaler, B. Schray-Utz, and R. Busse, *Nitric oxide modulates the expression of monocyte chemoattractant protein 1 in cultured human endothelial cells.* Circulation Research, 1995. **76**(6): p. 980-986.

266. Deshmane, S.L., S. Kremlev, S. Amini, and B.E. Sawaya, *Monocyte chemoattractant protein-1 (MCP-1): an overview.* Journal of Interferon Cytokine Research, 2009. **29**(6): p. 313-26.

267. Syapin, P.J., *Alcohol and nitric oxide production by cells of the brain.* Alcohol, 1998. **16**(2): p. 159-165.

268. McIlwain, D.R., T. Berger, and T.W. Mak, *Caspase functions in cell death and disease.* Cold Spring Harbor Perspectives in Biology, 2013. **5**(4): p. a008656.

269. Goldim, M.P.S., A. Della Giustina, and F. Petronilho, *Using evans blue dye to determine blood-brain barrier integrity in rodents.* Current Protocols in Immunology, 2019. **126**(1): p. e83.

270. Dasgupta, A., *Alcohol a double-edged sword: Health benefits with moderate consumption but a health hazard with excess alcohol intake*, in *Alcohol, Drugs, Genes and the Clinical Laboratory*, A. Dasgupta, Editor. 2017, Academic Press. p. 1-21.

271. Yu, H., C. Wang, X. Wang, H. Wang, C. Zhang, J. You, P. Wang, C. Feng, G. Xu, R. Zhao, X. Wu, and G. Zhang, *Long-term exposure to ethanol downregulates tight junction proteins through the protein kinase Cα signaling pathway in human cerebral microvascular endothelial cells.* Experimental and Therapeutic Medicine, 2017. **14**(5): p. 4789-4796.

272. Haorah, J., D. Heilman, B. Knipe, J. Chrastil, J. Leibhart, A. Ghorpade, D.W. Miller, and Y. Persidsky, *Ethanol-induced activation of myosin light chain kinase leads to dysfunction of tight junctions and blood-brain barrier compromise.* Alcoholism: Clinical and Experimental Research, 2005. **29**(6): p. 999-1009.

273. Kolios, G., V. Valatas, P. Manousou, C. Xidakis, G. Notas, and E. Kouroumalis, *Nitric oxide and MCP-1 regulation in LPS activated rat Kupffer cells.* Molecular and Cellular Biochemistry, 2008. **319**(1-2): p. 91-8.

274. Deng, X.S. and R.A. Deitrich, *Ethanol metabolism and effects: nitric oxide and its interaction.* Current Clinical Pharmacology, 2007. **2**(2): p. 145-53.

275. Eugenin, E.A., J.E. King, A. Nath, T.M. Calderon, R.S. Zukin, M.V. Bennett, and J.W. Berman, *HIV-tat induces formation of an LRP-PSD-95- NMDAR-nNOS complex that promotes apoptosis in neurons and astrocytes.* Proceedings of the National Academy of Sciences of the United States of America, 2007. **104**(9): p. 3438-43.

276. Ma, R., L. Yang, F. Niu, and S. Buch, *HIV Tat-mediated induction of human brain microvascular endothelial cell apoptosis involves endoplasmic reticulum stress and mitochondrial dysfunction.* Molecular Neurobiology, 2016. **53**(1): p. 132-142.

277. Yang, Y., I. Tikhonov, T.J. Ruckwardt, M. Djavani, J.C. Zapata, C.D. Pauza, and M.S. Salvato, *Monocytes treated with human immunodeficiency virus Tat kill uninfected CD4(+) cells by a tumor necrosis factor-related apoptosis-induced ligand-mediated mechanism.* Journal of Virology, 2003. **77**(12): p. 6700-6708.

278. Hargus, N.J. and S.A. Thayer, *Human immunodeficiency virus-1 Tat protein increases the number of inhibitory synapses between hippocampal neurons in culture.* The Journal of Neuroscience : the Official Journal of the Society for Neuroscience, 2013. **33**(45): p. 17908-17920.

279. Mishra, M., M. Taneja, S. Malik, H. Khalique, and P. Seth, *Human immunodeficiency virus type 1 Tat modulates proliferation and differentiation of human neural precursor cells: implication in NeuroAIDS.* Journal of NeuroVirology, 2010. **16**(5): p. 355-67.

280. Mohseni Ahooyi, T., B. Torkzaban, M. Shekarabi, F.G. Tahrir, E.A. Decoppet, B. Cotto, D. Langford, S. Amini, and K. Khalili, *Perturbation of synapsins homeostasis through HIV-1 Tat-mediated suppression of BAG3 in primary neuronal cells.* Cell Death and Disease, 2019. **10**(7): p. 473.

281. Teodorof-Diedrich, C. and S.A. Spector, *Human immunodeficiency virus type 1 gp120 and Tat induce mitochondrial fragmentation and incomplete mitophagy in human neurons.* Journal of Virology, 2018. **92**(22).

282. Belmadani, A., E.J. Neafsey, and M.A. Collins, *Human immunodeficiency virus type 1 gp120 and ethanol coexposure in rat organotypic brain slice cultures: Curtailment of gp120-induced neurotoxicity and neurotoxic mediators by moderate but not high ethanol concentrations.* Journal of Neurovirology, 2003. **9**(1): p. 45-54.

283. Belmadani, A., J.Y. Zou, M.J. Schipma, E.J. Neafsey, and M.A. Collins, *Ethanol pre-exposure suppresses HIV-1 glycoprotein 120-induced neuronal degeneration by abrogating endogenous glutamate/Ca2+-mediated neurotoxicity.* Neuroscience, 2001. **104**(3): p. 769-81.

284. Collins, M.A., E.J. Neafsey, and J.Y. Zou, *HIV-I gpI20 neurotoxicity in brain cultures is prevented by moderate ethanol pretreatment.* Neuroreport, 2000. **11**(6): p. 1219-22.

285. Olney, J.W., T. Tenkova, K. Dikranian, L.J. Muglia, W.J. Jermakowicz, C. D'Sa, and K.A. Roth, *Ethanol-induced caspase-3 activation in the in vivo developing mouse brain.* Neurobiological Diseases, 2002. **9**(2): p. 205-19.

286. Young, C., K.A. Roth, B.J. Klocke, T. West, D.M. Holtzman, J. Labruyere, Y.Q. Qin, K. Dikranian, and J.W. Olney, *Role of caspase-3 in ethanol-induced developmental neurodegeneration.* Neurobiology of Disease, 2005. **20**(2): p. 608-14.

287. León-Rivera, R., M. Veenstra, M. Donoso, E. Tell, E.A. Eugenin, S. Morgello, and J.W. Berman, *Central nervous system (CNS) viral seeding by mature monocytes and potential therapies to reduce CNS viral reservoirs in the cART era.* mBio, 2021. **12**(2).

288. CDC, *Human immunodeficiency virus (HIV) diagnoses, by year of diagnosis and selected characteristics: United States, 2012–2017.* Centers for Disease Control and Prevention, 2018: p. Accessed 02-20-2021 Retrieved from https://www.ncbi.nlm.nih.gov/books/NBK551099/table/ch3.tab11/?report=objectonly.

289. Panagiotoglou, D., M. Olding, B. Enns, D.J. Feaster, C. Del Rio, L.R. Metsch, R.M. Granich, S.A. Strathdee, B.D.L. Marshall, M.R. Golden, S. Shoptaw, B.R. Schackman, and B. Nosyk, *Building the case for localized approaches to HIV: structural conditions and health system capacity to address the HIV/AIDS epidemic in six US cities.* AIDS and Behavior, 2018. **22**(9): p. 3071-3082.

290. Arts, E.J. and D.J. Hazuda, *HIV-1 antiretroviral drug therapy.* Cold Spring Harbor Perspectives in Medicine, 2012. **2**(4): p. a007161.

291. McArthur, J.C., B.J. Brew, and A. Nath, *Neurological complications of HIV infection.* Lancet Neurology, 2005. **4**(9): p. 543-55.

292. Nath, A. and N. Sacktor, *Influence of highly active antiretroviral therapy on persistence of HIV in the central nervous system.* Current Opinion in Neurology, 2006. **19**(4): p. 358-61.

293. Spudich, S. and F. Gonzalez-Scarano, *HIV-1-related central nervous system disease: current issues in pathogenesis, diagnosis, and treatment.* Cold Spring Harbor Perspectives in Medicine, 2012. **2**(6): p. a007120.

294. Peluso, M.J., F. Ferretti, J. Peterson, E. Lee, D. Fuchs, A. Boschini, M. Gisslen, N. Angoff, R.W. Price, P. Cinque, and S. Spudich, *Cerebrospinal fluid HIV escape associated with progressive neurologic dysfunction in patients on antiretroviral therapy with well controlled plasma viral load.* Aids, 2012. **26**(14): p. 1765-74.

295. Cattaneo, D., A. Giacomelli, and C. Gervasoni, *Loss of control of HIV viremia with OTC weight-loss drugs: a call for caution?* Obesity (Silver Spring), 2018. **26**(8): p. 1251-1252.

296. Behrens, G.M., A.R. Boerner, K. Weber, J. van den Hoff, J. Ockenga, G. Brabant, and R.E. Schmidt, *Impaired glucose phosphorylation and transport in skeletal muscle cause insulin resistance in HIV-1-infected patients with lipodystrophy.* Journal of Clinical Investigation, 2002. **110**(9): p. 1319-27.

297. Jia, H.H., K.W. Li, Q.Y. Chen, X.Y. Wang, T.J. Harrison, S.J. Liang, Q.L. Yang, C. Wang, L.P. Hu, C.C. Ren, and Z.L. Fang, *High prevalence of HBV lamivudine-resistant mutations in HBV/HIV co-infected patients on antiretroviral therapy in the area with the highest prevalence of HIV/HBV co-infection in China.* Intervirology, 2018. **61**(3): p. 123-132.

298. Ranganathan, S. and P.A. Kern, *The HIV protease inhibitor saquinavir impairs lipid metabolism and glucose transport in cultured adipocytes.* Journal of Endocrinology, 2002. **172**(1): p. 155-62.

299. Baum, M.K., C. Rafie, S. Lai, S. Sales, J.B. Page, and A. Campa, *Alcohol use accelerates HIV disease progression.* AIDS Research on Human Retroviruses, 2010. **26**(5): p. 511-8.

300. Shuper, P.A., M. Neuman, F. Kanteres, D. Baliunas, N. Joharchi, and J. Rehm, *Causal considerations on alcohol and HIV/AIDS--a systematic review.* Alcohol Alcohol, 2010. **45**(2): p. 159-66.

301. Zhang, Y.L., Y.B. Ouyang, L.G. Liu, and D.X. Chen, *Blood-brain barrier and neuro-AIDS.* European Review for Medical and Pharmacological Sciences, 2015. **19**(24): p. 4927-39.

302. Tran, B.X., L.H. Nguyen, C.T. Nguyen, H.T. Phan, and C.A. Latkin, *Alcohol abuse increases the risk of HIV infection and diminishes health status of clients attending HIV testing services in Vietnam.* Harm Reduction Journal, 2016. **13**: p. 6.

303. Ferrari, L.F. and J.D. Levine, *Alcohol consumption enhances antiretroviral painful peripheral neuropathy by mitochondrial mechanisms.* European Journal of Neuroscience, 2010. **32**(5): p. 811-8.

304. Sullivan, L.E., J.L. Goulet, A.C. Justice, and D.A. Fiellin, *Alcohol consumption and depressive symptoms over time: a longitudinal study of patients with and without HIV infection.* Drug and Alcohol Dependence, 2011. **117**(2-3): p. 158-63.

305. Rosenbloom, M.J., E.V. Sullivan, and A. Pfefferbaum, *Focus on the brain: HIV infection and alcoholism: comorbidity effects on brain structure and function.* Alcohol Research and Health, 2010. **33**(3): p. 247-57.

306. DeLorenze, G.N., C. Weisner, A.L. Tsai, D.D. Satre, and C.P. Quesenberry, Jr., *Excess mortality among HIV-infected patients diagnosed with substance use dependence or abuse receiving care in a fully integrated medical care program.* Alcoholism: Clinical and Experimental Research, 2011. **35**(2): p. 203-10.

307. Freiberg, M.S., K.A. McGinnis, K. Kraemer, J.H. Samet, J. Conigliaro, R. Curtis Ellison, K. Bryant, L.H. Kuller, and A.C. Justice, *The association between alcohol consumption and prevalent cardiovascular diseases among HIV-infected and HIV-uninfected men.* Journal of Acquired Immune Deficiency Syndromes, 2010. **53**(2): p. 247-53.

308. Clary, C.R., D.M. Guidot, M.A. Bratina, and J.S. Otis, *Chronic alcohol ingestion exacerbates skeletal muscle myopathy in HIV-1 transgenic rats.* AIDS Research and Therapy, 2011. **8**: p. 30.

309. Katusiime, C., P. Ocama, and A. Kambugu, *Basis of selection of first and second line highly active antiretroviral therapy for HIV/AIDS on genetic barrier to resistance: a literature review.* African Health Sciences, 2014. **14**(3): p. 679-81.

310. Sebaaly, J.C. and D. Kelley, *HIV clinical updates: new single-tablet regimens.* Annals of Pharmacotherapy, 2019. **53**(1): p. 82-94.

311. Iacob, S.A., D.G. Iacob, and G. Jugulete, *Improving the adherence to antiretroviral therapy, a difficult but essential task for a successful HIV treatment-clinical points of view and practical considerations.* Frontiers in Pharmacology, 2017. **8**: p. 831.

312. Spreen, W.R., D.A. Margolis, and J.C. Pottage, Jr., *Long-acting injectable antiretrovirals for HIV treatment and prevention.* Current Opinion in HIV and AIDS, 2013. **8**(6): p. 565-71.

313. Perazzolo, S., L.M. Shireman, J. Koehn, L.A. McConnachie, J.C. Kraft, D.D. Shen, and R.J.Y. Ho, *Three HIV drugs, atazanavir, ritonavir, and tenofovir, coformulated in drug-combination nanoparticles exhibit long-acting and lymphocyte-targeting properties in nonhuman primates.* Journal of Pharmaceutical Sciences, 2018. **107**(12): p. 3153-3162.

314. Horwitz, J.A., A. Halper-Stromberg, H. Mouquet, A.D. Gitlin, A. Tretiakova, T.R. Eisenreich, M. Malbec, S. Gravemann, E. Billerbeck, M. Dorner, H. Buning, O. Schwartz, E. Knops, R. Kaiser, M.S. Seaman, J.M. Wilson, C.M. Rice, A. Ploss, P.J. Bjorkman, F. Klein, and M.C. Nussenzweig, *HIV-1 suppression and durable control by combining single broadly neutralizing antibodies and antiretroviral drugs in humanized mice.* Proceedings of the National Academy of Sciences of the United States of America, 2013. **110**(41): p. 16538-43.

315. Bertrand, L., M. Nair, and M. Toborek, *Solving the blood-brain barrier challenge for the effective treatment of HIV replication in the central nervous system.* Current Pharmaceutical Design, 2016. **22**(35): p. 5477-5486.

316. Eisfeld, C., D. Reichelt, S. Evers, and I. Husstedt, *CSF penetration by antiretroviral drugs.* CNS Drugs, 2013. **27**(1): p. 31-55.

317. Gibbs, J.E. and S.A. Thomas, *The distribution of the anti-HIV drug, 2'3'-dideoxycytidine (ddC), across the blood-brain and blood-cerebrospinal fluid barriers and the influence of organic anion transport inhibitors.* Journal of Neurochemistry, 2002. **80**(3): p. 392-404.

318. Krentz, H.B., S. Campbell, V.C. Gill, and M.J. Gill, *Patient perspectives on de-simplifying their single-tablet co-formulated antiretroviral therapy for societal cost savings.* HIV Medicine, 2018. **19**(4): p. 290-298.

319. Strazielle, N. and J.F. Ghersi-Egea, *Factors affecting delivery of antiviral drugs to the brain.* Reviews in Medical Virology, 2005. **15**(2): p. 105-33.

320. Varatharajan, L. and S.A. Thomas, *The transport of anti-HIV drugs across blood-CNS interfaces: summary of current knowledge and recommendations for further research.* Antiviral Research, 2009. **82**(2): p. A99-109.

321. Persidsky, Y., S.H. Ramirez, J. Haorah, and G.D. Kanmogne, *Blood-brain barrier: structural components and function under physiologic and pathologic conditions.* Journal of Neuroimmune Pharmacology, 2006. **1**(3): p. 223-36.

322. Letendre, S., J. Marquie-Beck, E. Capparelli, B. Best, D. Clifford, A.C. Collier, B.B. Gelman, J.C. McArthur, J.A. McCutchan, S. Morgello, D. Simpson, I. Grant, and R.J. Ellis, *Validation of the CNS penetration-effectiveness rank for quantifying antiretroviral penetration into the central nervous system.* Archives of Neurology, 2008. **65**(1): p. 65-70.

323. Banks, W.A., N. Ercal, and T.O. Price, *The blood-brain barrier in neuroAIDS.* Current HIV Research, 2006. **4**(3): p. 259-66.

324. Chomont, N., M. El-Far, P. Ancuta, L. Trautmann, F.A. Procopio, B. Yassine-Diab, G. Boucher, M.R. Boulassel, G. Ghattas, J.M. Brenchley, T.W. Schacker, B.J. Hill, D.C. Douek, J.P. Routy, E.K. Haddad, and R.P. Sekaly, *HIV reservoir size and persistence are driven by T cell survival and homeostatic proliferation.* Nature Medicine, 2009. **15**(8): p. 893-900.

325. Vandergeeten, C., R. Fromentin, S. DaFonseca, M.B. Lawani, I. Sereti, M.M. Lederman, M. Ramgopal, J.P. Routy, R.P. Sekaly, and N. Chomont, *Interleukin-7 promotes HIV persistence during antiretroviral therapy.* Blood, 2013. **121**(21): p. 4321-9.

326. Gendelman, H.E., J.M. Orenstein, M.A. Martin, C. Ferrua, R. Mitra, T. Phipps, L.A. Wahl, H.C. Lane, A.S. Fauci, D.S. Burke, and et al., *Efficient isolation and propagation of human immunodeficiency virus on recombinant colony-stimulating factor 1-treated monocytes.* Journal of Experimental Medicine, 1988. **167**(4): p. 1428-41.

327. Li, J.Z., B. Etemad, H. Ahmed, E. Aga, R.J. Bosch, J.W. Mellors, D.R. Kuritzkes, M.M. Lederman, M. Para, and R.T. Gandhi, *The size of the expressed HIV reservoir predicts timing of viral rebound after treatment interruption.* Aids, 2016. **30**(3): p. 343-53.

328. Finzi, D., J. Blankson, J.D. Siliciano, J.B. Margolick, K. Chadwick, T. Pierson, K. Smith, J. Lisziewicz, F. Lori, C. Flexner, T.C. Quinn, R.E. Chaisson, E. Rosenberg, B. Walker, S. Gange, J. Gallant, and R.F. Siliciano, *Latent infection of CD4+ T cells provides a mechanism for lifelong persistence of HIV-1, even in patients on effective combination therapy.* Nature Medicine, 1999. **5**(5): p. 512-7.

329. Brown, T.R., *I am the Berlin patient: a personal reflection.* AIDS Research on Human Retroviruses, 2015. **31**(1): p. 2-3.

330. Burke, B.P., M.P. Boyd, H. Impey, L.R. Breton, J.S. Bartlett, G.P. Symonds, and G. Hutter, *CCR5 as a natural and modulated target for inhibition of HIV.* Viruses, 2013. **6**(1): p. 54-68.

331. Deeks, S.G., *HIV: shock and kill.* Nature, 2012. **487**(7408): p. 439-40.

332. Kessing, C.F., C.C. Nixon, C. Li, P. Tsai, H. Takata, G. Mousseau, P.T. Ho, J.B. Honeycutt, M. Fallahi, L. Trautmann, J.V. Garcia, and S.T. Valente, *In vivo suppression of HIV rebound by didehydro-cortistatin A, a "block-and-lock" strategy for HIV-1 treatment.* Cell Reports, 2017. **21**(3): p. 600-611.

333. Giuliani, E., L. Vassena, S. Galardi, A. Michienzi, M.G. Desimio, and M. Doria, *Dual regulation of L-selectin (CD62L) by HIV-1: Enhanced expression by Vpr in contrast with cell-surface down-modulation by Nef and Vpu.* Virology, 2018. **523**: p. 121-128.

334. Hicks, C., P. Clay, R. Redfield, J. Lalezari, R. Liporace, S. Schneider, M. Sension, M. McRae, and J.P. Laurent, *Safety, tolerability, and efficacy of KP-1461 as monotherapy for 124 days in antiretroviral-experienced, HIV type 1-infected subjects.* AIDS Research on Human Retroviruses, 2013. **29**(2): p. 250-5.

335. Traore, Y.L., Y. Chen, and E.A. Ho, *Current state of microbicide development.* Clinical Pharmacology and Therapeutics, 2018. **104**(6): p. 1074-1081.

336. Frattari, G., L. Aagaard, and P.W. Denton, *The role of miR-29a in HIV-1 replication and latency.* Journal of Virus Eradication, 2017. **3**(4): p. 185-191.

337. Xu, W., H. Li, Q. Wang, C. Hua, H. Zhang, W. Li, S. Jiang, and L. Lu, *Advancements in developing strategies for sterilizing and functional HIV cures.* BioMed Research International, 2017. **2017**: p. 6096134.

338. Li, H., Y. Hai, S.Y. Lim, N. Toledo, J. Crecente-Campo, D. Schalk, L. Li, R.W. Omange, T.G. Dacoba, L.R. Liu, M.A. Kashem, Y. Wan, B. Liang, Q. Li, E. Rakasz, N. Schultz-Darken, M.J. Alonso, F.A. Plummer, J.B. Whitney, and M. Luo, *Mucosal antibody responses to vaccines targeting SIV protease cleavage sites or full-length Gag and Env proteins in Mauritian cynomolgus macaques.* PLoS One, 2018. **13**(8): p. e0202997.

339. Khalili, K., M.K. White, and J.M. Jacobson, *Novel AIDS therapies based on gene editing.* Cellular and Molecular Life Sciences, 2017. **74**(13): p. 2439-2450.

340. Ramakrishna, C., R.A. Atkinson, S.A. Stohlman, and C.C. Bergmann, *Vaccine-induced memory CD8+ T cells cannot prevent central nervous system virus reactivation.* Journal of Immunology, 2006. **176**(5): p. 3062-9.

341. Proust, A., C. Barat, M. Leboeuf, J. Drouin, and M.J. Tremblay, *Contrasting effect of the latency-reversing agents bryostatin-1 and JQ1 on astrocyte-mediated neuroinflammation and brain neutrophil invasion.* Journal of Neuroinflammation, 2017. **14**(1): p. 242.

342. Anstett, K., B. Brenner, T. Mesplede, and M.A. Wainberg, *HIV-1 resistance to dolutegravir is affected by cellular histone acetyltransferase activity.* Journal of Virology, 2017. **91**(21).

343. Qualls, Z.M., A. Choudhary, W. Honnen, R. Prattipati, J.E. Robinson, and A. Pinter, *Identification of novel structural determinants in MW965 env that regulate the neutralization phenotype and conformational masking potential of primary HIV-1 isolates.* Journal of Virology, 2018. **92**(5).

344. Ringel, O., V. Vieillard, P. Debre, J. Eichler, H. Buning, and U. Dietrich, *The hard way towards an antibody-based HIV-1 env vaccine: lessons from other viruses.* Viruses, 2018. **10**(4).

345. Balzarini, J., M.J. Perez-Perez, A. San-Felix, M.J. Camarasa, I.C. Bathurst, P.J. Barr, and E. De Clercq, *Kinetics of inhibition of human immunodeficiency virus type 1 (HIV-1) reverse transcriptase by the novel HIV-1-specific nucleoside analogue [2',5'-bis-O-(tert-butyldimethylsilyl)-beta-D-ribofuranosyl]-3'-spiro-5 "-(4"-amino-1",2"-oxathiole-2",2"-dioxide)thymine (TSAO-T).* Journal of Biological Chemistry, 1992. **267**(17): p. 11831-8.

346. Goff, S., P. Traktman, and D. Baltimore, *Isolation and properties of Moloney murine leukemia virus mutants: use of a rapid assay for release of virion reverse transcriptase.* Journal of Virology, 1981. **38**(1): p. 239-48.

347. Rosenberg, N. and D. Baltimore, *The effect of helper virus on Abelson virus-induced transformation of lymphoid cells.* Journal of Experimental Medicine, 1978. **147**(4): p. 1126-41.

348. Lee, J.J., D.J. Segar, J.F. Morrison, W.M. Mangham, S. Lee, and W.F. Asaad, *Subdural hematoma as a major determinant of short-term outcomes in traumatic brain injury.* Journal of Neurosurgery, 2018. **128**(1): p. 236-249.

349. Perel, P., I. Roberts, O. Bouamra, M. Woodford, J. Mooney, and F. Lecky, *Intracranial bleeding in patients with traumatic brain injury: A prognostic study.* BMC Emergency Medicine, 2009. **9**(1): p. 15.

350. Schweitzer, A.D., S.N. Niogi, C.T. Whitlow, and A.J. Tsiouris, *Traumatic brain injury: imaging patterns and complications.* RadioGraphics, 2019. **39**(6): p. 1571-1595.

351. East, J.M., J. Viau-Lapointe, and V.A. McCredie, *Transfusion practices in traumatic brain injury.* Current Opinion in Anaesthesiology, 2018. **31**(2): p. 219-226.

352. Stolla, M., F. Zhang, M.R. Meyer, J. Zhang, and J.-F. Dong, *Current state of transfusion in traumatic brain injury and associated coagulopathy.* Transfusion, 2019. **59**(S2): p. 1522-1528.

353. Salim, A., P. Hadjizacharia, J. DuBose, C. Brown, K. Inaba, L. Chan, and D.R. Margulies, *Role of anemia in traumatic brain injury.* Journal of the American College of Surgeons, 2008. **207**(3): p. 398-406.

354. Daglas, M. and P.A. Adlard, *The involvement of iron in traumatic brain injury and neurodegenerative disease.* Frontiers in Neuroscience, 2018. **12**: p. 981.

355. Ma, X., Y. Cheng, R. Garcia, and J. Haorah, *Hemorrhage associated mechanisms of neuroinflammation in experimental traumatic brain injury.* Journal of Neuroimmune Pharmacology, 2020. **15**(2): p. 181-195.

356. Ma, X., A. Aravind, B.J. Pfister, N. Chandra, and J. Haorah, *Animal models of traumatic brain injury and assessment of injury severity.* Molecular Neurobiology, 2019. **56**(8): p. 5332-5345.

357. Magnani, M., V. Stocchi, L. Cucchiarini, L. Chiarantini, and G. Fornaini, *Red blood cell phagocytosis and lysis following oxidative damage by phenylhydrazine.* Cell Biochemistry and Function, 1986. **4**(4): p. 263-9.

358. Wimmer, I., C. Scharler, T. Kadowaki, S. Hillebrand, B. Scheiber-Mojdehkar, S. Ueda, M. Bradl, T. Berger, H. Lassmann, and S. Hametner, *Iron accumulation in the choroid plexus, ependymal cells and CNS parenchyma in a rat strain with low-grade haemolysis of fragile macrocytic red blood cells.* Brain Pathology, 2021. **31**(2): p. 333-345.

359. Dev, S. and J.L. Babitt, *Overview of iron metabolism in health and disease.* Hemodialysis International, 2017. **21**(S1): p. S6-S20.

360. Russell, N.H., R.T. Black, N.N. Lee, A.E. Doperalski, T.M. Reeves, and L.L. Phillips, *Time-dependent hemeoxygenase-1, lipocalin-2 and ferritin induction after non-contusion traumatic brain injury.* Brain Research, 2019. **1725**: p. 146466.

361. Lowe, P.P., C. Morel, A. Ambade, A. Iracheta-Vellve, E. Kwiatkowski, A. Satishchandran, I. Furi, Y. Cho, B. Gyongyosi, D. Catalano, E. Lefebvre, L. Fischer, S. Seyedkazemi, D.P. Schafer, and G. Szabo, *Chronic alcohol-induced neuroinflammation involves CCR2/5-dependent peripheral macrophage infiltration and microglia alterations.* J Neuroinflammation, 2020. **17**(1): p. 296.

362. Teng SX, M.P., *Acute alcohol intoxication prolongs neuroinflammation without exacerbating neurobehavioral dysfunction following mild traumatic brain injury.* Journal of Neurotrauma, 2014. **31**(4): p. 378-386.

363. Smith, S., K. Fair, A. Goodman, J. Watson, C. Dodgion, and M. Schreiber, *Consumption of alcohol leads to platelet inhibition in men.* The American Journal of Surgery, 2019. **217**(5): p. 868-872.

364. Alikunju, S., P.M. Abdul Muneer, Y. Zhang, A.M. Szlachetka, and J. Haorah, *The inflammatory footprints of alcohol-induced oxidative damage in neurovascular components.* Brain, Behavior, and Immunity, 2011. **25**: p. S129-S136.

365. Cheng, Y., X. Ma, K.D. Belfield, and J. Haorah, *Biphasic effects of ethanol exposure on waste metabolites clearance in the CNS.* Molecular Neurobiology, 2021.

366. Ma, X., A. Agas, Z. Siddiqui, K. Kim, P. Iglesias-Montoro, J. Kalluru, V. Kumar, and J. Haorah, *Angiogenic peptide hydrogels for treatment of traumatic brain injury.* Bioact Mater, 2020. **5**(1): p. 124-132.

367. Izatt, R.M., G.D. Watt, C.H. Bartholomew, and J.J. Christensen, *Calorimetric study of Prussian blue and Turnbull's blue formation.* Inorganic Chemistry, 1970. **9**(9): p. 2019-2021.

368. Blomster, L.V., G.J. Cowin, N.D. Kurniawan, and M.J. Ruitenberg, *Detection of endogenous iron deposits in the injured mouse spinal cord through high-resolution ex vivo and in vivo MRI.* NMR in Biomedicine, 2013. **26**(2): p. 141-50.

369. Dietrich, W.D., O. Alonso, R. Busto, R. Prado, S. Dewanjee, M.K. Dewanjee, and M.D. Ginsberg, *Widespread hemodynamic depression and focal platelet accumulation after fluid percussion brain injury: a double-label autoradiographic study in rats.* Journal of Cerebral Blood Flow and Metabolism, 1996. **16**(3): p. 481-9.

370. McKee, A.C. and D.H. Daneshvar, *The neuropathology of traumatic brain injury.* Handbook of Clinical Neurology, 2015. **127**: p. 45-66.

371. Weisel, J.W. and R.I. Litvinov, *Red blood cells: the forgotten player in hemostasis and thrombosis.* Journal of Thrombosis and Haemostasis, 2019. **17**(2): p. 271-282.

372. Cheng, Y. and J. Haorah, *How does the brain remove its waste metabolites from within?* International Journal of Physiology, Pathophysiology, and Pharmacology, 2019. **11**(6): p. 238-249.

373. Shin, M.K., S.I. Kim, S.J. Kim, S.Y. Park, Y.H. Hyun, Y. Lee, K.E. Lee, S.S. Han, D.P. Jang, Y.B. Kim, Z.H. Cho, I. So, and G.M. Spinks, *Controlled magnetic nanofiber hydrogels by clustering ferritin.* Langmuir, 2008. **24**(21): p. 12107-11.

374. Arosio, P., L. Elia, and M. Poli, *Ferritin, cellular iron storage and regulation.* IUBMB Life, 2017. **69**(6): p. 414-422.

375. Abrahao, K.P., A.G. Salinas, and D.M. Lovinger, *Alcohol and the brain: neuronal molecular targets, synapses, and circuits.* Neuron, 2017. **96**(6): p. 1223-1238.

376. Xiao, X., B.S. Yeoh, P. Saha, R.A. Olvera, V. Singh, and M. Vijay-Kumar, *Lipocalin 2 alleviates iron toxicity by facilitating hypoferremia of inflammation and limiting catalytic iron generation.* Biometals, 2016. **29**(3): p. 451-65.

377. Chia, W.J., G.S. Dawe, and W.Y. Ong, *Expression and localization of the iron-siderophore binding protein lipocalin 2 in the normal rat brain and after kainate-induced excitotoxicity.* Neurochemistry International, 2011. **59**(5): p. 591-9.

378. Balter, L.J.T., J.A. Bosch, S. Aldred, M.T. Drayson, J.J.C.S. Veldhuijzen van Zanten, S. Higgs, J.E. Raymond, and A. Mazaheri, *Selective effects of acute low-grade inflammation on human visual attention.* NeuroImage, 2019. **202**: p. 116098.

379. McGarry, G.W., S. Gatehouse, and J. Hinnie, *Relation between alcohol and nose bleeds.* BMJ, 1994. **309**(6955): p. 640.

380. Whitfield, J.B., G. Zhu, A.C. Heath, L.W. Powell, and N.G. Martin, *Effects of alcohol consumption on indices of iron stores and of iron stores on alcohol intake markers.* Alcoholism: Clinical and Experimental Research, 2001. **25**(7): p. 1037-45.

381. Donat, C.K., G. Scott, S.M. Gentleman, and M. Sastre, *Microglial activation in traumatic brain injury.* Frontiers in Aging Neuroscience, 2017. **9**(208).

382. Murugan, M., A. Ravula, A. Gandhi, G. Vegunta, S. Mukkamalla, W. Mujib, and N. Chandra, *Chemokine signaling mediated monocyte infiltration affects anxiety-like behavior following blast injury.* Brain, Behavior, and Immunity, 2020. **88**: p. 340-352.

383. Fernandez-Lizarbe, S., M. Pascual, and C. Guerri, *Critical Role of TLR4 Response in the Activation of Microglia Induced by Ethanol.* The Journal of Immunology, 2009. **183**(7): p. 4733-4744.

384. Zhao, Y.-N., F. Wang, Y.-X. Fan, G.-F. Ping, J.-Y. Yang, and C.-F. Wu, *Activated microglia are implicated in cognitive deficits, neuronal death, and successful recovery following intermittent ethanol exposure.* Behavioural Brain Research, 2013. **236**: p. 270-282.

385. Molteni, M., S. Gemma, and C. Rossetti, *The role of toll-like receptor 4 in infectious and noninfectious inflammation.* Mediators Inflammation, 2016. **2016**: p. 6978936.

386. Klei, T.R., S.M. Meinderts, T.K. van den Berg, and R. van Bruggen, *From the cradle to the grave: the role of macrophages in erythropoiesis and erythrophagocytosis.* Frontiers in Immunology, 2017. **8**: p. 73.

387. Gánti, B., E. Molnár, R. Fazekas, B. Mikecs, Z. Lohinai, S. Mikó, and J. Vág, *Evidence of spreading vasodilation in the human gingiva evoked by nitric oxide.* Journal of Periodontal Research, 2019. **54**(5): p. 499-505.

388. Zazulia, A.R., M.N. Diringer, C.P. Derdeyn, and W.J. Powers, *Progression of mass effect after intracerebral hemorrhage.* Stroke, 1999. **30**(6): p. 1167-1173.

389. Hariprasad, D.S. and T.W. Secomb, *Motion of red blood cells near microvessel walls: effects of a porous wall layer.* Journal of Fluid Mechanics, 2012. **705**: p. 195-212.

390. Imai, T., S. Iwata, T. Hirayama, H. Nagasawa, S. Nakamura, M. Shimazawa, and H. Hara, *Intracellular Fe(2+) accumulation in endothelial cells and pericytes induces blood-brain barrier dysfunction in secondary brain injury after brain hemorrhage.* Scientific Reports, 2019. **9**(1): p. 6228.

391. Daruich, A., Q. Le Rouzic, L. Jonet, M.-C. Naud, L. Kowalczuk, J.-A. Pournaras, J.H. Boatright, A. Thomas, N. Turck, A. Moulin, F. Behar-Cohen, and E. Picard, *Iron is neurotoxic in retinal detachment and transferrin confers neuroprotection.* Science Advances, 2019. **5**(1): p. eaau9940.

392. Eid, R., N.T. Arab, and M.T. Greenwood, *Iron mediated toxicity and programmed cell death: A review and a re-examination of existing paradigms.* Biochimica et Biophysica Acta Molecular Cell Research, 2017. **1864**(2): p. 399-430.

393. Balla, J., G.M. Vercellotti, K. Nath, A. Yachie, E. Nagy, J.W. Eaton, and G. Balla, *Haem, haem oxygenase and ferritin in vascular endothelial cell injury.* Nephrology Dialysis Transplantation, 2003. **18**(suppl_5): p. v8-v12.

394. Timmer, T.C., R. de Groot, J.J.M. Rijnhart, J. Lakerveld, J. Brug, C.W.M. Perenboom, M.A. Baart, F.J. Prinsze, S. Zalpuri, E.C. van der Schoot, W.L.A.M. de Kort, and K. van den Hurk, *Dietary intake of heme iron is associated with ferritin and hemoglobin levels in Dutch blood donors: results from Donor InSight.* Haematologica, 2020. **105**(10): p. 2400-2406.

395. Li Volti, G., F. Galvano, A. Frigiola, S. Guccione, C. Di Giacomo, S. Forte, G. Tringali, M. Caruso, O.A. Adekoya, and D. Gazzolo, *Potential immunoregulatory role of heme oxygenase-1 in human milk: a combined biochemical and molecular modeling approach.* Journal of Nutritional Biochemistry, 2010. **21**(9): p. 865-71.

396. Moschen, A.R., T.E. Adolph, R.R. Gerner, V. Wieser, and H. Tilg, *Lipocalin-2: a master mediator of intestinal and metabolic inflammation.* Trends in Endocrinology and Metabolism, 2017. **28**(5): p. 388-397.

397. Tran, T.N., S.K. Eubanks, K.J. Schaffer, C.Y.J. Zhou, and M.C. Linder, *Secretion of ferritin by rat hepatoma cells and its regulation by inflammatory cytokines and iron.* Blood, 1997. **90**(12): p. 4979-4986.

398. Jin, Z., K.E. Kim, H.J. Shin, E.A. Jeong, K.A. Park, J.Y. Lee, H.S. An, E.B. Choi, J.H. Jeong, W. Kwak, and G.S. Roh, *Hippocampal lipocalin 2 is associated with neuroinflammation and iron-related oxidative stress in ob/ob mice.* Journal of Neuropathology and Experimental Neurology, 2020. **79**(5): p. 530-541.

399. Morita, A., A. Jullienne, A. Salehi, M. Hamer, E. Javadi, Y. Alsarraj, J. Tang, J.H. Zhang, W.J. Pearce, and A. Obenaus, *Temporal evolution of heme oxygenase-1 expression in reactive astrocytes and microglia in response to traumatic brain injury.* Brain Hemorrhages, 2020. **1**(1): p. 65-74.

400. McIntosh, A., V. Mela, C. Harty, A.M. Minogue, D.A. Costello, C. Kerskens, and M.A. Lynch, *Iron accumulation in microglia triggers a cascade of events that leads to altered metabolism and compromised function in APP/PS1 mice.* Brain Pathology, 2019. **29**(5): p. 606-621.

401. Mairuae, N., J.R. Connor, and P. Cheepsunthorn, *Increased cellular iron levels affect matrix metalloproteinase expression and phagocytosis in activated microglia.* Neuroscience Letters, 2011. **500**(1): p. 36-40.

402. Lan, X., X. Han, Q. Li, Q.W. Yang, and J. Wang, *Modulators of microglial activation and polarization after intracerebral haemorrhage.* Nature Reviews Neurology, 2017. **13**(7): p. 420-433.

403. Loane, D.J. and A. Kumar, *Microglia in the TBI brain: The good, the bad, and the dysregulated.* Experimental Neurology, 2016. **275**: p. 316-327.

404. Walter, T.J., R.P. Vetreno, and F.T. Crews, *Alcohol and stress activation of microglia and neurons: brain regional effects.* Alcoholism: Clinical and Experimental Research, 2017. **41**(12): p. 2066-2081.

405. Peng, H. and K. Nixon, *Microglia phenotypes following the induction of alcohol dependence in adolescent rats.* Alcoholism: Clinical and Experimental Research, 2021. **45**(1): p. 105-116.

406. Li, J., F. Cao, H.L. Yin, Z.J. Huang, Z.T. Lin, N. Mao, B. Sun, and G. Wang, *Ferroptosis: past, present and future.* Cell Death and Disease, 2020. **11**(2): p. 88.

407. Ioannou, G.N., J.A. Dominitz, N.S. Weiss, P.J. Heagerty, and K.V. Kowdley, *The effect of alcohol consumption on the prevalence of iron overload, iron deficiency, and iron deficiency anemia.* Gastroenterology, 2004. **126**(5): p. 1293-301.

408. Kärkkäinen, J.M., S. Miilunpohja, T. Rantanen, J.M. Koskela, J. Jyrkkä, J. Hartikainen, and H. Paajanen, *Alcohol abuse increases rebleeding risk and mortality in patients with non-variceal upper gastrointestinal bleeding.* Digestive Diseases and Sciences, 2015. **60**(12): p. 3707-15.